U.S. DEPARTMENT OF THE INTERIOR
U.S. GEOLOGICAL SURVEY

TO ACCOMPANY MAP I-2559

# GEOLOGIC MAP OF THE UNALAKLEET QUADRANGLE, WEST-CENTRAL ALASKA

By W.W. Patton, Jr. and E.J. Moll-Stalcup

## DESCRIPTION OF MAP UNITS

### OVERLAP ASSEMBLAGES

#### Surficial deposits

Qf **Flood-plain deposits (Holocene)**—Silt, sand, and gravel along floodplains of stream valleys. Light-gray micaceous silt along the Yukon River; chiefly sand and gravel along the Unalakleet River and along small streams that drain bedrock uplands. Characterized physiographically by bars, oxbow lakes, meander scrolls, abandoned channels, and other evidence of recent floodplain building. Mapped almost entirely from aerial photographs

Qc **Fluvial, colluvial, and eolian terrace and slope deposits, undivided (Holocene and Pleistocene)**—Chiefly silt and very fine sand. Terrace deposits appear to be largely fluvial; slope deposits probably include both colluvial and eolian deposits. Unit is characterized locally by thermokarst topography marked by many small lakes. Mapped almost entirely from aerial photographs

Qh **High-level eolian and colluvial deposits (Pleistocene)**—Windblown and reworked windblown deposits of silt and very fine sand that mantle hilly areas east of the Yukon River. Unit obscures all bedrock except for small exposures at highest elevations and in scattered cutbanks along the Innoko River. Mapped almost entirely from aerial photographs

#### St. Michael volcanic field

The St. Michael volcanic field covers over 3,000 km² in the southwestern part of the Unalakleet quadrangle and adjacent St. Michael quadrangle (Hoare and Condon, 1971). It forms a broad shield volcano composed of numerous basalt flows that are overlain by more than 55 highly alkalic monogenetic cones and short flows. Maar craters occur in the western part of the field. The oldest dated flow is 3.25±0.11 Ma; the youngest dated flow is less than 200 ka (table 1). The flows are mostly tholeiitic and alkali olivine basalt; the cones and short flows consist of more alkalic basalt and basanite (tables 2 and 3). The volcanic field is divided into three map units, units Qyt, Qya, and QTb, on the basis of age and composition.

Qyt **Younger tholeiitic basalt cones and flows (Holocene? and Pleistocene)**—Black glassy olivine tholeiite basalt flows that erupted from two small unnamed craters in the south-central part of the volcanic field. Flows have well-preserved pahoehoe structure including ropy flow surfaces and lava tubes; they lack vegetative cover. Flows and spatter are variably oxidized. Least oxidized parts have 3 percent olivine phenocrysts in a groundmass of plagioclase laths, fine-grained pyroxene, dark-brown glass, and magnetite; more oxidized parts have black olivine (a term used by Johnston and Stout, 1984, for olivine containing abundant linear tracks of opaque oxides) and sparse plagioclase microlites in a groundmass of dark, almost opaque glass. The more oxidized parts are interpreted to have formed from magma that reached the surface, but subsequently fell back into the magma chamber where it was oxidized at high temperatures by volatiles trapped in vesicles.

Unit yielded a whole-rock K-Ar age of 0.19±0.02 Ma (table 1) and is considered to be Pleistocene and possibly Holocene

Qya **Younger alkalic basalt cones and flows (Pleistocene)**—In the Unalakleet quadrangle this unit comprises more than 40 alkali basalt, basanite, and hawaiite cones, short flows, and maar craters. The cones and short flows have little or no vegetative cover, and some primary flow features are still preserved (fig.2). Almost all cones are aligned in two broad east-west-trending segments. Alkali basalts have phenocrysts of fine-grained euhedral and embayed olivine and pinkish-brown clinopyroxene in an intergranular groundmass of plagioclase laths, olivine, granular clinopyroxene, and magnetite. Olivine phenocrysts commonly contain inclusions of brown, octahedral, Cr-rich spinel. Some alkali basalts have xenoliths of pyroxenite, dunite, and (or) wehrlite. Basanites are petrographically similar to the alkali basalts, but commonly have interstitial black glass or very fine-grained, low-birefringent, dark

mesostasis of glass, abundant oxides, pyroxene, and possible nepheline. Basanites also contain more abundant xenoliths of harzburgite (olivine, minor orthopyroxene, and anhedral brown Cr-spinel), quartzofeldspathic material, plagioclase aggregate, anorthoclase, pyroxenite, and dunite. Some crystals, such as kink-banded olivine phenocrysts and crystals of orthopyroxene or clinopyroxene rimmed by tiny granular clinopyroxene crystals, appear to have come from disaggregating xenoliths. Hawaiite, which is relatively uncommon, consists of phenocrysts of olivine and plagioclase in a groundmass of plagioclase, brown clinopyroxene, and opaque oxides. Some hawaiite flows have clinopyroxene phenocrysts in addition to olivine and plagioclase; others contain clots of pyroxene or olivine (± subordinate plagioclase).

Unit is considered to be Pleistocene because it overlies and was erupted through unit QTb

QTb **Older basalt flows (Pleistocene and Pliocene)**—Abundant vesicular tholeiitic and alkali olivine basalt flows form a broad dissected shield volcano that composes the lowest unit in the St. Michael volcanic field. Exposures for the most part are confined to sea cliffs and to canyons cut by major drainages; elsewhere flows are generally covered by variable thicknesses of silt and tundra vegetation. Locally, along sea cliffs and canyons, unit uncomformably overlies Cretaceous sedimentary rocks (Ks, Kg) of the Yukon-Koyukuk basin. Flows are nearly horizontal, columnar jointed, and have a total thickness of at least 100 m along the Golsovia River; they consist of fine-grained, black to gray, vesicular, alkalic olivine and tholeiitic basalt. Alkali basalt contains medium- to fine-grained phenocrysts of olivine and subordinate greenish to brown clinopyroxene in a groundmass of plagioclase laths, magnetite, granular pyroxene, and sparse olivine. Olivine is partially altered to iddingsite. Tholeiitic basalt is characterized by diktytaxitic textures consisting of olivine, clinopyroxene, and plagioclase phenocrysts in a slightly finer grained groundmass of the same minerals plus ilmenite, magnetite, and oxide-rich brown to black interstitial glass. Some of the clinopyroxene subophitically encloses plagioclase.

Unit is considered to be Pleistocene and Pliocene in age on the basis of four K-Ar whole-rock ages of 1.39±0.04, 1.99±0.06, 2.8±0.1, and 3.25±0.11 Ma (table 1). The oldest age is from Tolstoi Point where the basalt flows unconformably overlie sedimentary rocks of unit Ks. A basalt flow from a topographically high area at Iprugalet Mountain yielded a K-Ar age of 2.8±0.1 Ma, whereas a flow from a small lobe more than 200 m below gave a younger age of 1.39±0.04 Ma, suggesting that Iprugalet Mountain is an eroded volcanic center and that the small lobe is a remnant of a younger flow

Deposits along Kaltag Fault

Ts **Clay shale and coal (Miocene or Oligocene)**—Poorly consolidated deposits of gray to brown clay shale, lignitic coal, and yellow volcanic ash mapped in one small area on the coast about 13 km south of Unalakleet along the inferred trace of the Kaltag Fault. The section appears to be about 10 m thick, but all exposures are badly slumped. Unit is assigned a late Oligocene (Seldovian) or early Miocene age based on pollen and spore assemblages from lignite (Estella Leopold, written commun., 1966). Similar small coal-bearing deposits of Oligocene to Pliocene age are scattered along the Kaltag Fault to the northeast in the Norton Bay, Melozitna, and Tanana quadrangles (Patton and others, 1994)

Blackburn Hills volcanic field

The Blackburn Hills volcanic field consists primarily of andesite lava flows (Ta), rhyolite domes and hypabyssal bodies (Td, Thr), altered tuff and tuff breccia (Tt), and a granitic stock (Tg). Small volumes of basalt and sodic rhyolite are interbedded with andesitic flows near the top of the stratigraphic section. The volcanic field is split into two segments that are left-laterally offset about 25 km along the Thompson Creek Fault. The northern segment has been studied in considerable detail (Moll-Stalcup and Patton, 1992; Moll-Stalcup and Arth, 1991); the southern segment, which was mapped more recently, has not been studied in the same detail. The northern segment forms the broadly folded Blackburn Syncline composed of a thick section of andesite and basalt lava flows (Ta) that are overlain and interbedded at the top of the section by rhyolite domes and flows (Td). The axis of the Blackburn Syncline is cut by a thick section of altered intracaldera tuff and tuff breccia (Tt) and is intruded by an elongate granite stock (Tg). The southern segment of the field consists of a homoclinal southeast-dipping section composed chiefly of andesite lava flows (Ta) and subordinate rhyolite domes (Td). Moll-Stalcup and Arth (1991) divided the andesite lava flows (Ta) in the northern segment into two subunits, groups 1 and 2, on the basis of chemical composition. Group 1 is the more widely distributed and has much higher heavy rare-earth-element (HREE) content than group 2, which is geographically restricted to the northwest corner of the northern segment. The composition of two andesite lava flows sampled from the southern segment of the volcanic field is similar to group 1 (fig. 10).

Ta **Andesite and basalt flows (Eocene and Paleocene)**—Well-exposed sequence more than 1,500 m thick of subaerial columnar-jointed andesite and basalt flows. Unit occurs at the base of the volcanic field on both flanks of the Blackburn Syncline and in the southern segment of the field that has been offset 25 km left-laterally along the Thompson Creek Fault. Most common rock types are one- and two-pyroxene andesite. Hornblende-bearing high-silica andesite and olivine-bearing basaltic andesite are much less common. Basalt is restricted to the uppermost part of the stratigraphic section where the unit is locally intercalated with rhyolite of unit Td. Pyroxene andesite has 1 to 2 modal percent phenocrysts of oscillatory-zoned plagioclase, clinopyroxene and (or) orthopyroxene, with or without altered olivine. Andesites usually have a hyaloophitic or intersertal groundmass that is composed of subparallel plagioclase microlites, pyroxene, ilmenite, and magnetite in dark glass. Hornblende-bearing high-silica andesite has 15 to 20 percent phenocrysts of plagioclase, gold-brown hornblende, and clinopyroxene in a groundmass of fine-grained plagioclase laths and opaque oxides in pale devitrified glass. Basalt has 3 to 15 percent phenocrysts of plagioclase, clinopyroxene, and olivine in a groundmass of the same minerals plus magnetite. Ilmenite is present in some flows.

Hornblende from an andesite flow near the base of the unit in the northern segment of the volcanic field yielded a K-Ar age of 65.2±3.9 Ma (table 1); an andesite flow near the top of the unit in the southern segment yielded a whole-rock K-Ar age of 51.9±1.6 Ma

Tg **Granite (Eocene or Paleocene)**—Stock composed of pink to light-gray granite and quartz monzonite (63 to 71 percent $SiO_2$, table 4) that intrudes the northern segment of the Blackburn Hills volcanic field. Occurs as crop or rubble on high ridges along the axis of the Blackburn Syncline. Composed of fine-grained hypidiomorphic granular or sparsely porphyritic granitic rocks characterized by plagioclase laths ($An_{38-16}$) mantled by orthoclase. Orthoclase usually occurs as thick rims on plagioclase or less commonly as interstitial crystals. Quartz is usually interstitial and locally occurs as crystals that are optically, but not physically, continuous over large areas or as graphic-intergrowths of quartz and potassium-feldspar. Most of the stock has about 10 percent hornblende and biotite and 5 percent iron-titanium oxides. More mafic parts of the stock (63 percent $SiO_2$) have up to 3 percent pyroxene. Pink granite dikes, presumably related to the stock, intrude unit Tt near its contact with the stock.

Unit is Paleocene or Eocene in age based on a K-Ar determination on biotite of 56.2±1.7 Ma (table 1)

Thr **Hypabyssal rhyolite (Eocene or Paleocene)**—Fine-grained porphyritic hypabyssal rhyolite intruded into units Ta and Ks along the southeast flank of the Blackburn Syncline. Hypabyssal rhyolite is characterized by fine- to medium-grained phenocrysts of plagioclase rimmed by orthoclase and is texturally and mineralogically similar to the rocks of the granitic stock (Tg). The rhyolite is interpreted to be the differentiated hypabyssal equivalent of the rocks of the central stock. Most of this unit is porphyritic, although some parts have a groundmass that is only slightly finer than the phenocrysts. The groundmass consists of fine- to medium-grained plagioclase, orthoclase, quartz, and altered mafic minerals. The original mafic minerals probably were biotite, hornblende, and magnetite, but have been completely replaced by muscovite, sphene, and iron oxides. Four samples of the porphyritic intrusive rhyolite were analyzed for major and trace elements (Moll-Stalcup and Patton, 1992); a typical analysis is given in table 4. The intrusive rhyolite is silicic, clustering at about 75 percent $SiO_2$, and is similar in major- and trace-element composition to the calc-alkalic rhyolite domes and tuffs of unit Td (table 4).

Unit is considered to be the same age (Eocene or Paleocene) as the granitic stock (Tg) because the two units form a compositional continuum (Moll-Stalcup and Arth, 1991) and are petrographically similar. Both units probably formed from a single evolving magma chamber

Td **Rhyolite domes and flows (Eocene or Paleocene)**—Unit consists of well-exposed erosional remnants of rhyolite domes and flows and associated basal breccia and tuff. Unit is exposed mainly along the axis and west flank of the Blackburn Syncline where it generally overlies unit Ta, but locally is interbedded with the uppermost part of unit Ta. In the southern segment of the field, this unit is also found at the top of the stratigraphic section. Rhyolite domes and flows generally have sparse phenocrysts in a groundmass of black hydrated glass and devitrified rhyolite. Glassy rocks are flow-banded, perlitic, and contain 1 to 5 percent fine-grained phenocrysts of ferrohedenbergite and a single feldspar of either unzoned oligoclase or oligoclase rimmed by anorthoclase. Devitrified rhyolite

generally has a groundmass of microcrystalline quartz and feldspar, locally containing very fine-grained needles of green pyroxene. Most devitrified and partially devitrified rocks are calc-alkalic rhyolite (table 4). Phenocrysts are chiefly plagioclase (3 to 20 modal percent), which shows normal or oscillatory zoning from andesine to oligoclase and commonly shows zonal arrangement of melt inclusions. Mafic minerals in the devitrified calc-alkalic rocks are usually altered but typically consist of biotite or hornblende, ilmenite, magnetite, and locally clinopyroxene and (or) orthopyroxene. Secondary chalcedony is common in the groundmass of the devitrified rocks. Associated volcanic breccia and tuff are composed of medium- to coarse-grained clasts of perlitic rhyolite, green to brown altered pumice, glass shards, crystals of feldspar and quartz, and andesite lithic clasts.

A sanidine mineral separate from a rhyolite dome sample yielded a K-Ar age of 56.0±1.7 Ma (table 1)

Tt **Tuff and tuff breccia (Eocene or Paleocene)**—Unit consists of more than 1,000 m of (1) green tuff and tuff breccia, (2) white rhyolite breccia, domes, and ash, (3) highly altered green andesite and dacite flows, and (4) minor pink granite dikes. Unit forms rubble and small outcrops in the axial part of the Blackburn Syncline. At least 500 m of this unit consists of green intracaldera tuff and tuff breccia that ranges from fine gray-green ash beds to coarse volcanic breccia containing clasts as long as 25 cm. Tuff is composed of abundant lithic fragments of rhyolite, dark-green partially welded pumice, and subordinate andesite lithic fragments in a groundmass of devitrified glass shards and crystals of altered plagioclase, quartz, and mafic minerals. Rhyolite lithic fragments consist of various lithologies of the rhyolite domes and flows (Td) unit, including devitrified and glassy fragments, some of which show remnant flow banding and perlitic cracks. Partially welded pumice is altered to chlorite and epidote. Mafic minerals are altered to chlorite and opaque oxides. Devitrified rhyolite glass is locally altered to zeolites. Rhyolite breccia consists of nearly monolithologic angular clasts of white flow-banded rhyolite and rare andesite clasts and pumice in a matrix of polycrystalline quartz. White flow-banded rhyolite is devitrified and fractured; quartz veins fill fractures. Green andesite and dacite flows are highly altered and are composed of 15 to 25 percent phenocrysts of chiefly plagioclase and mafic minerals altered to chlorite and epidote. Andesite has a highly altered groundmass composed of medium-grained plagioclase laths, chlorite, and opaque minerals. Dacite groundmass is composed of polycrystalline quartz and K-feldspar. Unit is locally cut by pink granite dikes lithologically similar to those of the central stock (Tg). Green tuff and breccia are interpreted to represent thick intracaldera deposits probably related to eruption of large siliceous ash-flow tuffs late in the evolution of the volcanic field. Unit appears to contain some outflow, near-source, altered flows and tuffs. The contact with andesite and basalt flows of unit Ta is uncertain due to similar alteration of both units along the south and north parts of the contact. Unit may also be present in a poorly mapped area at the northeast end of the Blackburn Syncline.

Unit was not isotopically dated owing to the lack of suitable unaltered material. It cuts unit Ta and, therefore, is younger than 65.2±3.9 Ma; it is intruded by unit Tg and, thus, is older than 56.2±1.7 Ma

Small volcanic and intrusive bodies

TKr **Rhyolite and dacite (early Tertiary and Late Cretaceous)**—Erosional remnants of rhyolite and dacite domes, sills, dikes, and tuffs that are widely distributed throughout the quadrangle. Unit consists of (1) rhyolite and dacite tuffs exposed along the Innoko River in the southeast corner of the quadrangle; (2) a large rhyolite dome and associated dacite flows exposed at Eagle Slide on the Yukon River; (3) rhyolite tuff and a dacite flow exposed along Runkels Creek in the Anvik River drainage near the south boundary of the quadrangle; and (4) numerous rhyolite domes, dikes, sills, and tuffs in the northern, central, and southwestern parts of the quadrangle. Rhyolite and dacite of this map unit commonly are associated spatially with andesite and basalt flows of unit TKa.

In the Innoko River area , unit consists of dacite and white rhyolite ash-flow tuff containing gray pumice. White rhyolite ash-flow tuff is composed of 30 percent phenocrysts of sanidine, quartz, and biotite in a groundmass of glass shards. Dacite consists of phenocrysts of plagioclase, quartz, sanidine, altered biotite, and orthopyroxene in a groundmass of plagioclase microlites, biotite, chlorite, and opaque oxides.

The rhyolite dome at Eagle Slide has 3 to 10 percent medium-grained phenocrysts of plagioclase, anorthoclase, quartz, and sanidine in a groundmass of partly devitrified pale-brown glass, tiny plagio-

clase microlites, sparse biotite, and magnetite. The more mafic parts of the dome also contain phenocrysts of biotite, and green hornblende.

Rhyolite tuff at Runkels Creek consists of blocks of flow-banded rhyolite vitrophyre in non-welded ash. The blocks have about 10 modal percent fine-grained phenocrysts of chiefly plagioclase, biotite, and subordinate sanidine in a groundmass of colorless glass and plagioclase microlites. The dacite flow at Runkels Creek consists of 7 percent medium-grained phenocrysts of plagioclase and amphibole in a groundmass of tiny plagioclase microlites and trace opaque oxides in colorless glass. A small dacite field along the Swift River north of Runkels Creek consists of fine-grained porphyritic dacite having 25 percent phenocrysts of plagioclase and biotite in a groundmass of devitrified glass.

Rhyolite domes elsewhere in the quadrangle typically occur as bare, round hills of platy rubble that weather to an orange color. Most of the domes are pervasively altered. A typical dome has 3 to 15 percent phenocrysts of plagioclase, quartz, biotite, and sanidine in a groundmass of very fine-grained quartz, feldspar, and opaque oxides. Mafic minerals are generally altered and some may be secondary. Dacite has hornblende and lacks sanidine. Plagioclase is commonly oscillatory zoned and has zonal concentrations of glass or mineral inclusions. Dacite dikes and sills, which occur throughout the quadrangle, typically contain 25 modal percent medium-grained phenocrysts of amphibole and plagioclase in a groundmass of fine-grained equigranular quartz and feldspar, opaque oxides, and chlorite.

Unit is considered to be Late Cretaceous and early Tertiary on the basis of two K-Ar determinations of 69.1±2.1 Ma (sanidine) and 66.4±2 Ma (biotite) on a rhyolite from the Runkels Creek area, one K-Ar determination of 53.2±1.6 Ma (sanidine) on a rhyolite dome from Eagle Slide, and one K-Ar determination of 66.8±2 Ma (hornblende) on a rhyolite dome in the south-central part of the quadrangle (table 1)

TKs **Tuff, sandstone, conglomerate, and shale (early Tertiary and Late Cretaceous)**—Nonmarine sedimentary rocks rich in volcanic components. Exposed in two small areas in the central and southeastern parts of the quadrangle where they underlie rhyolite and dacite flows and tuffs of unit TKr. In the Anvik River drainage in the central part of the quadrangle, unit is composed of well-sorted quartz-rich sandstone, conglomerate, siltstone, tuff, tuff breccia, and locally abundant carbonized plant debris and thin coaly layers. Unit appears to grade upward into rhyolite tuffs of unit TKr. Along the Innoko River in the southeast corner of the quadrangle, unit is composed of quartz-chert-pebble conglomerate, sandstone, and siltstone containing abundant plant fossils and thin coaly layers. Unit is assigned a Late Cretaceous and early Tertiary age on the basis of its gradational contact with unit TKr

TKa **Andesite and basalt (early Tertiary and Late Cretaceous)**—Chiefly andesite and basalt lava flows that are widely distributed in the eastern and southern parts of the quadrangle. In many places, the flows are spatially associated with rhyolite and dacite of unit TKr. Unit consists of: (1) thin basalt flows exposed along the Innoko River in the southeast corner of the quadrangle that are composed of fine-grained plagioclase, olivine, clinopyroxene, and ilmenite in an intergranular groundmass of devitrified glass; (2) hornblende andesite flows at the top of a low hill above Runkels Creek in the south-central part of the quadrangle consisting of 15 to 20 percent fine-to medium-grained phenocrysts of plagioclase, oxidized hornblende, and sparse clinopyroxene in a groundmass of aligned plagioclase microlites, golden-brown amphibole needles, and opaque oxides; (3) a small dissected andesite cone about 5 km west of Bullfrog Island in the Yukon River that consists chiefly of fine-grained plagioclase, orthopyroxene, clinopyroxene, and magnetite; and (4) several small erosional remnants bordering the Chiroskey Fault Zone in the central part of the quadrangle consisting of columnar-jointed flows having about 20 percent phenocrysts of olivine, plagioclase, and clinopyroxene in a groundmass of the same minerals plus altered opaque oxides and a trace interstitial altered glass. Unit also includes a compositionally unusual lamprophyre sill in the southwest corner of the quadrangle (map No. 57, sample No. 86Pa043, map sheet and table 5) consisting of highly zoned clinopyroxene phenocrysts in a groundmass of biotite, amphibole, opaque oxides, plagioclase, and apatite.

Unit is considered to be latest Cretaceous and early Tertiary on the basis of three K-Ar determinations of 64.4±1.9, 61.5±1.8, and 53.8±1.6 Ma (table 1). Some rocks in this unit are lithologically similar to, and may be contemporaneous with, andesite and basalt flows of unit Ta

TKu **Rhyolite, dacite, andesite, and basalt, undivided (early Tertiary and Late**

**Cretaceous)**—Volcanic and hypabyssal rocks of uncertain composition and age. Unit is poorly exposed and confined to low hills in the south-central and southeastern parts of the quadrangle and to several dike- or sill-like bodies in the southwest corner of the quadrangle. Unit is presumed to be approximately the same age as units TKa and TKr

Complexes of small intrusive bodies and altered sedimentary deposits

TKrs **Rhyolite and dacite (early Tertiary and Late Cretaceous), and sandstone, shale, and conglomerate deltaic deposits (Late and Early Cretaceous), undivided**—Complexes composed of small rhyolite and dacite hypabyssal bodies and thermally altered sandstone, shale, and conglomerate. The rhyolite and dacite bodies are too small and too numerous to be mapped separately at this map scale. Sedimentary host rocks are altered to an erosion-resistant hornfels. The complexes form broad domal topographic features in three separate parts of the quadrangle: (1) in the southwestern part between the Anvik and Andreafsky Rivers, (2) in the north-central part between Old Woman River and the lowlands of the Unalakleet River, and (3) in the east-central part between the Yukon River and the east edge of the quadrangle. The complexes are interpreted to represent the roofs of shallow plutons (map sheet, section A-A'). Hypabyssal rocks are generally similar to the rhyolite and dacite dikes of unit TKr, but are more altered and have a coarser grained groundmass. More felsic phases consist of 25 percent oscillatory zoned plagioclase, 10 percent quartz, and 2 percent biotite in a groundmass of quartz, feldspar, biotite, and opaque oxides. More mafic phases have phenocrysts of green amphibole (altered to chlorite and calcite), quartz, and plagioclase in a groundmass of altered feldspar.

A biotite separate from a hypabyssal rock collected from the complex in the southwestern part of the quadrangle yielded a K-Ar age determination of 68.8±3 Ma (table 1)

Yukon-Koyukuk basin sedimentary deposits

The Unalakleet quadrangle lies wholly within the Yukon-Koyukuk basin, a huge Cretaceous depression that occupies much of western Alaska south of the Brooks Range. The basin is filled with late Early and early Late Cretaceous (Albian and Cenomanian) terrigenous sedimentary rocks consisting of volcanic graywacke and mudstone turbidite deposits (Kg) in the lower part and sandstone, shale, and conglomerate deltaic deposits (Ks) in the upper part.

Ks **Sandstone, shale, and conglomerate deltaic deposits (Late and Early Cretaceous)**—Chiefly fluvial and shallow-marine deltaic deposits of well-sorted, medium- to coarse-grained, light-olive crossbedded sandstone, fine- to medium-grained, dark-gray to green silty sandstone, dark-gray micaceous shale, quartz-chert-pebble conglomerate, and thin seams of bituminous coal. Unit is best exposed in sea cliffs south of Unalakleet, in cutbanks along the Chiroskey and Anvik Rivers, and along the west bank of the Yukon River. Sandstones are composed chiefly of quartz, chert, and metamorphic rock detritus and generally contain subordinate amounts of volcanic rock fragments. Bituminous coal seams are generally less than 50 cm thick; a 1-m-thick coal seam was reported on the Yukon River at the Williams Mine 6 km upstream from Eagle Slide, and a 75- to 90-cm-thick seam was reported 20 km upstream from Blackburn (Chapman, 1963). On South River, unit includes some hard, fine- to medium-grained sandstone turbidites and mudstone of uncertain affinities.

Studies by J.M. Murphy (written commun., 1990) show that sandstone in this unit from west of the Anvik River contains fewer potassium feldspar, chert, and greenstone clasts than sandstone from east of the Anvik River. The quartzose nature of the lithic clasts (including polycrystalline quartz), as well as the relatively high proportions of potassium feldspar and micas, suggest a mixed metamorphic and granitic provenance. These data, when combined with limited paleocurrent data, indicate that unit Ks prograded westward from a source area in the Proterozoic(?) and early Paleozoic metasedimentary rocks and mid-Cretaceous granitic plutons of the Ruby terrane bordering the east margin of the Yukon-Koyukuk basin (Patton and others, 1994). A Ruby terrane provenance is further confirmed by the presence in this unit of detrital micas that yield K-Ar ages of 131 to 158 Ma (Harris and others, 1987). Similar mineral ages were obtained from metamorphic micas in the Ruby terrane by Patton and others (1984).

Unit Ks is assigned a late Early (Albian) and early Late (early Cenomanian) Cretaceous age. Marine mollusks of middle Albian to early Cenomanian age, including *Turrilites acutus* Passy, *Gastroplites (Gastroplites) kingi* McLearn, *Beaudanticeras (Grantziceras)* sp., and *Inoceramus* sp. (Elder and Miller, 1991), were found along the Chiroskey and Anvik Rivers, in the Old Woman River drainage, and in the uplands between the Unalakleet

and North Rivers. Fossil fresh- and brackish-water mollusks are common throughout the unit. Plant fossils, consisting of both conifers and angiosperms of probable Cenomanian age (R.A. Spicer, written commun., 1981), are also widely distributed in this unit. The unit unconformably overlies the andesitic volcaniclastic rocks (Kv) unit, the shoshonitic flows and tuffs (Kft) unit, and the volcanic graywacke and mudstone turbidites (Kg) unit. On the Yukon and lower Koyukuk Rivers, where this unit has been studied in greatest detail, the exposed section has an estimated thickness of 3,000 to 3,500 m. It grades upward from shallow-marine beds containing abundant mollusks of Albian age into nonmarine beds with plant fossils of Cenomanian and Turonian(?) age (Patton and Bickel, 1956; Patton, 1966; R.A. Spicer, oral commun., 1987)

Kg **Volcaniclastic graywacke and mudstone turbidites (Early Cretaceous)**—Dark-gray to green, hard, fine-grained to conglomeratic volcanic graywacke and dark-gray, finely laminated mudstone. Unit is best exposed in sea cliffs north of Unalakleet; elsewhere, exposures are largely reduced to frost-riven rubble. These strata make up a turbidite assemblage consisting of submarine-fan deposits, chiefly midfan channel, interchannel, and related overbank facies (Nilsen, 1989). Graywacke is composed mainly of intermediate and mafic volcanic rock detritus and chert; quartz and metamorphic rock debris are present in subordinate amounts. Unit appears to be transitional in composition between the andesitic volcaniclastic rocks (Kv) unit and the sandstone, shale, and conglomerate deltaic deposits (Ks) unit. Andesitic and basaltic lithic clasts dominate, but in the upper part of the unit metamorphic detritus, which is common in the overlying sandstone, shale, and conglomerate deltaic deposits (Ks) unit, makes its first appearance (J.M. Murphy, written commun., 1990). Some graywacke beds are characterized by a distinctly mottled appearance owing to the presence of laumontite (Hoare and others, 1964).

No fossils have been found in this unit. It is assigned an Early Cretaceous (Albian) age based on its stratigraphic position above the shoshonitic flows and tuffs (Kft) unit and below the sandstone, shale, and conglomerate deltaic deposits (Ks) unit

## LITHOTECTONIC TERRANES

### Koyukuk terrane

The Koyukuk (volcanic arc) terrane of west-central Alaska underlies a large part of the Yukon-Koyukuk basin and is widely exposed on a broad structural high that separates the Lower Yukon subbasin from the Kobuk-Koyukuk subbasin (Patton, 1973). In the Unalakleet quadrangle, the Koyukuk terrane is exposed on the Anvik-Chiroskey high, a north-trending uplift, which extends from the south edge of the quadrangle north to the Unalakleet River valley (fig. 1). The Koyukuk terrane is composed of two volcanic units (Kft, Kv) of Early Cretaceous age and two plutonic units (Jt, Ju) of Middle and Late Jurassic age.

Kft **Shoshonitic flows and tuffs (Early Cretaceous)**—Dark-gray to green lithic tuffs, pillowed flows, diabase, and volcanic conglomerate of shoshonitic composition exposed on several north-trending ridges near the Yellow River in the south-central part of the quadrangle. Unit also locally includes fine-grained tan to salmon-pink syenite intrusive rocks. Tuffs consist of poorly sorted medium- to coarse-grained volcanic rock fragments, crystals of plagioclase and clinopyroxene, opaque minerals, and pumice; interstitial prehnite and calcite is abundant. Tuffs contain abundant glass in the groundmass and in the clasts suggesting that quenching occurred. Some tuffs also include lithic clasts of pink syenite. Flows are generally vesicular and highly altered. A typical shoshonite flow has 48 to 50 percent $SiO_2$ and contains 2 percent clinopyroxene and plagioclase phenocrysts in a groundmass of fine-grained equigranular plagioclase laths, magnetite, ilmenite, and intersertal chlorite and calcite, and minor brown biotite and apatite. Some samples have olivine(?) pseudomorphs. Calcite and the pale-green microcrystalline chlorite occur primarily in interstices, where they appear to replace glass. Shoshonitic andesite flows consist of 15 to 25 percent zoned phenocrysts of andesine or labradorite, clinopyroxene, opaque minerals, and biotite in a groundmass of aligned plagioclase microlites, opaque oxides, chlorite, calcite, and dark devitrified glass. Apatite, prehnite and pumpellyite, and interstitial potassium feldspar occur locally. The more felsic shoshonitic andesites (as much as 59.6 percent $SiO_2$, table 6) have green-blue altered amphibole and interstitial quartz. Diabase is compositionally similar to the shoshonite flows and consists of even-textured plagioclase and clinopyroxene, biotite, interstitial calcite, apatite, and opaque minerals. The presence of biotite in the groundmass of the mafic rocks distinguishes this unit from the basalts and diabases of unit MzPzb. Conglomerate is composed of well-rounded cobbles of dark-reddish and greenish shoshonitic andesite porphyry in a dark tuffaceous matrix. Tan to salmon-pink syenite has 5 to 15 percent coarse-grained phenocrysts of Carlsbad-

twinned potassium feldspar in a groundmass of interlocking potassium feldspar, interstitial quartz, chlorite, biotite, and disseminated oxides, sphene, and apatite.

Unit unconformably underlies the volcaniclastic graywacke and turbidites (Kg) unit. It is assigned an Early Cretaceous (Barremian or Aptian) age on the basis of K-Ar age determinations of 117±3.5 and 118±3.5 Ma (table 1) obtained from biotite mineral separates from a shoshonitic andesite flow on a ridge west of the upper Yellow River and a shoshonitic andesite boulder in a cutbank on the Yellow River near south margin of quadrangle

Kv **Andesitic volcaniclastic rocks (Early Cretaceous)**—Dark-greenish-gray crystal and lithic tuff, fine cherty tuff, tuff breccia, and volcanic sandstone and conglomerate. Tuffs generally are present in cyclically repeated sequences that grade upward from coarse tuff breccia and lapilli tuff to very fine-grained cherty tuff and rare blue-green radiolarian chert. Tuffs are composed chiefly of fine-grained dark-red and green basalt and andesite clasts, plagioclase crystals, and mafic minerals in an altered matrix of devitrified glass. In upper part of unit, tuffs commonly are highly calcareous and locally contain abundant shelly debris, including *Buchia*. Tuffs grade into volcanic sandstone and conglomerate that are composed mostly of red and green basalt and andesite clasts and plagioclase crystals, but are better sorted than tuffs and have less matrix. Locally, tuffs contain felsic plutonic clasts derived from the underlying trondhjemite and tonalite (Jt) unit and less commonly clasts from the altered basalt and diabase (MzPzb) unit. Some basalt and andesite flows are present in unit in southern part of quadrangle.

In the Unalakleet quadrangle andesitic volcaniclastic rocks (Kv) unit is assigned an Early Cretaceous (Valanginian) age. It conformably underlies the shoshonitic flows and tuffs (Kft) unit and unconformably overlies the trondhjemite and tonalite (Jt) unit and the altered basalt and diabase (MzPzb) unit. Poorly preserved specimens of *Buchia* and brachiopods were found at several localities and a well-preserved specimen of *Buchia sublaevis* Keyserling of Valanginian age (Elder and Miller, 1991) was collected in the north-central part of the quadrangle east of the Chiroskey River. Radiolarians of possible Early Cretaceous (Valanginian) age (D.L. Jones, B. Murchey, and C.D. Blome, written commun., 1981) were found in chert along drainage divide between the Chiroskey and Anvik Rivers

Jt **Trondhjemite and tonalite (Late and Middle Jurassic)**—Trondhjemite, tonalite, and subordinate quartz diorite, diorite, and gabbro form a long narrow pluton extending from the Unalakleet River valley southward across the quadrangle and into the adjoining Holy Cross quadrangle (Béla Csejtey, Jr., written commun., 1992). The pluton is bordered over much of its length by the Chiroskey Fault Zone and is offset right laterally 17 to 30 km by the Anvik Fault. North of the Anvik Fault much of western part of the pluton has been metasomatized by K-rich fluids to pink granite and granodiorite. The presence of more abundant mafic rocks and the decrease in abundance of K-metasomatized rocks south of the fault suggests that the southern segment may expose deeper parts of the pluton. The pluton is cataclastically deformed locally in both the northern and southern segments. Moderately deformed rocks are granulated along thin (<1mm) bands or along grain boundaries and contain kink-banded or bent biotite. Some quartz grains show undulose extinction. In places, rocks are highly deformed and completely brecciated. Much of the pluton consists of lightly to moderately sericitized plagioclase that has more altered calcic cores. Biotite commonly is partly altered to chlorite. More mafic parts of the pluton have prehnite in veins and cavities. Most of the potassium feldspar is secondary and occurs as rims on plagioclase, in patches, or along veins replacing plagioclase. Trondhjemite consists of 50 to 60 percent plagioclase, 25 to 45 percent quartz, 4 to 8 percent mafic minerals (chiefly biotite and subordinate amphibole), and trace amounts of opaque oxides, potassium feldspar, and zircon. Tonalite has 50 to 55 percent plagioclase, about 20 percent quartz, 5 to 10 percent biotite, 15 to 25 percent amphibole, and trace amounts of sphene, epidote and apatite. Diorite and gabbro have as much as 30 percent mafic minerals, usually amphibole cored by minor clinopyroxene.

The faulted contact between this unit and the altered basalt and diabase (MzPzb) unit is locally marked by quartz-rich mylonite composed of bands of microcrystalline quartz, that have a high degree of preferred orientation. The bands are separated by very fine grained mica and locally by porphyroclasts of undulose quartz. Unit is unconformably overlain by the andesitic volcaniclastic rocks (Kv) unit, which contains clasts derived from the trondhjemite and tonalite (Jt) unit.

Unit is assigned a Middle and Late Jurassic age on the basis of five K-Ar age

determinations: 154±6 Ma on biotite from a trondhjemite, 166±7 and 173±9 Ma on biotite and hornblende from a tonalite, 148±4.4 Ma on hornblende from a tonalite, and 130±3.9 Ma on hornblende from a tonalite (table 1). The youngest age determination of 130 Ma suggests that part of the pluton may be as young as Early Cretaceous or that the isotopic age represents resetting by a younger thermal event

Ju **Ultramafic-mafic complexes (Late and Middle Jurassic)**—Chiefly dark greenish-black serpentinite and serpentinized pyroxenite, peridotite, and dunite. Gabbro is locally present in subordinate amounts. Ultramafic-mafic complexes typically form smooth dun-colored hills of small outcrops and rubble in the south-central part of the quadrangle. Some areas mapped as unit Ju locally contain sheared tonalite-trondhjemite belonging to unit Jt that are too small to be shown at this map scale. Ultramafic-mafic complexes are locally intruded by felsic dikes of unit TKr. Serpentinite consists of serpentine and less than 1 percent magnetite. Pyroxenite consists of serpentinized olivine and clinopyroxene; dunite has serpentine pseudomorphs after olivine. Gabbro, which is locally layered, has 10 to 25 percent olivine, 35 to 65 percent plagioclase, and 30 to 35 percent clinopyroxene, minor serpentine veinlets, Cr-spinel, and brown and green amphibole. Some rocks in this unit contain strained olivine or plagioclase, and grain boundaries are granulated as in the trondhjemite and tonalite (Jt) unit. Ultramafic-mafic complexes are spatially associated with unit Jt and are presumed to represent parts of a dismembered ophiolite that formed the base of the Koyukuk terrane volcanic arc.

Unit is provisionally assigned a Middle and Late Jurassic age because of its association with the trondhjemite and tonalite (Jt) unit and its tentative correlation with the ophiolites of the Kanuti thrust panel exposed along the southeast margin of the Yukon-Koyukuk basin. The Kanuti ophiolites were first assigned to the Angayucham terrane by Patton and Box (1989), but Patton (1993) suggested that they actually are part of the Koyukuk terrane

Angayucham(?) terrane

The Angayucham terrane is an assemblage of Devonian to Jurassic oceanic and oceanic-continent transition-zone rocks that are exposed around the rim of the Yukon-Koyukuk basin and dip inward beneath the basin (Patton and Box, 1989). In the Unalakleet quadrangle, rocks of similar composition and of probable oceanic affinities are exposed along the Anvik-Chiroskey high, an upfaulted block within the basin that extends north across the central part of the quadrangle from the south border to the Unalakleet River valley (fig. 1). These rocks are described below as the altered basalt and diabase (MzPzb) unit, and are assigned to the Angayucham (?) terrane.

MzPzb **Altered basalt and diabase (Mesozoic? and Paleozoic?)**—Variably altered and metamorphosed dark-green to gray basalt and diabase. Thin sections of less altered samples of the altered basalt and diabase unit show these rocks to be composed almost entirely of weakly twinned plagioclase laths subophitically enclosed by clinopyroxene, abundant disseminated oxides, and minor interstitial quartz. Clinopyroxene has been partly to totally replaced by pale-green fibrous amphibole ± sphene. The most highly metamorphosed rocks consist of fine-grained intergrown amphibole and plagioclase, and subordinate sphene, epidote, and disseminated opaque oxides. Many rocks have subordinate chlorite and pumpellyite and some contain clots of green chlorite and opaque oxides rimmed by fibrous actinolite. Unit is locally sheared and granulated and commonly cut by abundant prehnite veins and subordinate carbonate, chlorite, and quartz veins. Unit also contains subordinate chert, metachert, cherty tuff, mylonite, and limestone. Metachert is composed of recrystallized quartz, granular epidote, and prehnite. Mylonite is a very fine-grained laminated rock consisting of submillimeter foliation planes of microcrystalline quartz separated by bands of chlorite, muscovite, calcite, and magnetite. Highly strained quartz eyes that show undulatory extinction occur in the quartz-rich bands. Limestone is pink and consists of microcrystalline carbonate, minor volcanic lithic fragments and chert, and prehnite-filled veinlets.

Unit is assigned a late Paleozoic(?) and early Mesozoic(?) age. Although no diagnostic fossils have been found in the Unalakleet quadrangle, a similar assemblage of rocks in the Holy Cross and Russian Mission quadrangles to the south has produced conodont, radiolarian, coral, and molluscan faunas of Carboniferous, Permian, and Triassic ages (Patton and others, unpublished maps, 1992)

## GEOLOGIC SETTING

### YUKON-KOYUKUK BASIN

The Yukon-Koyukuk basin of western Alaska is a broad mid- and Late Cretaceous depression filled with terrigenous sedimentary rocks. In the Unalakleet

quadrangle, as elsewhere in the basin, the sedimentary fill is distributed in two vaguely defined subbasins, the Lower Yukon and the Kobuk-Koyukuk subbasins (Patton and Box, 1989). The Lower Yukon subbasin is located in the western part of the quadrangle and the Kobuk-Koyukuk subbasin in the eastern part. They are separated by the Anvik-Chiroskey high, a broad north-trending belt of older rocks that extends across the center of the quadrangle from the south border to the Kaltag Fault (fig. 1). North of the fault, the

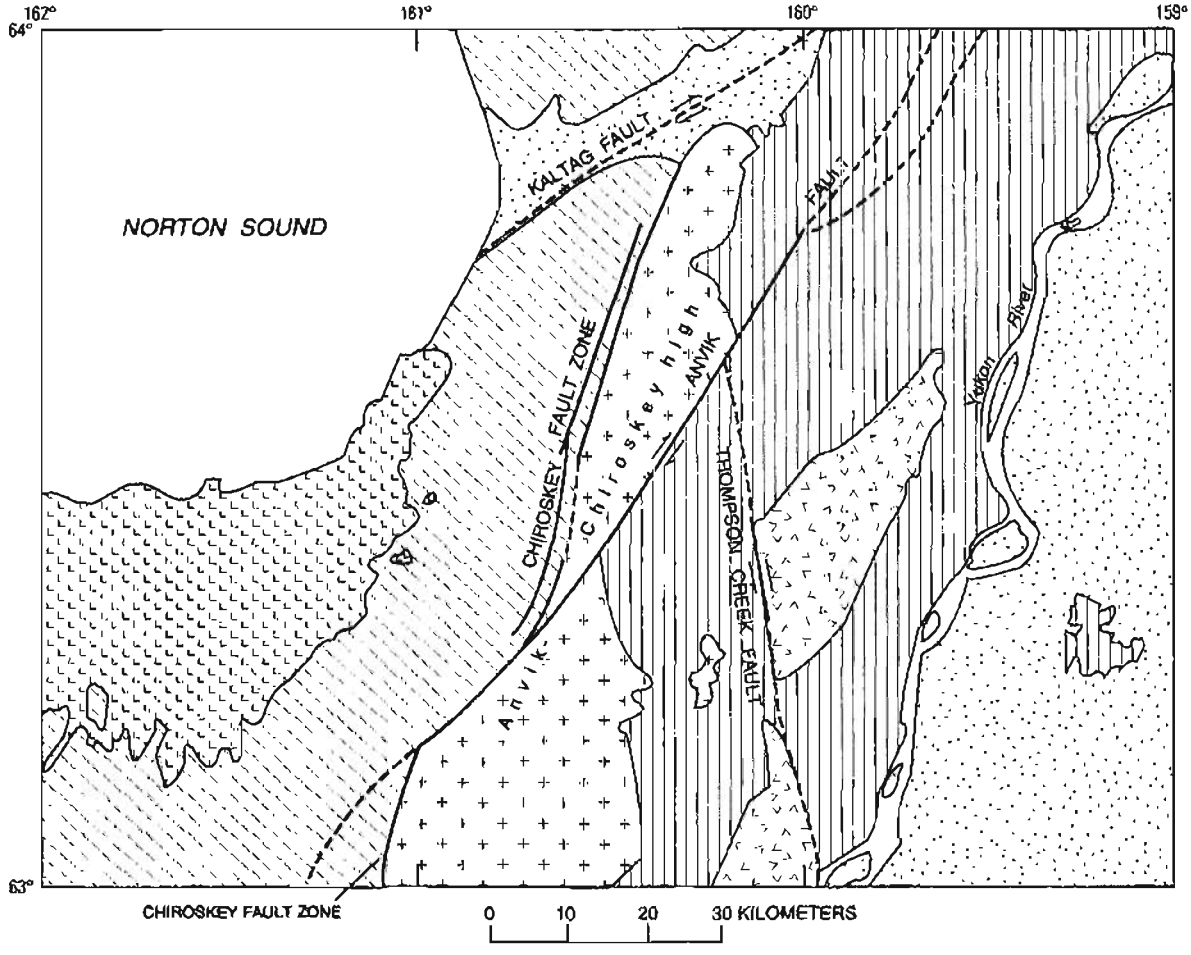


## EXPLANATION

Overlap assemblages

- Surficial deposits (Quaternary)
- St. Michael volcanic field (Quaternary and late Tertiary)
- Blackburn Hills volcanic field (early Tertiary and Late Cretaceous)
- Yukon-Koyukuk basin sedimentary deposits (Late and Early Cretaceous)
  - Lower Yukon subbasin
  - Kobuk-Koyukuk subbasin

Lithotectonic terranes

- Koyukuk terrane (Early Cretaceous and Late and Middle Jurassic) and Angayucham(?) terrane (Mesozoic? and Paleozoic?)
- Contact
- Fault, dashed where inferred. Arrows indicate direction of relative movement

**Figure 1.** Unalakleet quadrangle, west-central Alaska, showing major geologic features.

two subbbasins are dextrally offset about 100 km (Patton and Box, 1989). All of the basin sedimentary rocks in the Unalakleet quadrangle north of the Kaltag Fault belong in the Lower Yukon subbasin.

The sedimentary rocks in both subbasins are composed of a lower section of submarine-fan turbidites and an upper section of shallow-water and subaerial deltaic deposits. The aggregate thickness of this sedimentary fill in the Lower Yukon subbasin is uncertain, but sparse data from the adjoining Norton Bay and Nulato quadrangles to the north indicate that it may be as much as 10,000 m (Patton and Box, 1989). The thickness of the fill in the Kobuk-Koyukuk subbasin is also uncertain, but reconnaissance aeromagnetic data suggest that it is substantially less than in the Lower Yukon subbasin (Texas Instrument, Inc. 1976).

### ANVIK-CHIROSKEY HIGH

The Anvik-Chiroskey high exposes two lithotectonic terranes, the Koyukuk and Angayucham(?) terranes, which were assembled by Early Cretaceous time and subsequently overlapped by the mid- and Late Cretaceous terrigenous sedimentary rocks of the Yukon-Koyukuk basin (fig. 1). The Koyukuk terrane is composed of two Early Cretaceous volcanic rock units, shoshonitic flows and tuffs (Kft) and andesitic volcaniclastic rocks (Kv), and two Middle and Late Jurassic plutonic rock units, trondjhemite and tonalite (Jt) and ultramafic-mafic complexes (Ju). The two volcanic rock units and the trondhjemite and tonalite unit have the chemical characteristics of subduction-related magmatic rocks (Box and Patton, 1989). The ultramafic-mafic complexes represent a disrupted ophiolite assemblage. The volcanic rock units are separated from the plutonic rock units by a regional unconformity, but detrital clasts from the trondjhemite and tonallte unit have been incorporated in the overlying andesitic volcaniclastic rocks unit showing that these two units were linked together no later than Early Cretaceous (Valanginian). The altered basalt and diabase (MzPzb) unit, which is in fault contact with the Koyukuk terrane on the Anvik-Chiroskey high, is questionably correlated with the Devonian to Jurassic oceanic rocks of the Angayucham terrane that rim the Yukon-Koyukuk basin (Patton and Box, 1989). The altered basalt and diabase (MzPzb) unit shows strong oceanic geochemical affinities with and is chemically similar to basalt and diabase of the Angayucham terrane described elswhere in western Alaska by Pallister and others (1989) and Box and Patton (1989).

## STRUCTURE

All of the pre-latest Cretaceous rocks in the quadrangle, including the sedimentary deposits of the Yukon-Koyukuk basin, are strongly folded and broken by a complex pattern of closely spaced high-angle faults (map sheet, sections *A-A'*, *B-B'*). Only a few of the larger faults are shown on the map and cross sections. The folds and faults have a north to northeast orientation that appears to be related to an east-west compressional event which sharply constricted the Yukon-Koyukuk basin in Late Cretaceous (Campanian and Maastrichtian) time (Patton and Box, 1989). As indicated diagrammatically on the cross sections, there is a general increase in the degree of deformation with increasing age of the map units. The oldest map units, the trondhjemite and tonalite (Jt), ultramafic-mafic complexes (Ju), and altered basalt and diabase (MzPzb), are highly deformed and have undergone local mylonitization and cataclasis. All three of these units have been metamorphosed to the prehnite-pumpellyite facies. By contrast, the early Tertiary Blackburn Hills volcanic field and the latest Cretaceous and early Tertiary volcanic and intrusive bodies are characterized by broad open folds and mild geochemical alteration. The late Tertiary and Quaternary volcanic rocks of the St. Michael volcanic field are essentially flat lying and unaltered. The younger basalt flows of the St. Michael volcanic field in units Qyt and Qya preserve fresh unmodified eruptive features such as cinder cones and pahoehoe flow surfaces (fig. 2).

### KALTAG, ANVIK, AND THOMPSON CREEK STRIKE-SLIP FAULTS

The Kaltag Fault is a well-documented strike-slip fault that has been traced for more than 400 km from central Alaska to the shore of Norton Sound (Patton and Hoare, 1968). A short segment of this fault crosses the Unalakleet quadrangle along the Unalakleet River, where it is faintly visible in the surficial deposits on the south side of the valley (fig. 1). The trace of the fault becomes more obvious along the upper reaches of the Unalakleet River and across the drainage divide to the Yukon River in the adjoining Norton Bay quadrangle (Patton and Hoare, 1968). Right-lateral offset along this segment of the fault is estimated to be about 100 km (Patton and Tailleur, 1977).

The Anvik Fault is a splay of the Kaltag Fault that extends diagonally across the quadrangle from northeast to southwest. It is best exposed where it cuts across the Anvik-Chiroskey high in the central part of the quadrangle and offsets the map units of the Koyukuk and Angayucham(?) terranes right laterally as much as 35 km. The Anvik Fault merges with the Kaltag Fault to the northeast in the adjoining Norton Bay quadrangle near the Kaltag Portage. South of the Unalakleet quadrangle, the trace of the fault becomes less distinct and the strike-slip displacement appears to be distributed among several parallel faults. Along the southwestward projection of the Anvik Fault in the adjoining Kwiguk quadrangle, Hoare and Condon (1966) mapped a broad array of southwest-trending faults, many of which show right lateral-offsets of as much as 5 km.

The Thompson Creek Fault is part of the Anlak-Thompson Creek Fault system, which, according to Beikman (1980), can be traced from the Unalakleet quadrangle south for about 350 km to the Holitna Fault in southwestern Alaska. In the Unalakleet quadrangle, the Thompson Creek Fault offsets the Blackburn Hills volcanic field about 25 km left lat-

erally. The trace of the fault is most evident where it cuts across the Blackburn Syncline (map sheet, section A-A'). North of the Blackburn Syncline, the Thompson Creek Fault is inferred to extend as far as the Anvik Fault. An unnamed north-trending fault present along the Old Woman River may represent the offset continuation of the Thompson Creek Fault on the northwest side of the Anvik Fault.

### CHIROSKEY FAULT ZONE

The Chiroskey Fault Zone is composed of high-angle normal faults that border the west side of the Anvik-Chiroskey structural high (fig. 1). North of the Anvik Fault, the Chiroskey Fault Zone consists of two parallel normal faults separated by a narrow down-dropped block of Cretaceous sandstone, shale, and conglomerate deltaic deposits (Ks) (map sheet, section A-A'). South of the Anvik Fault, the Chiroskey Fault Zone is dextrally offset about 17 km and appears to be confined to a single fault bordering the west side of the Anvik-Chiroskey structural high. Another topographically prominent vertical fault, previously considered to be the part of the Chiroskey Fault Zone by Beikman (1980), bounds the lowlands on the west side of the Anvik River south of the Anvik Fault.

## GEOCHEMICAL CHARACTERISTICS OF VOLCANIC AND PLUTONIC ROCK UNITS

The rocks exposed in the Unalakleet quadrangle record a long and complex magmatic history starting in the Paleozoic(?) and continuing into the Quaternary. Samples from all the magmatic units were analyzed for major and trace-element composition (tables 2-8); their composition and tectonic affinities are discussed below. Many of the map units, especially in the lithotectonic terranes, were distinguished from each other on the basis of major- and trace-element compositions; the distinguishing characteristics of these units are summarized in table 9.

Nomenclature used in this paper generally follows that of Streckeisen (1979), Gill (1981), and Morrison (1980). Major oxides are normalized to 100 percent dry weight (without water and $CO_2$) before classification and plotting. On an anhydrous basis, basalts have less than 53 percent $SiO_2$, andesites have 53 to 63 percent $SiO_2$, dacites have 63 to 70 percent $SiO_2$, and rhyolites have more than 70 percent $SiO_2$. $Fe_2O_3/FeO$ was set to 0.15 for the late Cenozoic basalts in order to calculate normative mineralogies. The late Cenozoic rocks of the St. Michael volcanic field (Qyt, Qya, QTb) are classified as follows: Basalt

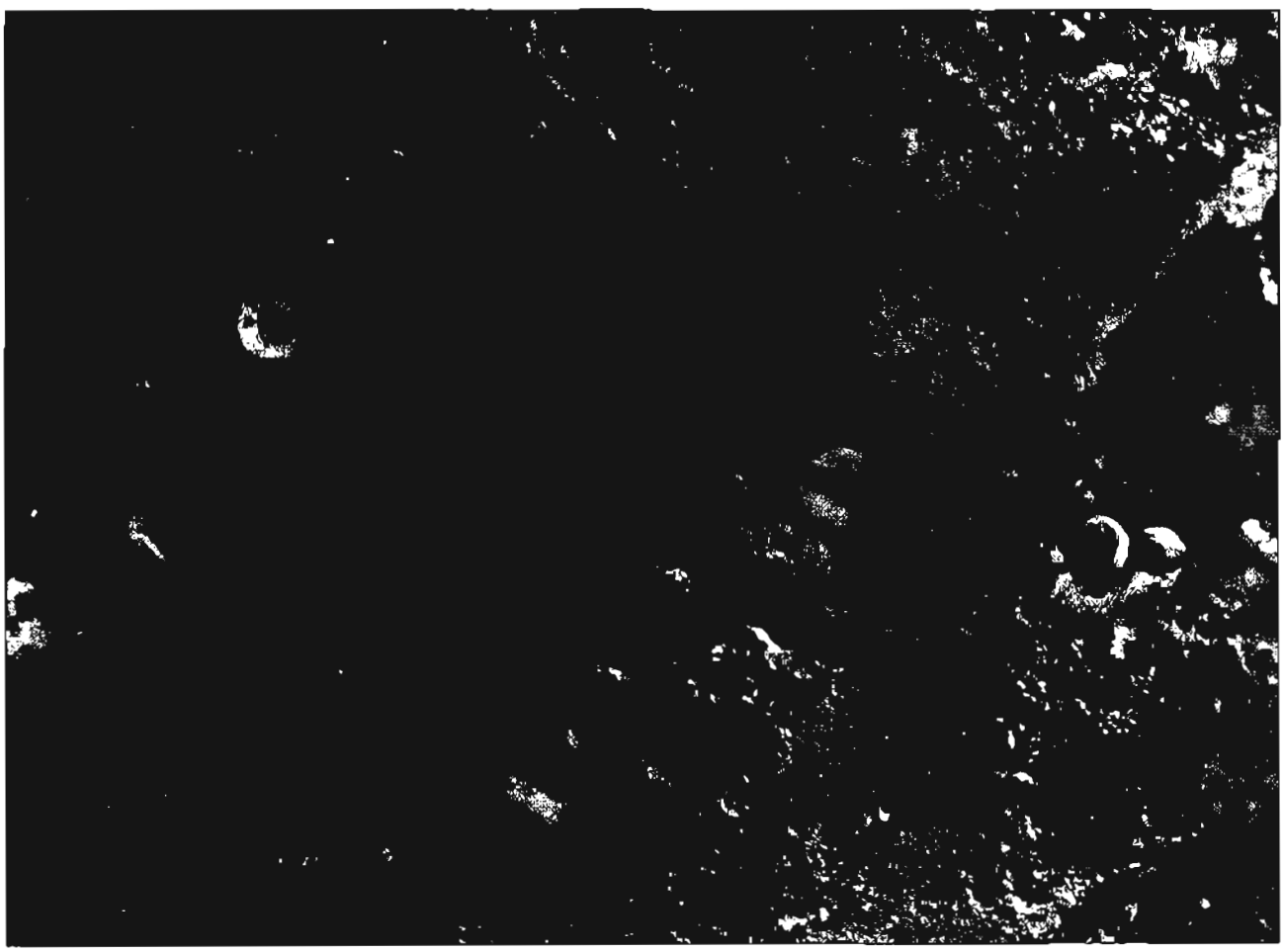

**Figure 2.** Aerial view of Pleistocene younger alkalic basalt flows and cones (Qya) unit at the Sisters in St. Michael volcanic field, Unalakleet quadrangle, west-central Alaska. Top is north. Width of photograph is about 6.5 km.

having normative nepheline is called alkali basalt or alkali olivine basalt if it contains more than 10 percent normative olivine. Basalt having normative hypersthene is called tholeiite or olivine tholeiite if it contains more than 10 percent normative olivine. Basanites have 10 to 20 percent normative nepheline; nephelinites have more than 20 percent normative nepheline. Hawaiites have more than 5 percent total alkalis ($Na_2O$ + $K_2O$) and less than 5 percent MgO. The Late Cretaceous and early Tertiary volcanic and plutonic rocks (Ta, Tg, Thr, Td, Tt, TKr, TKs, TKa, TKu) are classified using the Peacock index and are divided into low-, moderate-, or high-K types following Gill (1981) or shoshonitic following Morrison (1980).

## LATE CENOZOIC

### St. Michael volcanic field (Qyt, Qya, QTb)

The St. Michael volcanic field is one of a number of late Tertiary and Quaternary alkalic to subalkalic basalt fields along the west margin of Alaska and on islands in the Bering Sea that collectively are referred to as the Bering Sea basalt province (Moll-Stalcup, 1994). The province is characterized by broad fields of tholeiitic and alkaline olivine basalt flows and subordinate small cones, short flows, and ash of more alkalic basanite and nephelinite compositions (tables 2 and 3). The fields are compositionally similar to magmas erupted on oceanic islands like the Hawaiian Islands, but are generally more alkalic. These basaltic and ultrabasic rocks have small positive Nb and Ta anomalies relative to the light rare-earth elements (LREE) on multi-element spidergrams (fig. 3) that are complementary to the negative anomalies that characterize modern arcs (Hawkesworth and others, 1993). Rocks of the Bering Sea basalt province are distinct from Late Cretaceous and early Tertiary volcanic rocks in western Alaska because the former are generally more mafic, lack a negative Nb-Ta anomaly, and are tholeiitic, alkalic, or highly alkalic rather than having calc-alkalic to mildly alkalic compositions. Bering Sea basalts also can be distinguished from the Late Cretaceous and early Tertiary volcanic rocks in western Alaska on the basis of Nb/La ratios (fig. 4).

The St. Michael volcanic field in the southwestern part of the Unalakleet quadrangle consists of tholeiitic and alkali olivine basalts flows and subordinate amounts of more alkalic rocks including basanite and hawaiite. Total alkalis decrease with increasing $SiO_2$ content from nephelinite through tholeiite, similar to other volcanic fields in the Bering Sea basalt province and to unfractionated Hawaiian basalts (fig. 5). The alkalic-tholeiitic transition occurs at lower total alkalis than the transition in Hawaii because the rocks have higher MgO contents than most Hawaiian basalts. Trends of decreasing alkalis with increasing $SiO_2$ are thought to be indicative of an origin by varying degrees of partial melting of a mantle source (Frey and Clague, 1983). Small amounts of partial melting produces the highly alkalic nephelinites; increasingly large amounts of partial melting produces progressively less alkalic rocks. Moll-Stalcup (1994) made estimates of the degree of partial melting of Bering Sea basalts based on estimated concentrations of incompatible elements in the mantle. Since these estimates were made there has been increasing evidence that incompatible elements are enriched in the mantle source of ocean island-type basalts during metasomatism, prior to their formation, and therefore concentrations of incompatible elements in their mantle source are neither homogeneous nor typical of the mantle

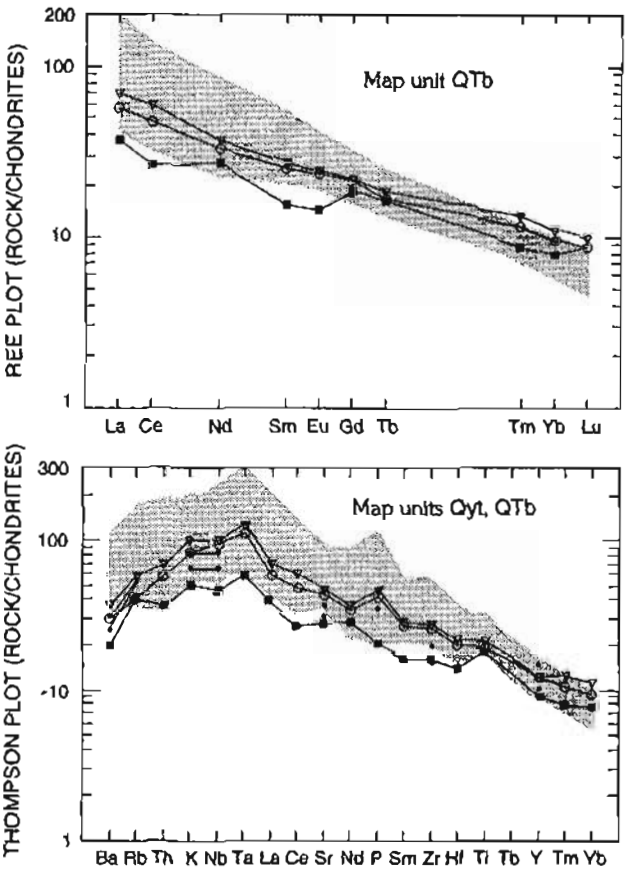


**Figure 3.** Rare-earth-element (REE) plot and spidergram for selected samples from St. Michael volcanic field, west-central Alaska. Although volcanic field consists of wide range of compositions from basanite and nephelinite to tholeiite, all three samples analyzed for REE were tholeiitic, from unit QTb. In basaltic volcanic fields like St. Michael volcanic field, concentrations of alkali elements and light-rare-earth elements (LREE) increase with alkalinity. Tholeiites tend to have lowest LREE contents, alkali basalts have higher LREE contents, and nephelinites have high LREE contents. A more complete data set showing entire range of compositions is shown as shaded field for Kookooligit volcanic field on St. Lawrence Island (Moll-Stalcup, unpub. data, 1994). Data in spidergram normalized to values given in Thompson and others (1984). Diagrams generated using program of Wheately and Rock (1988). See Description of Map Units for explanation of map-unit symbols.

in general. Recent models for the origin of ocean island basalt-type (OIB-type) magmas like those found in the St. Michael volcanic field suggest that they originate in residual oceanic lithosphere that was previously recycled into the mantle along a subduction zone (Weaver, 1991). This recycled lithosphere contains the Nb-Ta enriched residue left behind in the slab when other large-ion lithophile elements are transferred to the mantle wedge during subduction zone processes. Limited trace-element data on the St. Michael volcanic field suggest that the rocks are chemically similar to high μ(HIMU[1])-dominated OIB-type magmas in many respects. The volcanic field rocks have positive Nb and Ta anomalies on spiderplots, low La/Nb (0.66), and low Th/Nb (0.08); in contrast to typical HIMU-type lavas, they have slightly higher Ba/Nb (6.4-8.3), Rb/Nb (0.42-0.88), K/Nb (289-360), and Ba/La (11.1-11.7) and do not have elevated Pb isotope ratios. Data for the volcanic field plot along a mixing line between HIMU and continental crust (fig. 6). The data suggest that most Bering Sea basalts formed in a HIMU-type mantle, but have incorporated a small amount of continental crust that added Ba, Rb, and K to the system. The continental crust may have been added to the source of the magmas in the form of subducted sedimentary deposits (less than 3 percent) in their mantle source or the magmas may have been contaminated by continental crust near the surface. In the vicinity of the St. Michael volcanic field, the pre-mid-Cretaceous crust consists entirely of Paleozoic(?) and Mesozoic oceanic and island arc terranes, and evidence for old cratonal rocks is lacking. Weaver (1991) argues on the basis of isotopic data that the recycled lithosphere must be ancient, but ancient lithosphere is not required by the limited Bering Sea basalt data because they have Nd, Sr, and Pb isotope ratios that vary only slightly from that of mid-ocean-ridge basalts (MORB) (Moll-Stalcup, 1994). There is some evidence from Sr isotope data from Bering Sea basalt on Nunivak Island that the more alkalic rocks have more radiogenic Sr than the less alkalic rocks, but the differences are small (basanite, 0.70286; less alkalic basalt, 0.70311; Mark, 1971). This isotopic contrast led Menzies and Murthy (1980) to conclude that the source of Nunivak basalts was metasomatized by an alkali and rare-earth-element (REE)-rich component sometime within the last 200 m.y., because more time would have led to a greater isotopic contrast than that observed. The most likely source of the metasomatizing fluid is thought to be the earlier subduction episodes in the region, such as island arc magmatism during the Jurassic and Cretaceous or continental arc magmatism during the Late Cretaceous and early Tertiary.

[1]HIMU was first defined by Zindler and Hart (1986) as the mantle component that has very high $^{206}Pb/^{204}Pb$ ratios coupled with low $^{87}Sr/^{86}Sr$ and intermediate $^{143}Nd/^{144}Nd$ ratios. In order to generate such high $^{206}Pb/^{204}Pb$, the source must be enriched in U and Th relative to Pb and, therefore, have high μ ($^{238}U/^{204}Pb$).

Although the Bering Sea basalt province is located in a broad region behind the active Aleutian arc, the volcanic rocks are clearly not subduction-related nor do they have compositions that are typical of back-arc volcanoes. Many of the volcanic fields, including the St. Michael volcanic field, are associated with young faults and have clusters of cones that are aligned east-west, defining deep zones of magma intrusion. Studies of earthquake focal mechanisms (Nakumura and others, 1980) suggest that the area is undergoing north-south extension, which favors the formation of east-west-trending faults and facilitates the rise of mantle-formed magmas to the surface. Deep rift structures like these are common in oceanic islands (Carracedo, 1994).

## EARLY TERTIARY AND LATE CRETACEOUS

### Blackburn Hills volcanic field (Ta, Tg, Thr, Td, Tt)

### Small volcanic and intrusive bodies (TKr, TKs, TKa, TKu)

A vast Late Cretaceous and early Tertiary magmatic province extends from the Arctic Circle to Bristol

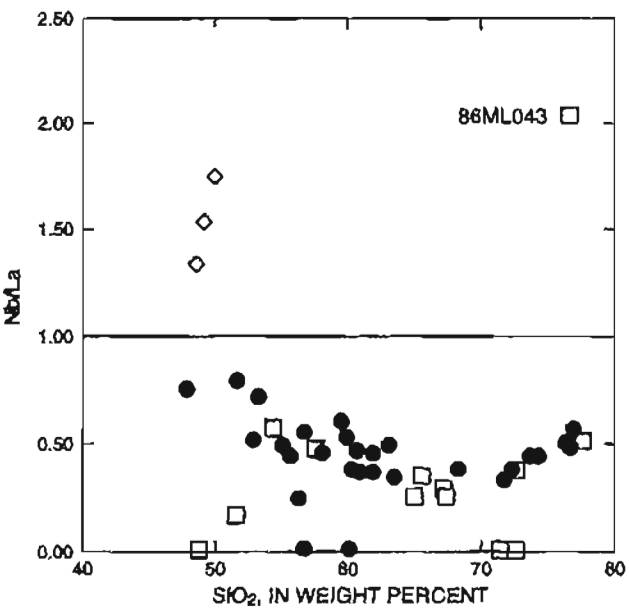


**Figure 4.** Plot of Nb/La compared with $SiO_2$ for Late Cretaceous and Cenozoic rocks of Unalakleet quadrangle, west-central Alaska. This plot can be used to distinguish volcanic rocks of the two age groups. Late Tertiary and Quaternary basaltic rocks of St. Michael volcanic field have higher Nb/La than nearly all Late Cretaceous and early Tertiary rocks, except for one sample of rhyolite (86ML043, table 5) from Runkels Creek. See Description of Map Units for explanation of map-unit symbols.

Bay and from the Alaska Range to the Bering Sea (Moll-Stalcup, 1994). Erosional remnants of this magmatic province are exposed throughout the Unalakleet quadrangle as volcanic fields and isolated cones, domes, dikes, and sills. Most of the rocks are calc-alkalic basalt, andesite, dacite, and rhyolite that range in age from 69.1 to 51.9 Ma. Magmatism is dominantly extrusive or shallow hypabyssal, but a small pluton is exposed in the Blackburn Hills. Approximately 50 samples of this magmatic suite were analyzed for major and trace elements. Most of the samples are from a large well-exposed volcanic field in the Blackburn Hills that was previously studied in considerable detail (Moll-Stalcup and Arth, 1991; Moll-Stalcup and Patton, 1992). Compositions of representative samples from this field are given in table 4. More than 1,500 m of andesite, rhyolite, and granite are exposed in the Blackburn Hills along the Blackburn Syncline west of the Yukon River. Samples were also analyzed from a number of isolated domes, intrusive bodies, and dikes and from two smaller volcanic fields exposed along the Innoko River and Runkels Creek (table 5).

Much of the Late Cretaceous and early Tertiary magmatic province consists of a compositionally coherent suite ranging from basalt and andesite to dacite and rhyolite (fig. 7). Chemical data for most of the rocks in the Unalakleet quadrangle plot within a narrow field defined by the Blackburn Hills data with some notable exceptions discussed below. The andesites, dacites, and rhyolites generally have negative Nb and Ta anomalies on spidergrams (figs. 8, 9, and 10),

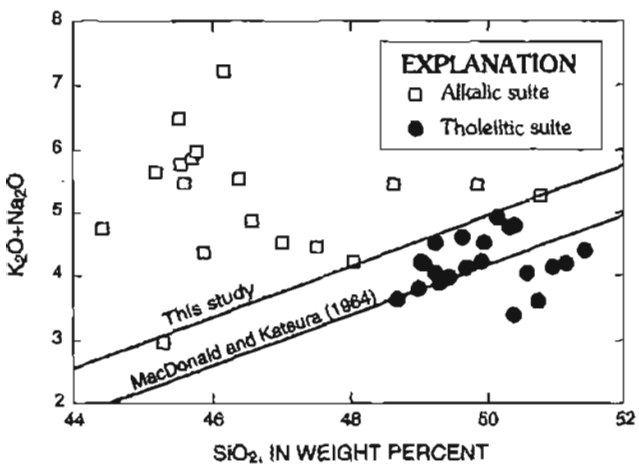


**Figure 5.** Plot of total alkali compared with $SiO_2$ for late Tertiary and Quaternary rocks (QTb, Qya, Qyt) of St. Michael volcanic field, west-central Alaska. The data show decreasing total alkalis with increasing $SiO_2$. The line dividing alkalic from subalkaline (tholeiitic) suites for St. Michael volcanic field (this study) divides rocks having normative nepheline (alkalic) from those having normative hypersthene (subalkaline or tholeiitic). The line below from MacDonald and Katsura (1964) divides Hawaiian rocks having modal hypersthene or pigeonite (subalkaline) from those lacking hypersthene or pigeonite (alkalic), even though normative hypersthene is present in some rocks that plot in the alkalic field. $Fe_2O_3/FeO$ was set to 0.15 for normative mineralogy calculations. See Description of Map Units for explanation of map-unit symbols.

typical of subduction-related magmatism. Mafic rocks with less than 53 percent $SiO_2$ (on an anhydrous basis) are much less common than intermediate or siliceous rocks. Most of the mafic rocks were erupted after 56 Ma and are restricted to the top of the stratigraphic section. They usually lack negative Nb and Ta anomalies and are mildly alkalic. Exceptions are the diabase intrusion (sample No. 86ML004, table 5) and the lamprophyre dike (sample No. 86Pa043, table 5), both of which have pronounced negative Nb and Ta anomalies (fig. 9). The lamprophyre dike is older than the other mafic rocks (64.4±1.9 Ma; table 1) and is strongly enriched in alkali, alkaline earth, and LREE elements. It also has lower FeO* and $TiO_2$, and slightly less MgO (fig. 7) than the rest of the Late Cretaceous and early Tertiary suite. The diabase intrusion is undated, but has higher $Al_2O_3$ and CaO and lower FeO* and $TiO_2$ than the other rocks (fig. 7). We are not entirely certain if this intrusion is part of the andesite and basalt (TKa) unit, because it was not dated, and its composition is different from most of the Late Cretaceous and early Tertiary volcanic rocks. The intrusion may be part of the surrounding andesitic volcaniclastic rocks (Kv) unit.

All of the high-silica rhyolites (more than 75 percent $SiO_2$) and some of the other rhyolites have unusual concentrations of certain trace elements. Barium concentrations drop at about 70 percent $SiO_2$ after increasing systematically from 48 to 68 percent $SiO_2$ (fig. 11). The decrease is most striking in the high-silica rhyolites and in rhyolite dikes. Sample 86ML043 has an unusual spidergram that shows LREE contents lower than normalized Nb or Ta contents,

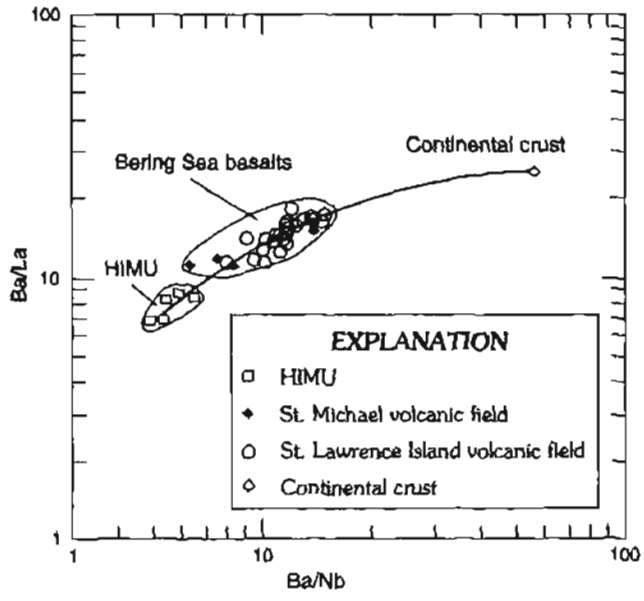


**Figure 6.** Plot of Ba/La compared with Ba/Nb for rocks from Bering Sea basalts including data from St. Lawrence Island (Moll-Stalcup, unpub. data, 1994) and St. Michael volcanic field (table 2). Also shown are fields for high-μ (HIMU) type basalts (see text for definition) from oceanic islands and for composition of continental crust from Weaver (1991).

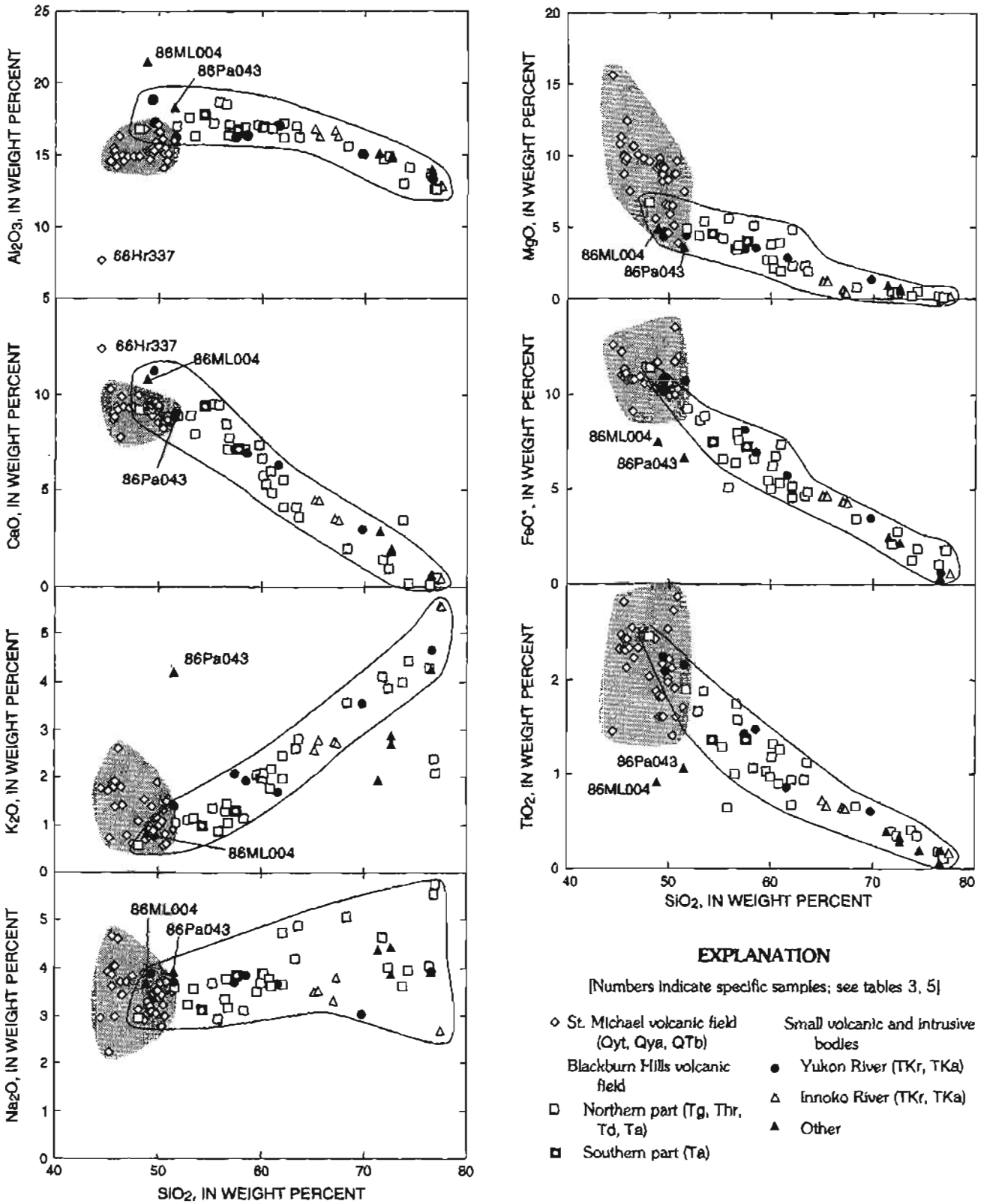


**Figure 7.** Plots of major-element oxides against $SiO_2$ for latest Cretaceous and Cenozoic volcanic rocks of Unalakleet quadrangle, west-central Alaska. All rocks, except those from St. Michael volcanic field, are part of the latest Cretaceous and early Tertiary magmatic province. Shaded area marks the field for most of the late Cenozoic basaltic rocks from St. Michael volcanic field. Outlined area marks the main trend for the Late Cretaceous and early Tertiary volcanic and plutonic rocks. See Description of Map Units for explanation of map-unit symbols.

opposite to that of most of the Late Cretaceous and early Tertiary rocks (fig. 9). Some of the rhyolites in the Blackburn Hills volcanic field are unusual in containing anorthoclase and Fe-rich hedenbergite phenocrysts and in having low $K_2O$ and high $Na_2O$ contents (Moll-Stalcup and Arth, 1991).

The Late Cretaceous and early Tertiary magmatic province was interpreted by Moll-Stalcup (1994) as the inland part of an unusually wide continental-margin arc formed in response to subduction of the Kula plate under the south margin of Alaska. The mildly alkalic basalts and sodic rhyolites that are exposed at the top of the stratigraphic section are believed to mark the end of the subduction-related magmatism and the transition to post-subduction tectonics.

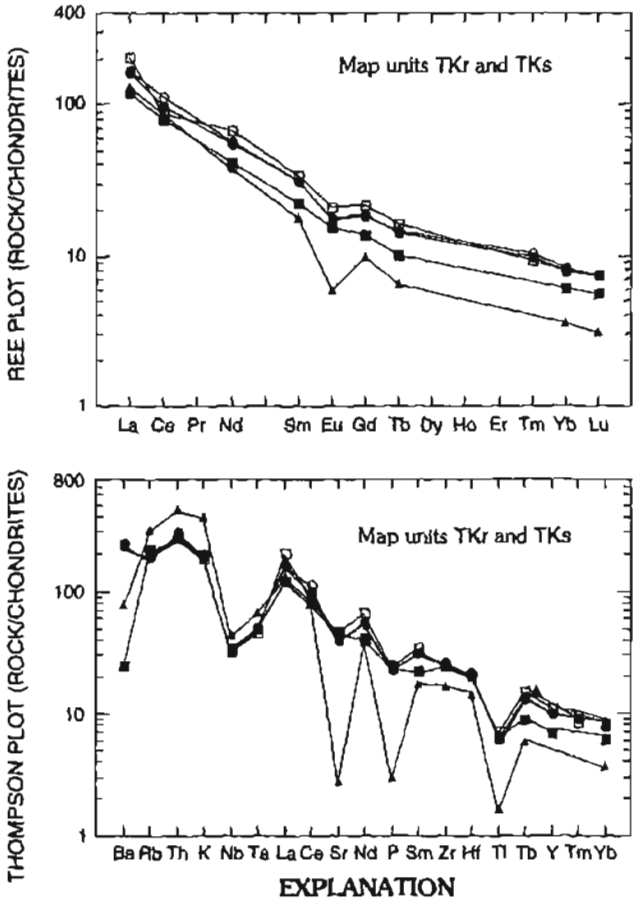


**Figure 8.** Rare-earth-element (REE) plot and spidergram for rhyolite and dacite samples (TKr, TKs) from banks of the Innoko River in southeast corner of Unalakleet quadrangle, west-central Alaska. Sample 86Pa100 is a high-silica rhyolite. Its highly evolved composition can be seen in deep spikes at Sr, P, and Ti. The other samples are dacites. Data in spidergram normalized to values given in Thompson and others (1984) and plotted using program of Wheately and Rock (1988). See Description of Map Units for explanation of map-unit symbols.

## EARLY CRETACEOUS AND LATE AND MIDDLE JURASSIC

### Koyukuk terrane

#### *Shoshonitic flows and tuffs (Kft)*

Shoshonitic volcanic rocks are exposed in the Yellow River drainage in the south-central part of the quadrangle. Unit Kft has a very distinctive chemical

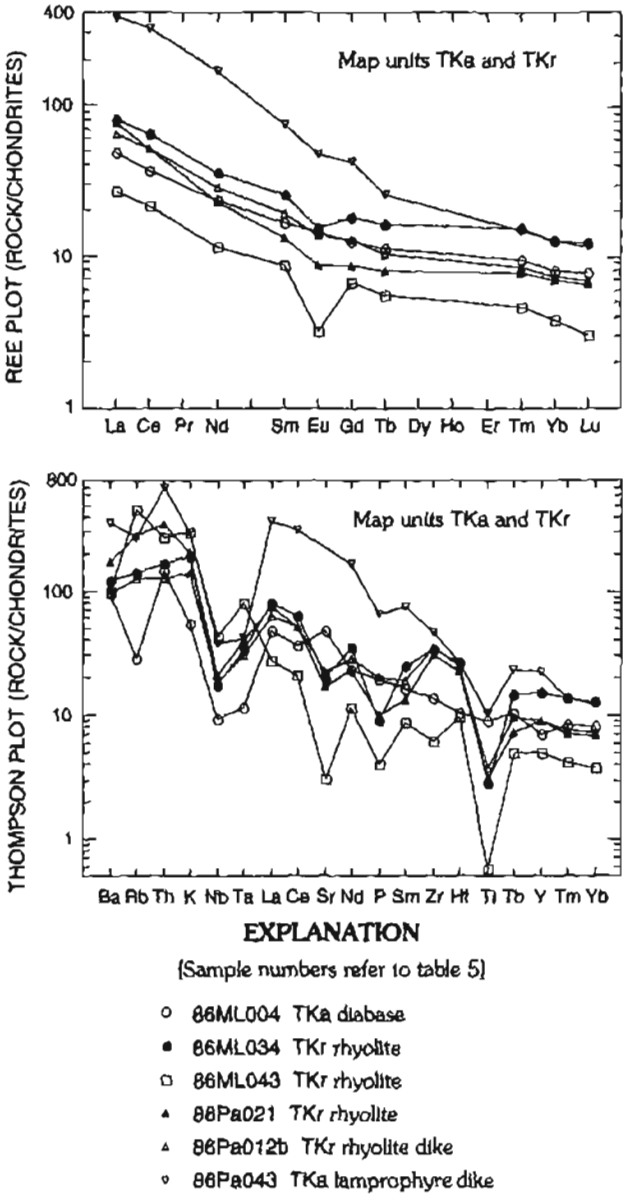


**Figure 9.** Rare-earth-element (REE) plot and spidergram for various volcanic rocks from units TKa and TKr in Unalakleet quadrangle, west-central Alaska. Most rocks are chemically similar to those in Blackburn Hills volcanic field (fig. 7). Sample 86Pa043 from a lamprophyre dike has extremely high light-rare-earth elements (LREE) and is highly enriched in incompatible elements. Sample 86ML043 from a rhyolite block in unconsolidated tuff has LREE lower than Nb and Ta. Data in spidergram normalized using values given in Thompson and others (1984) and plotted using program of Wheately and Rock (1988). See Description of Map Units for explanation of map-unit symbols.

composition and was first recognized on the basis of its extremely high $K_2O$, Rb, and Ba contents and low $TiO_2$ content (table 6). The rocks are termed shoshonitic rather than alkalic because they have $K_2O$ greater than $Na_2O$, low $TiO_2$, and are enriched in alkaline, alkaline-earth, and LREE elements relative to Nb and Ta, similar to subduction-related rocks (figs. 12 to 16) (Morrison, 1980; Gill and Whelan, 1989). Although Nb and Ta are depleted relative to other incompatible elements, the suite has high absolute abundance of all large-ion lithophile elements, including Nb and Ta (table 6 and fig. 16). This unit is easily identified on the basis of chemical composition because it has higher K, Rb, Ba, Th, Zr, and Nb contents than any other suite in the quadrangle (figs. 12B-16, tables 2-9). All of the rocks are LREE enriched (fig. 12A). Most of the samples have no Eu anomalies, but two samples with high-silica contents (62 to 63 percent) have moderately negative Eu anomalies, and two samples with moderate $SiO_2$ contents have small positive Eu anomalies (fig. 12A). Negative and positive Eu anomalies are probably the result, respectively, of fractionation and accumulation of plagioclase.

The age of the rocks and their composition indicate that they were generated at the end of subduction-related magmatism and represent the last eruptive products of the Koyukuk Arc. Earlier workers (Patton and Box, 1989) suggested that the Koyukuk Arc initially formed away from the continental margin of Alaska in an ocean-to-ocean subduction environment. As subduction progressed, the subducting oceanic crust was consumed, resulting in short-lived continental-margin subduction and eventually in arc-continent collision. The

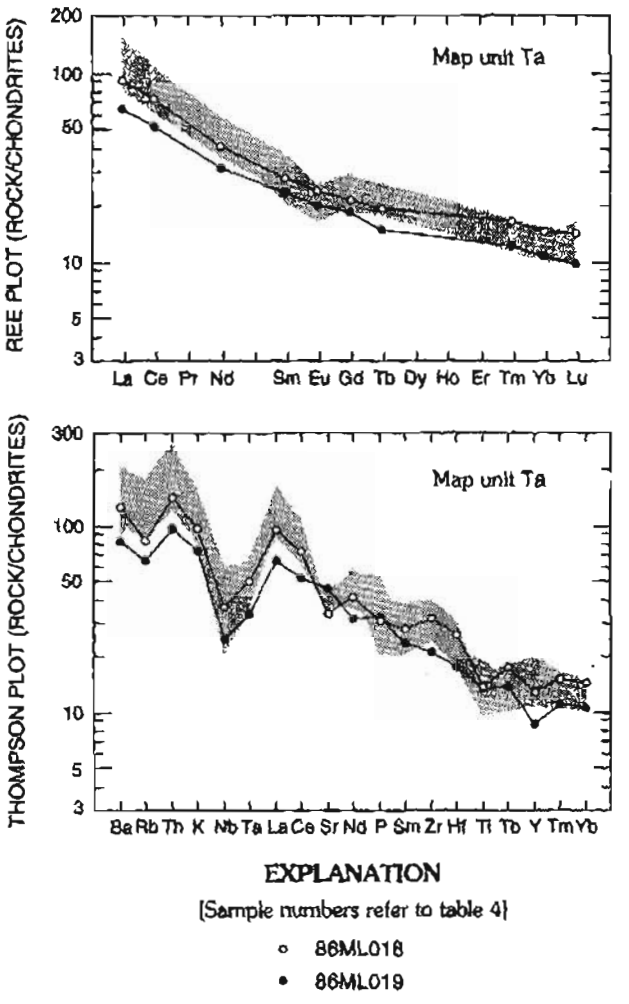


**Figure 10.** Rare-earth-element (REE) plot and spidergram of two samples from the southern part of Blackburn Hills volcanic field, Unalakleet quadrangle, west-central Alaska. This part of the volcanic field has been offset left laterally relative to the northern part of field. Shaded area is for andesites of group 1 from the northern part of the volcanic field (Moll-Stalcup and Arth, 1991). Data in spidergram normalized to values given in Thompson and others (1984) and plotted using program of Wheately and Rock (1988). See Description of Map Units for explanation of map-unit symbol.

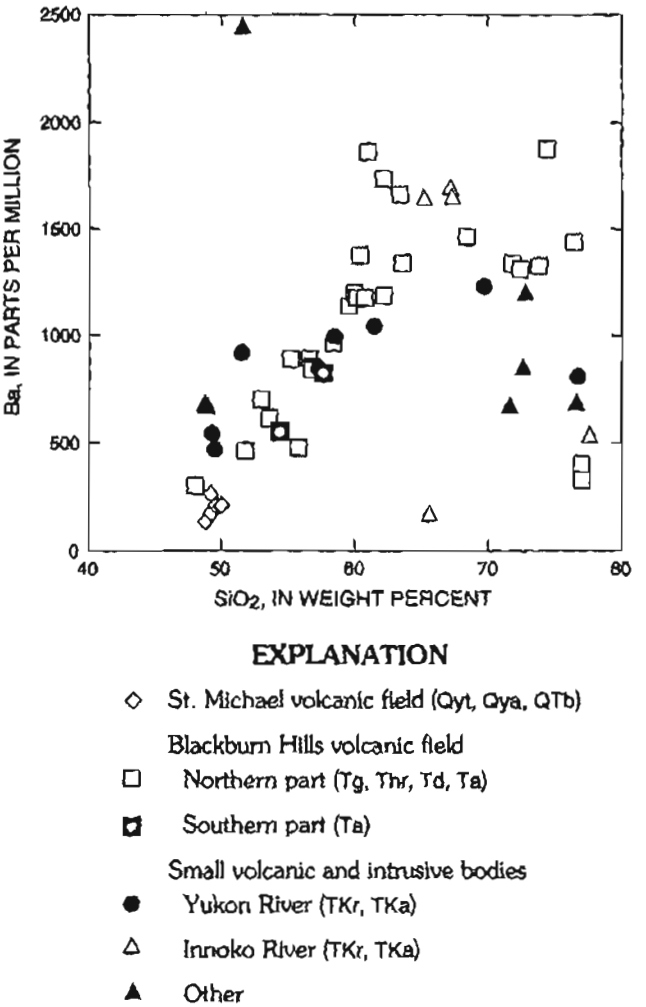


**Figure 11.** Barium compared with $SiO_2$ for Late Cretaceous and Cenozoic volcanic rocks from Unalakleet quadrangle, west-central Alaska. Most of the suite shows increasing Ba with increasing $SiO_2$, but most of the highly evolved rocks, which have more than 70 percent $SiO_2$, show a trend of declining Ba content with increasing $SiO_2$. These trends suggest that the highly evolved rocks are losing Ba, possibly to vapor phase transport. See Description of Map Units for explanation of map-unit symbols.

shoshonitic volcanic field represents the final magmatic products of this subduction system, and its incompatible element-enriched composition may be related to the subduction of continental crust.

*Andesitic volcaniclastic rocks (Kv)*

Early Cretaceous andesitic volcanic and volcaniclastic rocks, typically of volcanic-arc composition, are widespread in western Alaska. In the Unalakleet quadrangle, they are composed dominantly of volcaniclastic rocks that are not generally suitable for chemical analyses. We analyzed three samples of lava flows interbedded with the volcaniclastic rocks, but the flow rocks were too altered to yield reliable results. Plots of REE and spidergrams for unit Kv in other parts of the Yukon-Koyukuk basin (Box and Patton, 1989) are shown in figure 17. Compositions range from arc tholeiitic to high-K calc-alkalic and appear to become more enriched in K and other alkali elements with time (Box and Patton, 1989), perhaps owing to increased involvement of continental-derived material as the island arc drew near the continent prior to colliding.

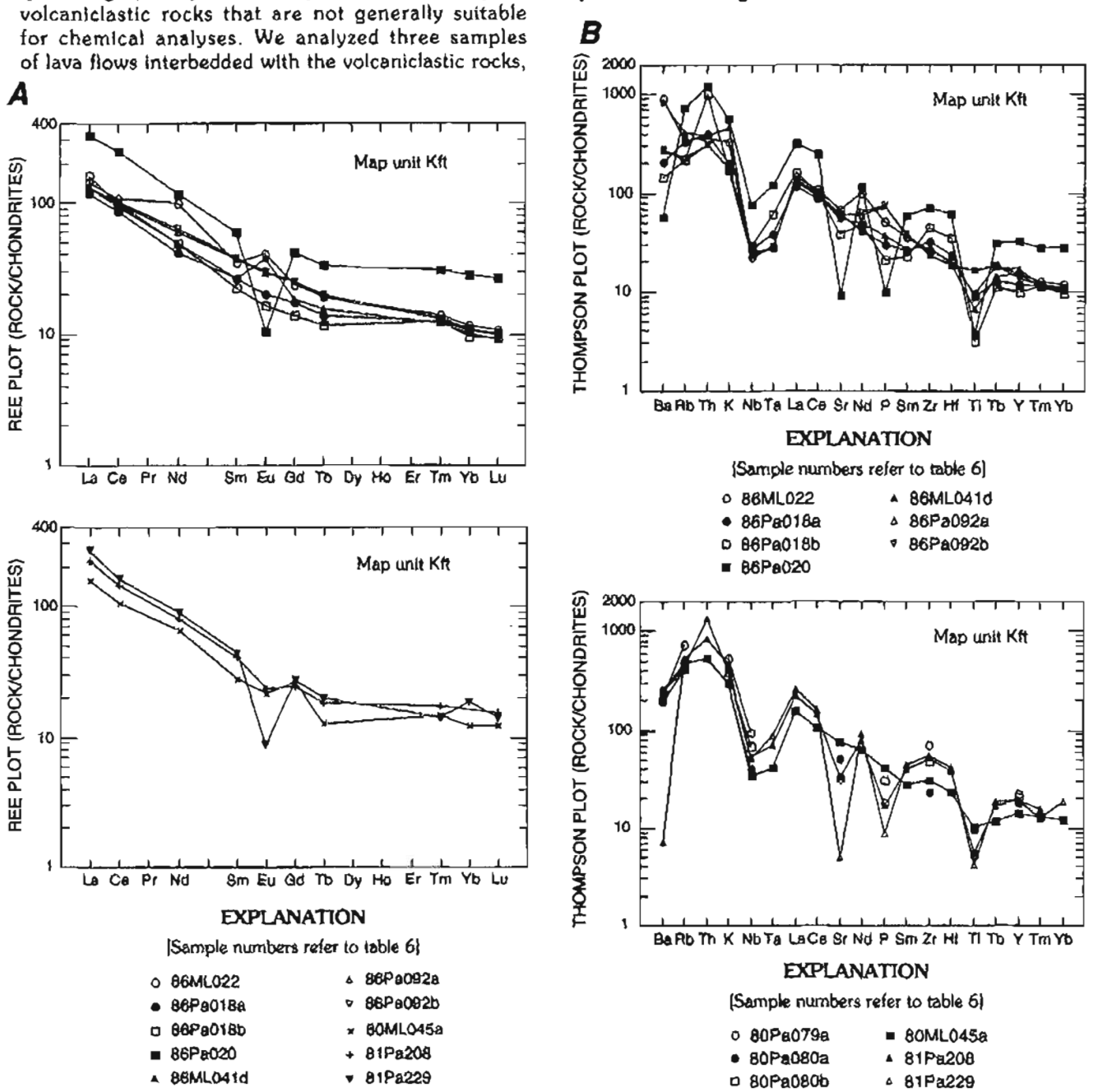


**Figure 12.** Rare-earth-element (REE) plots and spidergrams for shoshonitic volcanic and plutonic rocks (Kft) from Unalakleet quadrangle, west-central Alaska. *A*, REE plots. Two samples (86Pa020 and 81Pa229) have large negative Eu anomalies and contain more than 60 percent $SiO_2$. Two samples have small positive Eu anomalies, a shoshonitic andesite (86ML022) and a syenite (86ML041d). Negative anomalies indicate plagioclase fractionation; positive anomalies indicate plagioclase accumulation. *B*, Spidergrams showing high concentrations of incompatible elements and very high alkali and alkaline-earth contents. Samples 80Pa079a, 80Pa080a, and 80Pa080b have partial data sets. Data in spidergrams normalized to values from Thompson and others (1984). Data plotted using program of Wheately and Rock (1988). See Description of Map Units for explanation of map-unit symbol.

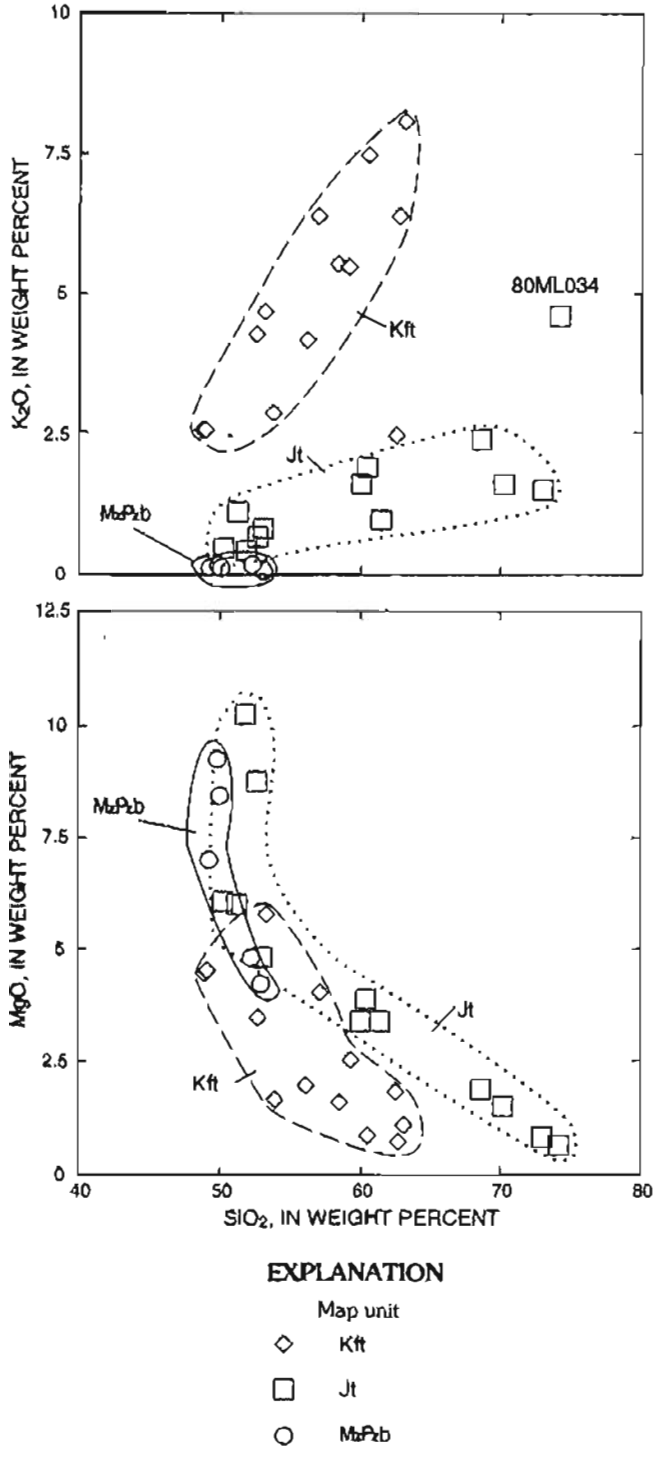


**Figure 13.** Plots of $K_2O$ and MgO compared to $SiO_2$ for Early Cretaceous and older map units in Unalakleet quadrangle, west-central Alaska. Unit Kft is characterized by very high $K_2O$. Unit MzPzb has low $K_2O$. Most of unit Jt has moderate $K_2O$ that increases with increasing $SiO_2$. Metasomatized parts of unit Jt (sample 80ML034, table 7) have much higher $K_2O$ than the rest of the unit. MgO decreases with increasing $SiO_2$ in all units. Outlined areas show general range of compositions for units Kft, Jt, and MzPzb. See Description of Map Units for explanation of map-unit symbols.

*Trondhjemite and tonalite (Jt)*

Spidergrams of intermediate and felsic samples of the trondhjemite and tonalite (Jt) unit are similar in shape to those of rocks from the andesitic volcaniclastic rocks (Kv) unit. Both have negative Nb and Ta anomalies relative to the alkali elements and

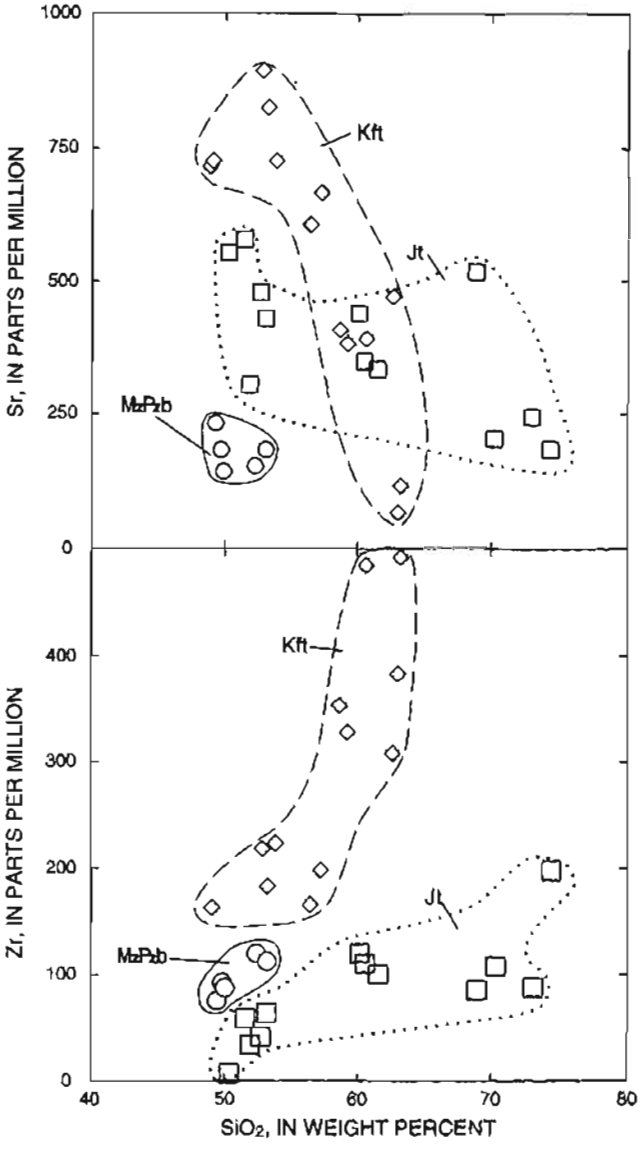


**Figure 14.** Zirconium (Zr) and strontium (Sr) compared with $SiO_2$ for Early Cretaceous and older map units in Unalakleet quadrangle, west-central Alaska. Unit MzPzb has low Sr and moderate Zr. Unit Jt has moderate Zr and Sr. Unit Kft has high Zr and Sr that increase and decrease, respectively, with increasing $SiO_2$. Outlined areas show general range of compositions for units Kft, Jt, and MzPzb. See Description of Map Units for explanation of map-unit symbols.

the LREE elements (fig. 18). Gabbroic rocks have flatter REE patterns and positive spikes at Eu (fig. 18) suggesting that these rocks are cumulate parts of the pluton that have accumulated significant plagioclase relative to their parent magmas. This conclusion is supported by their high-Sr contents (fig. 18) relative to other elements. Metasomatized parts of unit Jt have much higher $K_2O$ contents than the rest of the suite and plot outside the field defined by the rest of the data on plots of $K_2O$ vs. $SiO_2$ (fig. 13, sample No. 80ML034).

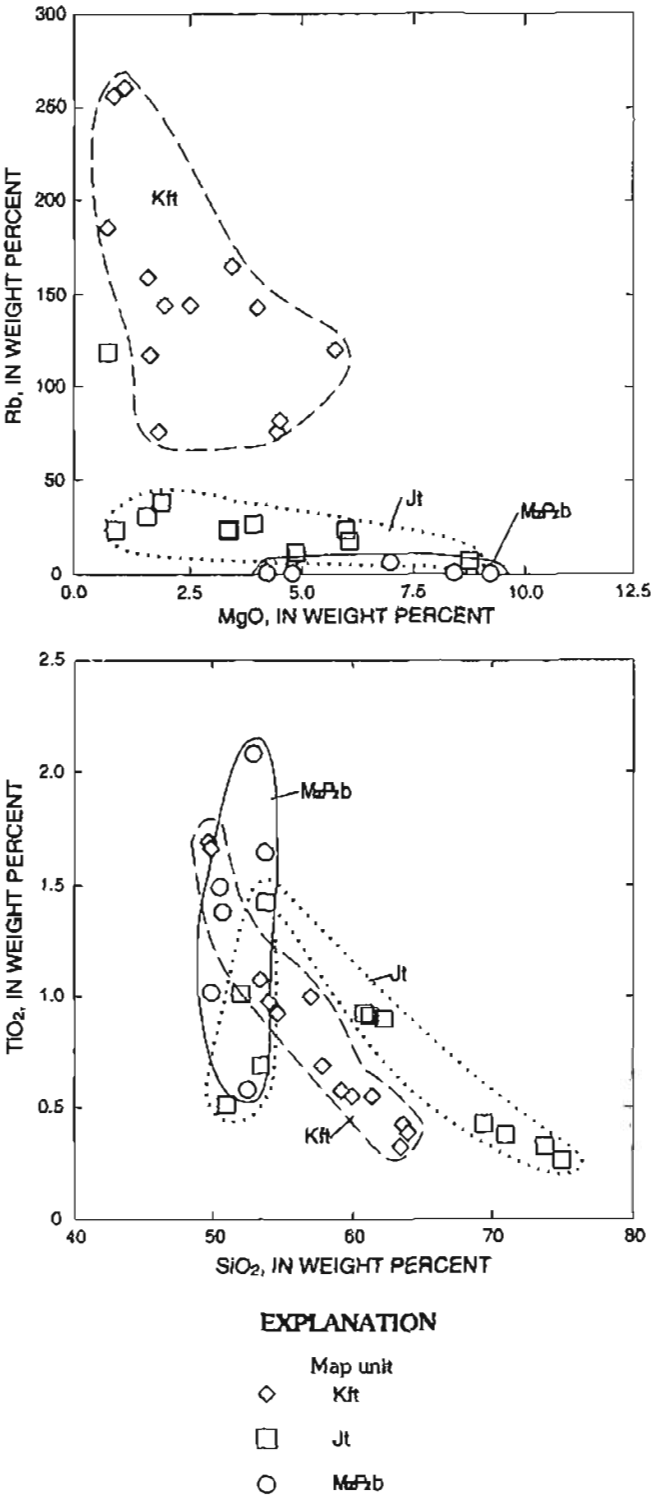


**Figure 15.** Rubidium (Rb) compared to MgO and $TiO_2$ compared to $SiO_2$ for Early Cretaceous and older map units in Unalakleet quadrangle, west-central Alaska. Outlined areas show general range of compositions for units Kft, Jt, and MzP1b. See Description of Map Units for explanation of map-unit symbols.

## MESOZOIC(?) AND PALEOZOIC(?)

### Angayucham(?) terrane (MzP1b)

Rocks of unit MzP1b are primarily metamorphosed basalts and diabases that are chemically similar to modern basalts generated at mid-ocean ridges (MORB). Chemical analyses of six rocks from this unit are given in table 8. Rocks of unit MzP1b are most often confused in the field with adjacent dark fine-grained rocks of arc-related units Jt or Kv. Unit MzP1b rocks are distinguished from both of these arc-related units on the basis of their flat to LREE-depleted REE patterns, lack of Nb or Ta anomaly, and by lower $K_2O$, Rb, and Sr contents (figs. 13, 14, 15, 19). In addition, unit MzP1b has higher Zr contents than unit Jt (fig.

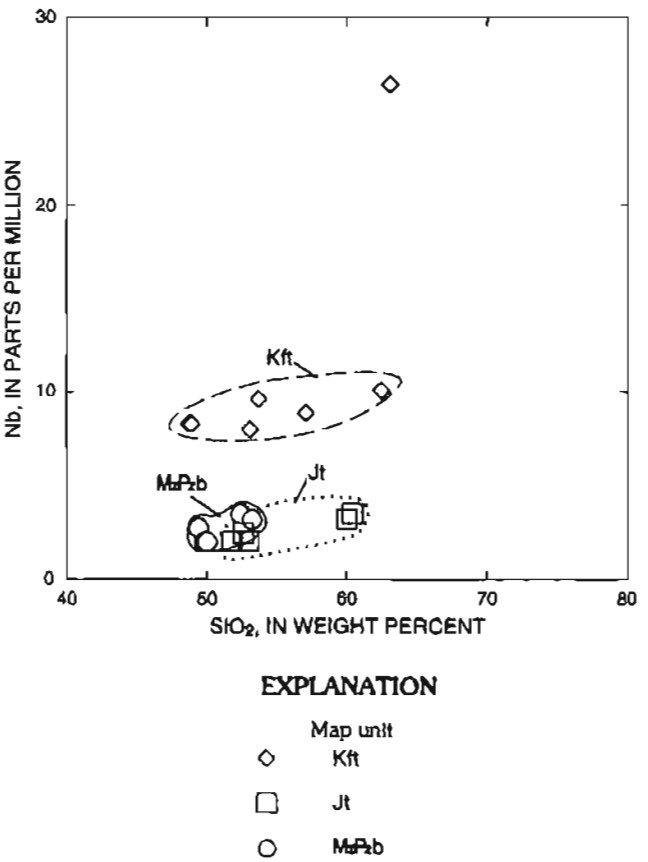


**Figure 16.** Niobium (Nb) compared with $SiO_2$ for Early Cretaceous and older rocks in Unalakleet quadrangle, west-central Alaska. Although unit Kft has low Nb and Ta relative to light-rare-earth elements (LREE) and alkali elements on spiderplots, it has higher Nb contents than any of the older units. Unit MzP1b has slightly higher Nb than unit Jt. Outlined areas show general range of compositions for units Kft, Jt, and MzP1b. See Description of Map Units for explanation of map-unit symbols.

14). Unit MzPzb in the Unalakleet quadrangle is questionably correlated with chemically similar basalts from the Angayucham terrane, which are exposed around the margins of the Yukon-Koyukuk basin. Unit MzPzb most closely resembles the Triassic basalt unit in the Angayucham terrane described by Pallister and others (1989), but has even lower LREE and a more MORB-like chemical composition.

## ACKNOWLEDGMENTS

Field data for compilation of the geologic map were collected at intervals between 1956 and 1986 by: W.W. Patton, Jr., 1956-1986; E.J. Moll-Stalcup, 1980-1986; J.M. Hoare, 1960-1966; W.H. Condon, 1961-1966; R.S. Bickel, 1956; I.L. Tailleur, 1958; Bond Taber, 1958; A.R. Tagg, 1962; R.J. Monroe, 1962; T.P. Miller, 1966; and J.M. Murphy, 1986. K.L. Wheeler prepared the computer database files for the field notes and for the geochemical and geochronological analyses. The geologic map was compiled by Patton and Moll-Stalcup and digitized by Wheeler using ARC/INFO software. The map and pamphlet greatly benefited from the careful reviews of M.L. Miller and A.B. Ford.

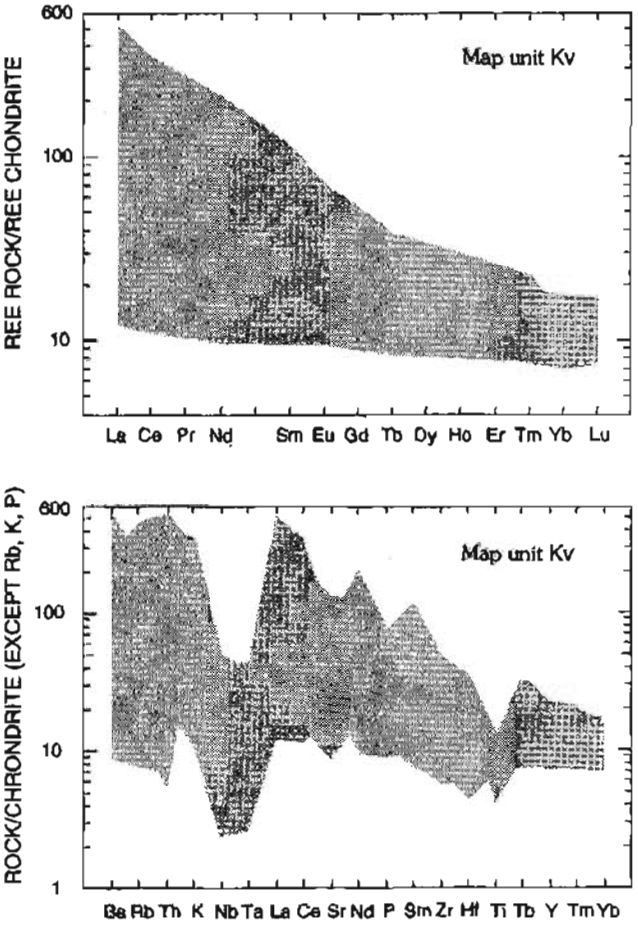


**Figure 17.** Rare-earth-element (REE) plot and spidergram for samples from unit Kv in Yukon-Koyukuk basin of west-central Alaska, outside the Unalakleet quadrangle. Shaded area indicates range of compositions for unit Kv in other parts of Yukon-Koyukuk basin. In Unalakleet quadrangle, most of this unit is clastic or highly altered and is not suitable for chemical analyses. Data from Box and Patton (1989). Data in spidergram normalized to values given in Thompson and others (1984) and plotted using program of Wheately and Rock (1988). See Description of Map Units for explanation of map-unit symbol.

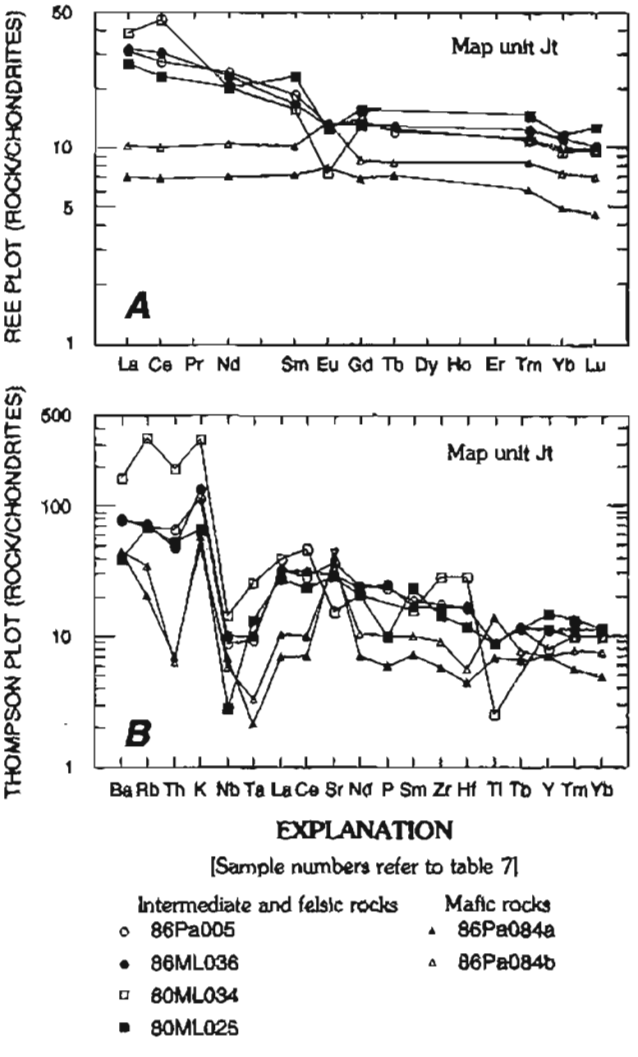


**Figure 18.** Rare-earth-element (REE) plot, *A*, and spidergram, *B*, for rocks from unit Jt in Unalakleet quadrangle, west-central Alaska. REE data for more felsic rocks (more than 57 percent $SiO_2$) are light-rare-earth element (LREE) enriched. Gabbros (samples 86Pa084a and 86Pa084b) have flat or LREE-depleted patterns and positive Eu and Sr anomalies indicating they are probably parts of the pluton that have accumulated significant plagioclase. Felsic samples yield spidergrams that are similar to spidergrams for modern island arcs. Typically these spidergrams have negative Nb and Ta anomalies (that is, Nb and Ta are low relative to the alkali elements, Ba, Rb, Th, and K, and to the LREE elements, La and Ce). Data in spidergram normalized to values given in Thompson and others (1984) and plotted using program of Wheately and Rock (1988). See Description of Map Units for explanation of map-unit symbol.

## REFERENCES CITED


Baedecker, 1987, Methods for geochemical analysis: U.S. Geological Survey Bulletin 1770, p. 132.

Beikman, H. M. (Compiler), 1980, Geologic map of Alaska: U.S. Geological Survey, scale 1:2,500,000.

Box, S.E., and Patton, W.W., Jr., 1989, Igneous history of the Koyukuk terrane, western Alaska: Constraints on the origin, evolution, and ultimate collision of an accreted island arc terrane: Journal of Geophysical Research 94 (B11), p. 15,843-15,867.

Carracedo, J.C., 1994, The Canary Islands, an example of structural control on the growth of large oceanic-island volcanoes: Journal of Volcanology and Geothermal Research, v. 60, p. 225-241.

Chapman, R.M., 1963, Coal deposits along the Yukon River between Ruby and Anvik, Alaska, *in* Contributions to economic geology of Alaska: U.S. Geological Survey Bulletin 1155, p. 18-29.

Elder, W.P., and Miller, J.W., 1991, Maps showing fossil localities and checklists of Jurassic and Cretaceous macrofauna of western Alaska: U.S. Geological Survey Open-File Report 91-629, 71 p., 3 pls., scale 1:500,000.

Frey, F.A., and Clague, D.A., 1983, Geochemistry of diverse basalt types from Loihi Seamount, Hawaii: Petrogenic implications: Earth and Planetary Science Letters, v. 66, p. 337-355.

Fries, Terry, Christie, J., and Pribble, S., 1990, Flame photometric determination of $K_2O$ and $Na_2O$ in rocks and mineral separates, *in* Arbogast, B.F., Quality Assurance Manual for the Branch of Geochemistry: U.S. Geological Survey Open-file Report 90-668, p. 107-110.

Gill, J., 1981, Orogenic andesites and plate tectonics: Springer-Verlag, New York, 390 p.

Gill, J., and Whelan, P., 1989, Early rifting of an oceanic island arc (Fiji) produced shoshonitic to tholeiitic basalts: Journal of Geophysical Research, v. 94, no. B4, p. 4,561-4,578.

Harris, R.A., Stone, D.B., and Turner, D.L., 1987, Tectonic implications of paleomagnetic and geochronologic data from the Yukon-Koyukuk province, Alaska: Geological Society of America Bulletin 99, p. 362-375.

Hawkesworth, C.J., Gallagher, K, Hergt, J.M., and McDermott, F., 1993, Mantle and slab contributions in arc magmas: Annual Review of Earth and Planetary Science, v. 21, p. 175-204.

Hoare, J.M., and Condon, W.H., 1966, Geologic map of the Kwiguk and Black quadrangles, western Alaska: U.S. Geological Survey Miscellaneous Investigations Map I-469, scale 1:250,000.

———1971, Geologic map of the St. Michael quadrangle, Alaska: U.S. Geological Survey Miscellaneous Geologic Investigations Map I-682, scale 1:250,000.

Hoare, J.M., Condon, W.H., and Patton, W.W., Jr., 1964, Occurrence and origin of laumontite in Cretaceous sedimentary rocks in western Alaska: U.S. Geological Survey Professional Paper 501-C, p. C74-C78.

Johnston, A.D., and Stout, J.H., 1984, A highly oxidized ferrian salite-, kennedyite-, forsterite-, and rhonite-bearing alkali gabbro from Kauai, Hawaii, and its mantle xenoliths: American Mineralogist, v. 69, p. 57-68.

MacDonald, G.A., and Katsura, T., 1964, Chemical composition of Hawaiian lavas: Journal of Petrology, v. 6, p. 82-133.

Mark, R. K., 1971, Strontium isotopic study of basalts from Nunivak Island, Alaska: Stanford University, unpublished Ph.D. thesis, 50 p.

Menzies, Martin, and Murthy, V.R., 1980, Nd and Sr isotope geochemistry of hydrous mantle nodules and their host alkali basalts: Implications for local


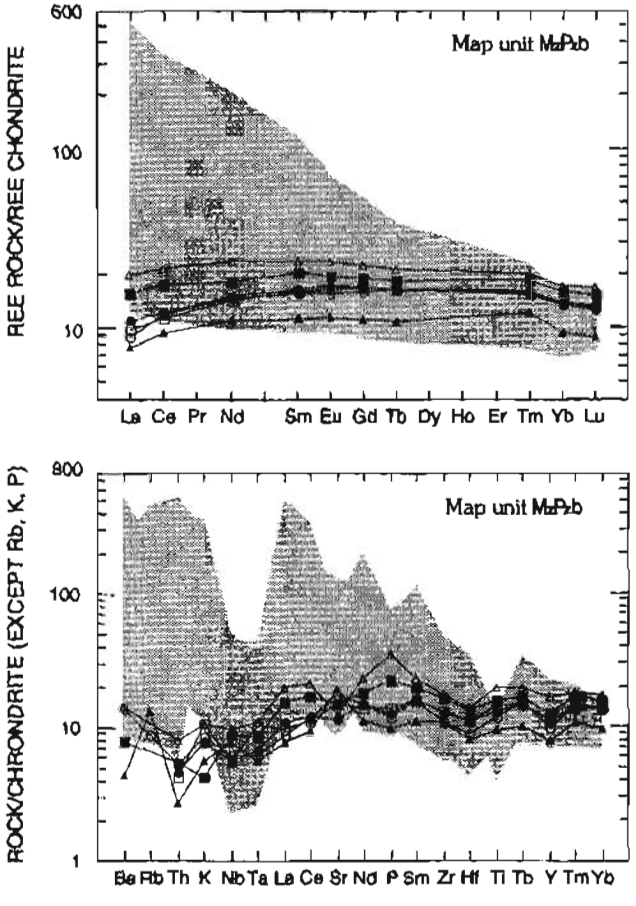


**Figure 19.** Rare-earth-element (REE) plot and spidergram for samples from unit MzPzb in Unalakleet quadrangle, west-central Alaska, compared with data for unit Kv in Yukon-Koyukuk basin outside Unalakleet quadrangle (shaded area). REE patterns for unit MzPzb are distinct from all other units in Unalakleet quadrangle because spidergrams do not have negative Nb or Ta anomalies or high alkalis. These patterns are typical of MORB (mid-ocean ridge basalts). Data for unit Kv from Box and Patton (1989). Data in spidergram normalized to values given in Thompson and others (1984) and plotted using program of Wheately and Rock (1988). See Description of Map Units for explanation of map-unit symbols.

heterogeneities in metasomatically veined mantle: Earth and Planetary Science Letters, v. 46, p. 323-334.

Moll-Stalcup, E.J., 1994, Latest Cretaceous and Cenozoic magmatism in mainland Alaska, *in* Plafker, G. and Berg, H.C., eds., The Geology of Alaska: Boulder, Colorado, Geological Society of America, The Geology of North America, v. G-1, p. 589-619.

Moll-Stalcup, E.J., and Arth, J.G., 1991, Isotopic and chemical constraints on the petrogenesis of Blackburn Hills volcanic field, western Alaska: Geochimica et Cosmochimica Acta, v. 55, no. 12, p. 3,753-3,776.

Moll-Stalcup, E.J., and Patton, W.W., Jr., 1992, Geologic map of the Blackburn Hills volcanic field, western Alaska: U.S. Geological Survey Miscellaneous Field Studies Map MF-2199, 1:63,360 scale.

Morrison, G.W., 1980, Characteristics and tectonic setting of the shoshonite rock association: Lithos, v. 13, p. 97-108.

Nakamura, K., Plafker, G., Jacob, K.H., and Davies, J.N., 1980, A tectonic stress trajectory map of Alaska using information from volcanoes and faults: Bulletin of the Earthquake Research Institute, v. 55, p. 89-100.

Nilsen, T.H., 1989, Stratigraphy and sedimentology of the mid-Cretaceous deposits of the Yukon-Koyukuk basin, west-central Alaska: Journal of Geophysical Research 94 (B11), p. 15,925-15,940.

Norton, D.R., and Papp, C.S., 1990, Determination of moisture and total water in silicate rocks, *in* Arbogast, B.F., Quality Assurance Manual for the Branch of Geochemistry: U.S. Geological Survey Open-file Report 90-668, p. 73-82.

Pallister, J.S., Budahn, J.R., and Murchey, B.L., 1989, Pillow basalts of the Angayucham terrane: Oceanic plateau and island crust accreted to the Brooks Range: Journal of Geophysical Research 94 (B11), p. 15,901-15,925.

Papp, C.S.E., Aruscavage, P., and Brandt, E., 1990, Determination of ferrous oxide in gologic materials by potentiometric titration, *in* Arbogast, B.F., Quality Assurance Manual for the Branch of Geochemistry: U.S. Geological Survey Open-file Report 90-668, p. 139-145.

Patton, W.W., Jr., 1966, Regional geology of Kateel River quadrangle, Alaska: U.S. Geological Survey Miscellaneous Geologic Investigations Map I-437, scale 1:250,000.

———1973, Reconnaissance geology of the northern Yukon-Koyukuk province, Alaska: U.S. Geological Survey Professional Paper 774-A, p. A1-A17.

———1993, Ophiolitic terranes of northern and central Alaska and their correlatives in Canada and northeastern Russia: Geological Society of America Abstracts with Programs, v. 25, no. 5, p. 132.

Patton, W.W., Jr., and Bickel, R.S., 1956, Geologic map and structure sections along part of the lower Yukon River, Alaska: U.S. Geological Survey Miscellaneous Geologic Investigations Map I-226, scale 1:80,000.

Patton, W.W., Jr. and Box, S.E., 1989, Tectonic setting of the Yukon-Koyukuk basin and its borderlands, western Alaska: Journal of Geophysical Research 94 (B11), p. 15,807-15,820.

Patton, W.W., Jr., Box, S.E., Moll-Stalcup, E.J., and Miller, T.P., 1994, Geology of west-central Alaska, *in* Plafker, G., and Berg, H.C., eds., Geology of Alaska: Boulder, Colorado, Geological Society of America, The Geology of North America, v. G-1, p. 241-269.

Patton, W.W., Jr., and Hoare, J.M., 1968, The Kaltag fault, west-central Alaska: Geological Research, 1968: U.S. Geological Survey Professional Paper 600-D, p. D147-D153.

Patton, W.W., Jr., and Moll, E.J., 1985, Geologic map of northern and central parts of Unalakleet quadrangle, Alaska: U.S. Geological Survey Miscellaneous Field Studies Map MF-1749, scale 1:250,000.

Patton, W.W., Jr., Moll, E.J., Lanphere, M.A., and Jones, D.L., 1984, New age data for the Kaiyuh Mountains, west-central Alaska, *in* W.L. Coonrad and R.L Elliott, *eds.*, U.S. Geological Survey in Alaska—Accomplishments during 1981: U.S. Geological Survey Circular 868, p. 30-32.

Patton, W.W., Jr. and Tailleur, I.L., 1977, Evidence in the Bering Strait region for differential movement between North America and Eurasia: Geological Society of America Bulletin 88, p. 1,298-1,304.

Shapiro, Leonard, and Brannock, W.W., 1962, Rapid analysis of silicate, carbonate, and phosphate rocks, U.S. Geological Survey Bulletin 1144-A, p. A1-A56.

Streckeisen, A., 1979, Classification and nomenclature of volcanic rocks, lamprophyres, carbonatites, and melitic rocks; Recommendations and suggestions of the IUGS Subcommission of the Systematics of Igneous Rocks: Geology, v. 7, p. 331-335.

Taggart, J.E., Jr., Bartel, A., and Siems, D.F., 1990, High precision major element analyses of rocks and minerals by wavelength dispersive X-ray fluorescence spectroscopy, *in* Arbogast, B.F., Quality Assurance Manual for the Branch of Geochemistry: U.S. Geological Survey Open-file Report 90-668, p. 166-172.

Texas Instrument, Inc., 1976, Aerial gamma-ray survey of the Bethel and Yukon areas, Alaska: U.S. Energy Research and Development Administration Open-file Report GJBX 5(77), scale 1:500,000.

Thompson, R.N., Morrison, M.A., Hendry, G.L., and Parry, S.J., 1984, An assessment of the relative roles of crust and mantle in magma genesis: an elemental approach: Philosophical Transactions Royal Society of London A, v. 310, p. 549-590.

Weaver, B.L, 1991, The origin of ocean island basalt end-member compositions: Trace element and isotopic constraints: Earth and Planetary Science Letters, v. 104, p. 381-397.

Wheately, M.R., and Rock, N.M.S., 1988, Spider: A Macintosh program to generate normalized multi-element "spidergrams": American Mineralogist, v. 73, p. 919-921, Version 3.01.

Zindler, A., and Hart, S., 1986, Chemical geodynamics: Annual Review of Earth and Planetary Science, v. 14, p. 493-571.

# TABLES 1–9

**Table 1.** Potassium-argon ages for samples from the Unalakleet quadrangle, west-central Alaska

| Map locality | Field No. | Location | | Mineral or whole rock | Map unit | $K_2O$ (percent) | $^{40}Ar$ rad (moles/gram) | $^{40}Ar$ rad/ $^{40}Ar$ total | Calculated age (Ma) | References |
|---|---|---|---|---|---|---|---|---|---|---|
| | | Township | Range | | | | | | | |
| A | 80Pa123a | T26S | R16W | basalt | Qyt | 0.890 | $0.0239\times10^{-11}$ | 0.002 | 0.19±0.02 | D. Turner, written commun., 1984 |
| | | | | | | 0.900 | | | | |
| B | 86Pa045 | T28S | R17W | basalt | QTb | 1.439 | $4.112\times10^{-12}$ | 0.13 | 1.99±0.06 | M. Lanphere, written commun., 1988 |
| C | 86Pa052 | T27S | R16W | basalt | QTb | 1.141 | $2.288\times10^{-12}$ | 0.32 | 1.39±0.04 | M. Lanphere, written commun., 1988 |
| D | 80Pa125a | T27S | R15W | basalt | QTb | 1.200 | $0.488\times10^{-11}$ | 0.10 | 2.8±0.1 | D. Turner, written commun., 1984 |
| | | | | | | 1.900 | | | | |
| E | 80ML057b | T22S | R12W | basalt | QTb | 0.730 | $0.341\times10^{-11}$ | 0.28 | 3.25±0.11 | D. Turner, written commun., 1984 |
| | | | | | | 0.730 | | | | |
| F | 81Pa223 | T24S | R6W | biotite | Tg | 7.85 | $6.452\times10^{-10}$ | 0.85 | 56.2±1.7 | Patton and Moll, 1985 |
| G | 80ML039d | T24S | R7W | sanidine | Td | 3.75 | $3.08\times10^{-10}$ | 0.86 | 56.0±1.7 | Patton and Moll, 1985 |
| | | | | | | 3.77 | | | | |
| H | 86ML018 | T28S | R8W | andesite | Ta | 1.362 | $1.032\times10^{-10}$ | 0.67 | 51.9±1.6 | M. Lanphere, written commun., 1988 |
| I | 80ML012b | T23S | R7W | hornblende | Ta | 0.668 | $0.6920\times10^{-10}$ | 0.35 | 65.2±3.9 | Patton and Moll, 1985 |
| | | | | | | 0.660 | $0.5865\times10^{-10}$ | 0.29 | | |
| J | 81Pa330 | T19S | R3W | sanidine | TKr | 5.34 | $4.139\times10^{-10}$ | 0.66 | 53.2±1.6 | Patton and Moll, 1985 |
| | | | | | | 5.31 | | | | |
| K | 86ML043 | T28S | R11W | biotite | TKr | 8.955 | $8.721\times10^{-10}$ | 0.86 | 66.4±2 | M. Lanphere, written commun., 1988 |
| | | | | | | 10.565 | $1.071\times10^{-9}$ | 0.96 | 69.1±2.1 | |
| L | 86Pa012b | T28S | R10W | hornblende | TKr | 0.348 | $3.407\times10^{-11}$ | 0.36 | 66.8±2 | M. Lanphere, written commun., 1988 |
| M | 82Pa080 | T20S | R4W | andesite | TKa | 1.224 | $9.650\times10^{-11}$ | 0.89 | 53.8±1.6 | Patton and Moll, 1985 |
| | | | | | | 1.224 | | | | |
| | | | | | | 1.227 | | | | |
| | | | | | | 1.233 | | | | |
| N | 86Pa043 | T28S | R17W | hornblende | TKa | 1.954 | $1.846\times10^{-10}$ | 0.51 | 64.4±1.9 | M. Lanphere, written commun., 1988 |
| O | 80Pa116a | T24S | R10W | basalt | TKa | 1.612 | $1.457\times10^{-10}$ | 0.41 | 61.5±1.8 | Patton and Moll, 1985 |
| | | | | | | 1.628 | | | | |
| | | | | | | 1.617 | | | | |
| | | | | | | 1.609 | | | | |
| P | 62Hr218 | T28S | R14W | biotite | TKrs | 8.08 | $8.155\times10^{-10}$ | 0.85 | 68.8±3 | Hoare and Condon, 1966 |
| Q | 86Pa018b | T28S | R9W | biotite | Kft | 6.305 | $1.101\times10^{-9}$ | 0.91 | 117±3.5 | M. Lanphere, written commun., 1988 |
| R | 81Pa208 | T25S | R8W | biotite | Kft | 6.91 | $1.219\times10^{-9}$ | 0.96 | 118±3.5 | Patton and Moll, 1985 |
| | | | | | | 6.96 | | | | |
| S | 86ML036 | T27S | R12W | hornblende | Jt | 0.721 | $1.400\times10^{-10}$ | 0.31 | 130±3.9 | M. Lanphere, written commun., 1988 |
| T | 86Pa005 | T27S | R11W | hornblende | Jt | 0.733 | $1.631\times10^{-10}$ | 0.55 | 148±4.4 | M. Lanphere, written commun., 1988 |
| U | 80Pa015a | T20S | R8W | biotite | Jt | 4.52 | $10.33\times10^{-10}$ | 0.67 | 154±6 | Patton and Moll, 1985 |
| | | | | | | 4.51 | $10.55\times10^{-10}$ | 0.79 | | |
| V | 80ML025 | T22S | R9W | biotite | Jt | 2.32 | $5.645\times10^{-10}$ | 0.70 | 166±7 | Patton and Moll, 1985 |
| | | | | | | 2.33 | $5.990\times10^{-10}$ | 0.68 | | |
| | | | | hornblende | | 0.662 | $1.730\times10^{-10}$ | 0.62 | 173±9 | |
| | | | | | | 0.660 | $1.729\times10^{-10}$ | 0.42 | | |

$^{40}K$ decay constants: $\lambda_\varepsilon = 0.581 \times 10^{-10}\ yr^{-1}$; $\lambda_\beta = 4.963 \times 10^{-10}\ yr^{-1}$. Abundance ratio: $^{40}K/K = 1.167 \times 10^{-4}$ atom percent.

**Table 2.** Major oxide and trace-element composition of Tertiary and Quaternary basalts (Qyt, Qya, QTb) from the St. Michael volcanic field, Unalakleet quadrangle, west-central Alaska

[Major elements in weight percent; trace elements in parts per million. All major oxides except FeO, $CO_2$, $H_2O+$, and $H_2O-$ by X-ray fluorescence following methods of Taggart and others (1990). FeO by titration following method of Papp and others (1990). $CO_2$ and $H_2O$ by methods of Norton and Papp (1990). Trace elements by instrumental neutron activation analysis (INAA) unless otherwise noted in first column by following acronyms: XRF, energy-dispersive X-ray fluorescence; ICP, inductively coupled plasma-emission spectrometry. Methods described in USGS Bulletin 1770 (Baedecker, 1987). nd, not accurately determined; - -, not analyzed. USGS analysts: J.S. Wahlberg, J.E. Taggart, J.W. Baker, H.G. Neiman, B. Anderson, F.D. Newman, G.R. Mason, L.A. Bradley, J.R. Budahn, R.J. Knight, and D.M. McKown, Lakewood, Colo.; R.G. Johnson, H.J. Rose, B.A. McCall, G. Sellers, and J. Lindsay, Reston, Va.; S.T. Neil and D.V. Vivit, Menlo Park, Calif. $SiO_2$ anhydrous is recalculated $SiO_2$ content after major oxides are normalized to 100% total weight without $H_2O$ or $CO_2$.]

| Sample No. | 80Pa123a | 86Pa045 | 86Pa052 | 80Pa125 | 80ML057b |
|---|---|---|---|---|---|
| Map Unit | Qyt | QTb | QTb | QTb | QTb |
| Rock Type | Tholeiite | Tholeiite | Tholeiite | Tholeiite | Tholeiite |
| Map No. | 1 | 2 | 3 | 4 | 5 |
| Township | T26S | T28S | T27S | T27S | T22S |
| Range | R16W | R17W | R16W | R15W | R12W |
| $SiO_2$ | 49.1 | 49.2 | 48.4 | 50.1 | 48.4 |
| $Al_2O_3$ | 14.7 | 15.4 | 15.0 | 16.1 | 15.2 |
| $Fe_2O_3$ | 3.3 | 1.9 | 2.2 | 3.6 | 2.4 |
| FeO | 7.44 | 8.02 | 8.63 | 7.38 | 9.43 |
| MgO | 9.26 | 8.19 | 8.09 | 6.70 | 9.08 |
| CaO | 9.72 | 9.19 | 8.78 | 9.67 | 9.08 |
| $Na_2O$ | 3.30 | 3.03 | 3.08 | 3.50 | 2.90 |
| $K_2O$ | 0.90 | 1.13 | 1.37 | 1.14 | 0.69 |
| $TiO_2$ | 1.83 | 1.93 | 2.12 | 2.11 | 1.86 |
| $P_2O_5$ | 0.34 | 0.40 | 0.45 | 0.46 | 0.20 |
| MnO | 0.17 | 0.15 | 0.16 | 0.18 | 0.16 |
| $CO_2$ | <0.01 | 0.11 | 0.13 | <0.01 | 0.01 |
| $H_2O$ | 0.32 | 0.67 | 0.35 | 0.22 | 0.45 |
| Total | 100.4 | 99.3 | 98.8 | 101.2 | 99.9 |
| $SiO_2$ anhydrous | 49.2 | 50.0 | 49.3 | 49.8 | 48.7 |
| $K_2O+Na_2O$ | 4.21 | 4.22 | 4.53 | 4.61 | 3.61 |
| Total $Fe_2O_3$ | 11.6 | 10.8 | 11.8 | 11.8 | 12.9 |
| Rb (XRF) | 19 | 14 | 20 | 21 | 14 |
| Cs | - - | 0.164 | 0.410 | - - | 0.40 |
| Sr (XRF) | 367 | 490 | 540 | 410 | 321 |
| Ba (XRF) | 178 | 210 | 260 | 209 | 133 |
| La | - - | 18.9 | 22.2 | - - | 12.0 |
| Ce | - - | 40.7 | 51.2 | - - | 23.0 |
| Nd | - - | 20.7 | 23.1 | - - | 17.0 |
| Sm | - - | 5.29 | 5.57 | - - | 3.20 |
| Eu | - - | 1.78 | 1.88 | - - | 1.13 |
| Gd | - - | 5.87 | 6.00 | - - | 5.10 |
| Tb | - - | 0.798 | 0.873 | - - | 0.37 |
| Tm | - - | 0.363 | 0.416 | - - | 0.27 |
| Yb | - - | 2.06 | 2.43 | - - | 1.70 |
| Lu | - - | 0.295 | 0.338 | - - | 0.30 |
| Y (XRF) | 21 | 24 | 24 | 29 | 18 |
| Y (ICP) | - - | 21 | 23 | - - | - - |
| Zr (XRF) | 103 | 170 | 180 | 130 | 110 |
| Hf | - - | 3.87 | 4.22 | - - | 2.80 |
| Nb (XRF) | 22 | 33 | 34 | 28 | 16 |
| Nb (ICP) | - - | 26.5 | 31 | - - | - - |
| Ta | - - | 2.18 | 2.52 | - - | 1.15 |
| Th | - - | 2.4 | 2.8 | - - | 1.5 |
| U | - - | 0.92 | 0.962 | - - | 0.60 |
| Co (ICP) | - - | 48 | 51 | - - | - - |
| Co | - - | 49.6 | 51.5 | - - | 57.1 |
| Cr (ICP) | - - | 339 | 315 | - - | - - |
| Cr | - - | 313 | 242 | - - | 243 |
| Ni (ICP) | - - | 194 | 196 | - - | - - |
| Ni | - - | 192 | 196 | - - | - - |
| Sc (ICP) | - - | 25 | 24 | - - | - - |
| V (ICP) | - - | 186 | 200 | - - | - - |
| Zn | - - | 110 | 118 | - - | 97 |
| Sb | - - | nd | 0.149 | - - | 4.30 |

**Table 3.** Major oxide composition of additional Tertiary and Quaternary basalts (Qyt, Qya, QTb) from the St. Michael volcanic field, Unalakleet quadrangle, west-central Alaska

[All major oxides except $K_2O$ and $Na_2O$ analyzed in 1972 by rapid rock methods described in Shapiro and Brannock (1962) supplemented by atomic absorption. USGS analysts: Paul Elmore, Hezekiah Smith, James Kelsey, R. Moore, J. Glenn, and Leonard Shapiro, Washington, D.C.; L.B. Schlocker, Menlo Park, Calif. $K_2O$ and $Na_2O$ analyzed by flame photometry using methods described in Fries and others (1990). $SiO_2$ anhydrous is recalculated $SiO_2$ content after major oxides are normalized to 100% total weight without $H_2O$ or $CO_2$.]

| Sample No. | 66Hr254 | 66Hr255 | 66Hr271 | 66Hr273 | 66Hr305 | 66Hr308 | 66Hr313 | 66Hr314 |
|---|---|---|---|---|---|---|---|---|
| Map Unit | Qyt | Qya | Qya | Qya | Qya | Qya | Qya | Qya |
| Rock Type | Tholeiite | Hawaiite | Basanite | Basanite | Alkali basalt | Basanite | Alkali basalt | Basanite |
| Map No. | 6 | 7 | 8 | 9 | 10 | 11 | 12 | 13 |
| Township | T26S | T26S | T24S | T24S | T25S | T25S | T25S | T25S |
| Range | R16W | R15W | R13W | R14W | R17W | R17W | R16W | R16W |
| $SiO_2$ wt. % | 49.1 | 49.7 | 45.6 | 45.2 | 45.6 | 44.9 | 47.6 | 45.9 |
| $Al_2O_3$ | 15.2 | 14.8 | 16.1 | 15.1 | 14.1 | 14.5 | 14.8 | 14.8 |
| $Fe_2O_3$ | 5.4 | 4.8 | 9.6 | 6.1 | 4.0 | 6.1 | 1.6 | 2.5 |
| FeO | 5.45 | 7.4 | 2.0 | 5.7 | 7.1 | 5.4 | 9.0 | 6.7 |
| MgO | 9.0 | 3.8 | 7.4 | 9.8 | 12.3 | 10.7 | 9.5 | 10.5 |
| CaO | 9.5 | 8.5 | 7.7 | 8.6 | 9.2 | 9.1 | 9.9 | 9.8 |
| $Na_2O$ | 3.08 | 3.64 | 4.57 | 3.59 | 2.97 | 3.90 | 3.12 | 3.67 |
| $K_2O$ | 0.86 | 1.48 | 2.57 | 1.80 | 1.36 | 1.70 | 1.06 | 1.77 |
| $TiO_2$ | 1.6 | 2.8 | 2.3 | 2.4 | 2.1 | 2.3 | 2.0 | 2.5 |
| $P_2O_5$ | 0.30 | 0.74 | 0.69 | 0.65 | 0.49 | 0.59 | 0.35 | 0.56 |
| MnO | 0.22 | 0.22 | 0.21 | 0.21 | 0.20 | 0.20 | 0.20 | 0.22 |
| $CO_2$ | <0.05 | <0.05 | <0.05 | <0.05 | <0.05 | <0.05 | <0.05 | <0.05 |
| Total $H_2O$ | 0.34 | 0.88 | 0.81 | 0.98 | 0.57 | 0.65 | 0.63 | 0.66 |
| Total | 100.1 | 98.8 | 99.6 | 100.1 | 100.0 | 100.0 | 99.8 | 99.6 |
| $SiO_2$ anhydrous | 49.2 | 50.8 | 46.2 | 45.6 | 45.9 | 45.2 | 48.0 | 46.4 |
| $K_2O+Na_2O$ | 3.97 | 5.25 | 7.29 | 5.46 | 4.37 | 5.66 | 4.22 | 5.51 |

| Sample No. | 66Hr316 | 66Hr319 | 66Hr323 | 66Hr330 | 66Hr333 | 66Hr337 | 66CO490 | 66Hr249 |
|---|---|---|---|---|---|---|---|---|
| Map Unit | Qya | Qya | Qya | Qya | Qya | Qya | Qya | QTb |
| Rock Type | Basanite | Alkali basalt | Hawaiite | Basanite | Basanite | Alkali basalt | Hawaiite | Tholeiite |
| Map No. | 14 | 15 | 16 | 17 | 18 | 19 | 20 | 21 |
| Township | T25S | T25S | T25S | T24S | T24S | T23S | T24S | T26S |
| Range | R15W | R15W | R15W | R14W | R15W | R14W | R13W | R11W |
| $SiO_2$ wt. % | 45.6 | 46.2 | 48.4 | 45.6 | 45.3 | 45.5 | 49.4 | 50.6 |
| $Al_2O_3$ | 15.3 | 14.5 | 16.7 | 14.8 | 15.1 | 7.9 | 16.9 | 14.6 |
| $Fe_2O_3$ | 5.1 | 3.4 | 6.6 | 3.2 | 2.2 | 8.4 | 5.2 | 1.6 |
| FeO | 6.4 | 7.6 | 4.4 | 7.7 | 9.0 | 5.3 | 5.7 | 8.8 |
| MgO | 9.6 | 10.5 | 5.6 | 9.8 | 10.0 | 16.0 | 4.6 | 9.6 |
| CaO | 8.8 | 9.3 | 9.3 | 9.3 | 9.0 | 12.7 | 8.5 | 8.9 |
| $Na_2O$ | 4.04 | 3.42 | 3.87 | 4.03 | 3.86 | 3.04 | 3.49 | 3.00 |
| $K_2O$ | 1.79 | 1.39 | 1.52 | 1.92 | 1.87 | 1.80 | 1.87 | 0.59 |
| $TiO_2$ | 2.3 | 2.2 | 2.4 | 2.4 | 2.3 | 1.5 | 2.5 | 1.6 |
| $P_2O_5$ | 0.67 | 0.53 | 0.57 | 0.68 | 0.64 | 0.12 | 0.73 | 0.21 |
| MnO | 0.21 | 0.20 | 0.16 | 0.19 | 0.21 | 0.2 | 0.16 | 0.22 |
| $CO_2$ | <0.05 | <0.05 | <0.05 | <0.05 | <0.05 | <0.05 | <0.05 | <0.05 |
| Total $H_2O$ | 0.48 | 0.91 | 0.74 | 0.61 | 0.58 | 0.44 | 1.39 | 0.61 |
| Total | 100.3 | 100.2 | 100.3 | 100.2 | 100.0 | 102.9 | 100.4 | 100.3 |
| $SiO_2$ anhydrous | 45.7 | 46.6 | 48.6 | 45.8 | 45.5 | 44.4 | 49.9 | 50.7 |
| $K_2O+Na_2O$ | 5.86 | 4.86 | 5.44 | 5.98 | 5.76 | 4.75 | 5.43 | 3.60 |

**Table 3.** Major oxide composition of additional Tertiary and Quaternary basalts (Qyt, Qya, QTb) from the St. Michael volcanic field, Unalakleet quadrangle, west-central Alaska.—*Continued*

| Sample No. | 66Hr251 | 66Hr252 | 66Hr253 | 66Hr268a | 6Hr268b | 66Hr269 | 66Hr269a | 66Hr278 |
|---|---|---|---|---|---|---|---|---|
| Map Unit | QTb | Qyt? | QTb | QTb | QTb | QTb | QTb | QTb |
| Rock Type | Tholeiite | Tholeiite | Tholeiite | Alkali basalt | Alkali basalt | Alkali basalt | Tholeiite | Tholeiite |
| Map No. | 22 | 23 | 24 | 25 | 26 | 27 | 28 | 29 |
| Township | T27S | T27S | T28S | T24S | T24S | T24S | T24S | T23S |
| Range | R15W | R16W | R17W | R12W | R12W | R12W | R12W | R13W |
| $SiO_2$ wt. % | 48.9 | 48.8 | 49.5 | 46.4 | 47.1 | 44.1 | 51.2 | 49.8 |
| $Al_2O_3$ | 15.0 | 15.0 | 16.4 | 14.7 | 14.8 | 14.2 | 15.9 | 16.5 |
| $Fe_2O_3$ | 1.4 | 1.5 | 5.2 | 2.3 | 3.1 | 3.8 | 2.1 | 3.8 |
| FeO | 9.4 | 9.2 | 5.6 | 8.7 | 7.6 | 8.4 | 7.3 | 7.1 |
| MgO | 9.2 | 9.4 | 6.5 | 10.0 | 9.7 | 11.0 | 7.5 | 5.9 |
| CaO | 9.4 | 9.1 | 8.7 | 9.2 | 9.3 | 10.0 | 9.0 | 9.4 |
| $Na_2O$ | 3.05 | 3.20 | 3.51 | 3.67 | 3.82 | 2.18 | 3.48 | 3.52 |
| $K_2O$ | 0.80 | 1.00 | 1.13 | 0.78 | 0.60 | 0.71 | 0.91 | 0.99 |
| $TiO_2$ | 1.6 | 1.8 | 2.0 | 2.3 | 2.5 | 2.4 | 1.7 | 2.2 |
| $P_2O_5$ | 0.27 | 0.30 | 0.46 | 0.50 | 0.51 | 0.43 | 0.28 | 0.36 |
| MnO | 0.15 | 0.22 | 0.19 | 0.16 | 0.15 | 0.19 | 0.16 | 0.09 |
| $CO_2$ | <0.05 | <0.05 | 0.11 | <0.05 | <0.05 | <0.05 | <0.05 | <0.05 |
| Total $H_2O$ | 0.86 | 0.50 | 0.76 | 1.30 | 0.50 | 1.33 | 0.72 | 0.39 |
| Total | 100.0 | 100.0 | 100.0 | 100.0 | 99.7 | 98.7 | 100.3 | 100.1 |
| $SiO_2$ anhydrous | 49.3 | 49.0 | 49.9 | 47.0 | 47.5 | 45.3 | 51.4 | 50.0 |
| $K_2O+Na_2O$ | 3.88 | 4.22 | 4.69 | 4.51 | 4.46 | 2.97 | 4.41 | 4.54 |

| Sample No. | 66Hr293 | 66Hr296 | 6Hr315 | 66Hr324 | 66Hr325b | 66Hr326b | 66CO545 |
|---|---|---|---|---|---|---|---|
| Map Unit | QTb | QTb | QTb | QTb | QTb | QTb | QTb |
| Rock Type | Tholeiite | Basanite | Tholeiite | Tholeiite | Tholeiite | Tholeiite | Tholeiite |
| Map No. | 30 | 31 | 32 | 33 | 34 | 35 | 36 |
| Township | T23S | T23S | T25S | T24S | T22S | T22S | T25S |
| Range | R16W | R14W | R16W | R15W | R12W | R13W | R16W |
| $SiO_2$ wt. % | 48.7 | 45.3 | 50.0 | 50.6 | 50.1 | 50.2 | 49.1 |
| $Al_2O_3$ | 15.2 | 15.4 | 16.0 | 15.5 | 15.0 | 14.0 | 15.5 |
| $Fe_2O_3$ | 3.9 | 4.2 | 8.2 | 2.4 | 2.2 | 5.1 | 3.1 |
| FeO | 6.9 | 7.0 | 2.8 | 7.8 | 9.6 | 8.8 | 7.7 |
| MgO | 9.7 | 8.7 | 6.5 | 8.7 | 8.7 | 5.1 | 8.7 |
| CaO | 9.1 | 8.9 | 8.4 | 8.6 | 8.6 | 8.2 | 9.2 |
| $Na_2O$ | 3.03 | 4.66 | 3.67 | 3.23 | 2.77 | 3.44 | 3.21 |
| $K_2O$ | 0.76 | 1.79 | 1.06 | 0.81 | 0.58 | 1.32 | 0.83 |
| $TiO_2$ | 1.6 | 2.8 | 2.1 | 1.9 | 1.4 | 2.7 | 1.8 |
| $P_2O_5$ | 0.32 | 0.71 | 0.46 | 0.32 | 0.26 | 0.46 | 0.35 |
| MnO | 0.19 | 0.13 | 0.15 | 0.17 | 0.19 | 0.22 | 0.19 |
| $CO_2$ | <0.05 | <0.05 | <0.05 | <0.05 | <0.05 | <0.05 | <0.05 |
| Total $H_2O$ | 0.67 | 0.71 | 0.74 | 0.34 | 1.00 | 0.68 | 0.51 |
| Total | 100.1 | 100.3 | 100.1 | 100.4 | 100.4 | 100.2 | 100.2 |
| $SiO_2$ anhydrous | 49.0 | 45.5 | 50.3 | 50.6 | 50.4 | 50.4 | 49.3 |
| $K_2O+Na_2O$ | 3.82 | 6.49 | 4.79 | 4.04 | 3.37 | 4.80 | 4.06 |

**Table 4.** Major oxide and trace-element composition of Tertiary volcanic rocks (Tg, Thr, Td, Ta) from the Blackburn Hills volcanic field, Unalakleet quadrangle, west-central Alaska

[Major elements in weight percent; trace elements in parts per million. All major oxides except FeO, $CO_2$, $H_2O+$, and $H_2O-$ by X-ray fluorescence following methods of Taggart and others (1990). FeO by titration following method of Papp and others (1990). $CO_2$ and $H_2O$ by methods of Norton and Papp (1990). Trace elements by instrumental neutron activation analysis (INAA) unless otherwise noted in first column by following acronyms: XRF, energy-dispersive X-ray fluorescence; ICP, inductively coupled plasma-emission spectrometry. Methods described in USGS Bulletin 1770 (Baedecker, 1987). nd, not accurately determined; - -, not analyzed. Rb, Sr, Ba, Nb, Zr, and Y by X-ray fluorescence, except Ba and Zr values in italics, which were analyzed by instrumental neutron activation, and Rb and Sr values in italics, which were analyzed by isotope dilution mass spectrometry. Th and U values in italics were analyzed by delayed neutron activation. Nb partial analyses were determined using inductively coupled plasma-atomic emission spectrometry (ICP-AES) using method developed by T.L. Fries of USGS, Menlo Park, Calif. USGS analysts: J.W. Baker, M. Coughlin, S. Danahey, J. Storey, J.E. Taggert, Jr., B. Vaughn, and J.S. Wahlberg, Lakewood, Colo.; R.G. Johnson, D. Kobilas, J.R. Linsey, B. McCall, H.J. Rose, G. Sellers, and L.J. Schwarz, Reston, Va.; T.L. Fries and B.S. King, Menlo Park, Calif.]

| Sample No. | 81ML024 | 81Pa222 | 81Pa223 | 81ML020a | 80ML005c | 80ML040a | 80ML042b | 80ML050a |
|---|---|---|---|---|---|---|---|---|
| Map Unit | Tg | Tg | Tg | Thr | Td | Td | Td | Td |
| Rock Type | Granite | Granite | Qtz monz | Rhyolite | Rhyolite | Rhyolite | Rhyolite | Rhyolite |
| Map No. | 37 | 38 | 39 | 40 | 41 | 42 | 43 | 44 |
| Township | T24S | T24S | T24S | T24S | T25S | T24S | T24S | T24S |
| Range | R6W | R6W | R6W | R6W | R6W | R7W | R7W | R7W |
| $SiO_2$ | 67.3 | 70.8 | 62.6 | 74.8 | 70.4 | 75.1 | 72.0 | 72.3 |
| $Al_2O_3$ | 15.4 | 14.5 | 16 | 13.4 | 14.5 | 11.0 | 11.8 | 11.8 |
| $Fe_2O_3$ | 2.0 | 1.5 | 3.1 | 0.86 | 2.6 | 3.4 | 1.0 | 1.1 |
| FeO | 1.60 | 0.80 | 2.13 | 0.24 | 0.4 | 0.22 | 0.76 | 0.63 |
| MgO | 0.84 | 0.5 | 1.84 | 0.21 | 0.4 | <0.1 | <0.1 | 0.10 |
| CaO | 1.94 | 1.33 | 3.57 | 0.06 | 0.89 | 0.39 | 0.40 | 0.44 |
| $Na_2O$ | 4.99 | 4.6 | 4.82 | 3.97 | 3.90 | 4.60 | 5.40 | 4.60 |
| $K_2O$ | 3.51 | 4.04 | 2.79 | 4.2 | 3.77 | 4.22 | 1.95 | 2.64 |
| $TiO_2$ | 0.65 | 0.38 | 1.1 | 0.18 | 0.34 | 0.25 | 0.09 | 0.10 |
| $P_2O_5$ | 0.17 | 0.08 | 0.42 | <0.05 | <0.1 | <0.1 | <0.1 | <0.1 |
| MnO | 0.09 | 0.05 | 0.15 | <0.02 | <0.02 | 0.07 | 0.04 | 0.04 |
| $CO_2$ | 0.02 | 0.03 | 0.13 | 0.02 | <0.01 | <0.01 | 0.02 | <0.01 |
| $H_2O+$ | 0.69 | 0.2 | 0.7 | 0.77 | 0.91 | 0.24 | 5.26 | 5.13 |
| $H_2O-$ | 0.2 | 0.28 | 0.42 | 0.39 | 1.15 | 0.05 | 0.23 | 0.54 |
| Total | 99.4 | 99.1 | 99.8 | 99.8 | 99.3 | 99.5 | 99.0 | 99.4 |
| Rb (XRF) | 107 | 146 | 79 | 137 | 120 | 79 | 198 | 227 |
| Cs | 4.2 | 3.7 | 3.6 | 1.1 | 2.4 | 1.0 | 11.6 | 12.4 |
| Sr (XRF) | 261 | 189 | 458 | 73 | 111 | 12 | 19 | 76 |
| Ba (XRF) | 1460 | 1340 | 1340 | 1440 | 1313 | 399 | 320 | 1123 |
| La | 51 | 50 | 53 | 50 | 56 | 98 | 55 | 55 |
| Ce | 92 | 82.5 | 94 | 85 | 89 | 165 | 101 | 103 |
| Nd | 39 | 32 | 39 | 27 | 41 | 57 | 35 | 36 |
| Sm | 7.1 | 5.3 | 7.2 | 4.5 | 6.65 | 11.7 | 9.4 | 8.2 |
| Eu | 1.55 | 0.83 | 1.68 | 0.46 | 1.01 | 1.29 | 0.43 | 0.44 |
| Gd | 6.9 | 4.25 | 6.3 | 4.4 | 7.2 | 9.4 | 10.4 | 11.4 |
| Tb | 1.08 | 0.66 | 0.89 | 0.52 | 0.67 | 1.01 | 1.05 | 0.97 |
| Tm | 0.57 | 0.39 | 0.38 | 0.34 | 0.43 | 0.74 | 0.79 | 1.1 |
| Yb | 3.9 | 3.15 | 3.3 | 2.4 | 3.6 | 5.6 | 5.7 | 5.7 |
| Lu | 0.59 | 0.44 | 0.47 | 0.36 | 0.55 | 0.89 | 0.86 | 0.89 |
| Y (XRF) | 38 | 32 | 31 | 29 | 41 | 50 | 50 | 40 |
| Y (ICP) | - - | - - | - - | - - | - - | - - | - - | - - |
| Zr (XRF) | 392 | 318 | 256 | 224 | 303 | 579 | 384 | 241 |
| Hf | 9.5 | 7.3 | 6.6 | 5.4 | 7.7 | 13.6 | 9.7 | 9.9 |
| Nb (XRF) | 19 | 16 | 18 | 25 | 21 | 21 | 31 | 22 |
| Nb (ICP-AES) | - - | - - | - - | - - | - - | - - | - - | - - |
| Ta | 1.77 | 1.77 | 1.55 | 1.82 | 1.8 | 1.96 | 2.47 | 2.44 |
| Th | 15.1 | 19.9 | 11.3 | *22.7* | *22.5* | *20.1* | *30.9* | *22.4* |
| U | 4.2 | 4 | 3.1 | 5.0 | *7.51* | *3.77* | *8.8* | *8.91* |
| Co (ICP) | - - | - - | - - | - - | - - | - - | - - | - - |
| Co | 4.7 | 2.1 | 8.7 | 0.8 | 0.7 | 0.5 | 0.2 | 0.2 |
| Cr (ICP) | - - | - - | - - | - - | - - | - - | - - | - - |
| Cr | 6.5 | 4.9 | 3.5 | 2.9 | 1.3 | 0.1 | 3.4 | <0.7 |
| Ni (ICP) | - - | - - | - - | - - | - - | - - | - - | - - |
| Ni | - - | - - | - - | - - | - - | - - | - - | - - |
| Sc | 8.21 | 4.54 | 10.7 | 2.88 | 5.1 | 3.09 | 1.83 | 1.69 |
| Sc (ICP) | - - | - - | - - | - - | - - | - - | - - | - - |
| V (ICP) | - - | - - | - - | - - | - - | - - | - - | - - |
| Zn | 80 | 42.5 | 115 | 22 | 62 | 55 | 72 | 72 |
| Sb | 2.1 | 0.4 | 2.1 | 0.3 | 1.8 | 1.9 | 2.2 | 1.5 |

**Table 4.** Major oxide and trace-element composition of Tertiary volcanic rocks (Tg, Thr, Td, Ta) from the Blackburn Hills volcanic field, Unalakleet quadrangle, west-central Alaska—*Continued*

| Sample No. | 80ML060d | 80ML001c | 80ML001h | 80ML009f | 80ML011c | 80ML012a | 86ML018 | 86ML019 |
|---|---|---|---|---|---|---|---|---|
| Map Unit | Td | Ta | Ta | Ta | Ta | Ta | Ta | Ta |
| Rock Type | Rhyolite | Andesite | Andesite | Basalt | Andesite | Andesite | Andesite | Andesite |
| Map No. | 45 | 46 | 47 | 48 | 49 | 50 | 51 | 52 |
| Township | T24S | T25S | T25S | T23S | T23S | T23S | T28S | T28S |
| Range | R7W | R7W | R7W | R7W | R7W | R7W | R8W | R8W |
| $SiO_2$ | 73.1 | 55.6 | 58.5 | 51.6 | 58.7 | 60.4 | 56.6 | 53.2 |
| $Al_2O_3$ | 13.9 | 16.0 | 16.5 | 17.0 | 16.5 | 16.7 | 16.4 | 17.5 |
| $Fe_2O_3$ | 1.4 | 4.2 | 4.6 | 3.2 | 3.4 | 4.6 | 3.3 | 3.3 |
| FeO | 0.58 | 4.01 | 1.91 | 6.31 | 1.94 | 0.98 | 4.28 | 4.54 |
| MgO | 0.51 | 3.3 | 2.6 | 4.9 | 3.70 | 2.20 | 3.94 | 4.43 |
| CaO | 0.14 | 6.99 | 5.62 | 8.86 | 6.56 | 4.03 | 6.97 | 9.15 |
| $Na_2O$ | 3.90 | 3.70 | 3.80 | 3.60 | 3.60 | 4.60 | 3.71 | 3.06 |
| $K_2O$ | 4.37 | 1.42 | 1.93 | 1.05 | 1.95 | 2.40 | 1.29 | 0.98 |
| $TiO_2$ | 0.33 | 1.71 | 1.15 | 1.89 | 0.95 | 0.92 | 1.35 | 1.33 |
| $P_2O_5$ | <0.1 | 0.52 | 0.30 | 0.50 | 0.30 | 0.40 | 0.29 | 0.30 |
| MnO | 0.02 | 0.14 | 0.09 | 0.16 | 0.08 | 0.04 | 0.13 | 0.14 |
| $CO_2$ | <0.01 | 0.33 | 0.02 | 0.01 | 0.51 | 0.14 | 0.09 | 0.20 |
| $H_2O+$ | 0.81 | 0.49 | 0.69 | 0.56 | 0.63 | 1.35 | 0.23 | 0.26 |
| $H_2O-$ | 0.39 | 1.24 | 1.59 | 0.65 | 1.03 | 0.65 | 0.75 | 0.78 |
| Total | 99.5 | 99.7 | 99.3 | 100.3 | 99.8 | 99.4 | 99.4 | 99.2 |
| Rb (XRF) | 125 | 50 | 57 | 20 | 62 | 76 | 28 | 22 |
| Cs | 1.2 | 1.1 | 1.2 | 1.2 | 1.5 | 3.2 | 0.972 | 1.02 |
| Sr (XRF) | 92 | 497 | 400 | 538 | 757 | 696 | 390 | 520 |
| Ba (XRF) | 1874 | 854* | 1180* | 458 | 1200 | 1733 | 830 | 550 |
| La | 50 | 33 | 37 | 24 | 36 | 56 | 29.5 | 20.8 |
| Ce | 83 | 60 | 62 | 48 | 61 | 85 | 60.2 | 43.5 |
| Nd | 32 | 33 | 24 | 25 | 27 | 33 | 25.1 | 19.3 |
| Sm | 4.3 | 5.5 | 4.5 | 4.75 | 3.95 | 5.55 | 5.50 | 4.55 |
| Eu | 0.67 | 1.62 | 1.38 | 1.63 | 1.08 | 1.41 | 1.77 | 1.51 |
| Gd | 4.5 | 6.5 | 5.6 | 5.6 | 4.6 | 5.0 | 5.70 | 4.88 |
| Tb | 0.4 | 0.64 | 0.53 | 0.54 | 0.305 | 0.42 | 0.891 | 0.692 |
| Tm | 0.3 | 0.55 | 0.42 | 0.41 | 0.28 | 0.25 | 0.494 | 0.366 |
| Yb | 2.6 | 3.15 | 2.65 | 2.7 | 1.2 | 1.25 | 3.10 | 2.27 |
| Lu | 0.38 | 0.5 | 0.4 | 0.48 | 0.16 | 0.17 | 0.468 | 0.323 |
| Y (XRF) | 25 | -- | -- | 25 | 14 | 16 | 25 | 17 |
| Y (ICP) | -- | -- | -- | -- | -- | -- | 27 | 20 |
| Zr (XRF) | 231 | 216* | 215* | 200 | 170 | 198 | 210 | 140 |
| Hf | 5.9 | 4.4 | 4.6 | 4.1 | 3.7 | 4.4 | 5.03 | 3.38 |
| Nb (XRF) | 22 | -- | -- | 19 | 19 | 25 | 14 | 12 |
| Nb (ICS-AES) | -- | -- | -- | -- | -- | -- | 12.5 | 8.5 |
| Ta | 1.93 | 1.1 | 1.13 | 1.45 | 1.09 | 1.53 | 0.978 | 0.656 |
| Th | 22.2 | 7.2 | 10.25 | 2.85 | 9.75 | 13.9 | 5.61 | 3.89 |
| U | 6.75 | 2.7 | 3.45 | 1 | 3.1 | 5.05 | 1.78 | 1.17 |
| Co (ICP) | -- | -- | -- | -- | -- | -- | 26 | 28 |
| Co | 2.1 | 21.5 | 19.3 | 29.8 | 19.4 | 15.4 | 24.6 | 27.8 |
| Cr (ICP) | -- | -- | -- | -- | -- | -- | 30 | 119 |
| Cr | 3.0 | 25.5 | 10.4 | 75.7 | 114 | 82.2 | 20.5 | 86.4 |
| Ni (ICP) | -- | -- | -- | -- | -- | -- | 19 | 39 |
| Ni | -- | -- | -- | -- | -- | -- | 30.0 | 55.8 |
| Sc | 3.83 | 20.9 | 14.95 | 24.7 | 11.6 | 9.84 | 23.0 | 25.8 |
| Sc (ICP) | -- | -- | -- | -- | -- | -- | 22 | 23 |
| V (ICP) | -- | -- | -- | -- | -- | -- | 161 | 186 |
| Zn | 38 | 75 | 61 | 81 | 55 | 64 | 79.4 | 76.5 |
| Sb | 0.9 | 0.8 | 1.3 | 1.2 | 2.1 | 1.1 | 0.301 | 0.240 |

**Table 5.** Major oxide and trace-element composition of Late Cretaceous and Tertiary and volcanic and plutonic rocks (TKr, TKa, TKa) from the Unalakleet quadrangle, west-central Alaska

[Major elements in weight percent; trace elements in parts per million. All major oxides except FeO, $CO_2$, $H_2O+$, and $H_2O-$ by X-ray fluorescence following methods of Taggart and others (1990). FeO by titration following method of Papp and others (1990). $CO_2$ and $H_2O$ by methods of Norton and Papp (1990). Trace elements by instrumental neutron activation analysis (INAA) unless otherwise noted in first column by following acronyms: XRF, energy-dispersive X-ray fluorescence; ICP, inductively coupled plasma-emission spectrometry. Nb analyses labeled (ICP-AES) were determined using inductively coupled plasma-atomic emission spectrometry using unpublished method developed by T.L. Fries of USGS, Menlo Park, Calif. Other methods described by Baedecker (1987). nd, not accurately determined; - -, not analyzed. USGS analysts: D. Kobilis, R.G. Johnson, L.J. Schwarz, and B. Scott, Reston, Va.; S.T. Neil and D.V. Vivit, Menlo Park, Calif.; A.J. Bartel, K. Stewart, J.E. Taggart, Jr., B. Anderson, L. Bradley, J.R. Budahn, R.J. Knight, and D.M. McKown, Lakewood, Colo.]

| Sample No. | 86ML034 | 86Pa021 | 81Pa330 | 86ML004 | 86Pa043 | 81Pa332b | 81Pa334 |
|---|---|---|---|---|---|---|---|
| Map Unit | TKr | TKr | TKr | TKa | TKa | TKa | TKa |
| Rock Type | Rhyolite | Rhyolite | Rhyolite | Diabase | Lamprophyre dike | Basalt | Andesite |
| Map No. | 53 | 54 | 55 | 56 | 57 | 58 | 59 |
| Township | T29S | T27S | T19S | T27S | T28S | T20S | T20S |
| Range | R16W | R9W | R3W | R10W | R17W | R3W | R3W |
| $SiO_2$ | 70.9 | 69.5 | 75.3 | 46.2 | 48.4 | 48.7 | 57.3 |
| $Al_2O_3$ | 14.5 | 14.3 | 13.1 | 20.3 | 17.2 | 18.4 | 16.0 |
| $Fe_2O_3$ | 2.03 | 1.89 | 0.61 | 3.74 | 5.01 | 4.26 | 4.26 |
| FeO | 0.39 | 0.49 | 0.08 | 4.16 | 2.17 | 6.10 | 3.00 |
| MgO | 0.60 | 0.66 | 0.15 | 4.60 | 3.40 | 4.24 | 3.45 |
| CaO | 1.87 | 1.88 | 0.41 | 10.20 | 8.40 | 9.31 | 6.86 |
| $Na_2O$ | 4.34 | 3.70 | 3.87 | 3.50 | 3.70 | 3.77 | 3.75 |
| $K_2O$ | 2.64 | 2.76 | 4.58 | 0.74 | 3.94 | 0.81 | 1.89 |
| $TiO_2$ | 0.28 | 0.32 | 0.16 | 0.86 | 1.00 | 2.17 | 1.43 |
| $P_2O_5$ | 0.09 | 0.10 | <0.05 | 0.18 | 0.62 | 0.66 | 0.39 |
| MnO | 0.06 | 0.06 | <0.02 | 0.13 | 0.14 | 0.19 | 0.11 |
| $CO_2$ | <0.05 | 0.40 | 0.02 | 0.62 | 0.21 | 0.02 | 0.02 |
| $H_2O+$ | 0.97 | 1.81 | 0.5 | 2.45 | 3.70 | 0.83 | 0.83 |
| $H_2O-$ | 0.70 | 1.00 | 0.43 | 1.48 | 0.44 | 0.5 | 0.94 |
| Total | 99.4 | 98.9 | 99.2 | 99.2 | 98.3 | 100.0 | 100.2 |
| Pb | 57.3 | 99.3 | 121.0 | 17.1 | 71.9 | 12.0 | 46.0 |
| Rb (XRF) | 50 | 98 | 128 | 10 | 96 | 17 | 50 |
| Cs | 1.34 | 3.23 | 1.80 | 1.19 | 41.10 | 0.50 | 2.00 |
| Sr (XRF) | 240 | 196 | 32 | 560 | >1500 | 603 | 475 |
| Ba (XRF) | 850 | 1200 | 800 | 670 | 2450 | 543 | 990 |
| La | 26.3 | 24.8 | 68.0 | 15.9 | 124.0 | 30.0 | 32.0 |
| Ce | 54.4 | 43.9 | 118.0 | 31.6 | 274.0 | 62.0 | 60.0 |
| Nd | 22.3 | 14.3 | 47.0 | 14.4 | 106.0 | 37.0 | 30.0 |
| Sm | 5.09 | 2.67 | 7.90 | 3.32 | 15.10 | 7.90 | 6.10 |
| Eu | 1.170 | 0.669 | 0.38 | 1.110 | 3.630 | 2.23 | 1.65 |
| Gd | 4.91 | 2.39 | 6.10 | 3.46 | 11.40 | 7.50 | 5.70 |
| Tb | 0.759 | 0.376 | 0.98 | 0.535 | 1.210 | 1.08 | 0.86 |
| Tm | 0.464 | 0.239 | 0.44 | 0.288 | 0.460 | 0.5 | 0.41 |
| Yb | 2.760 | 1.500 | 4.1 | 1.750 | 2.740 | 3.9 | 3.2 |
| Lu | 0.407 | 0.217 | 0.52 | 0.258 | 0.388 | 0.56 | 0.48 |
| Y (XRF) | 30 | 18 | 37 | 14 | 44 | 32 | 30 |
| Y (ICP) | 19 | 14 | -- | 18 | 31 | -- | -- |
| Zr (XRF) | 230 | 205 | 207 | 94 | 310 | 209 | 191 |
| Hf | 5.26 | 4.50 | 6.00 | 2.04 | 5.26 | 4.60 | 4.60 |
| Nb (XRF) | 10 | <10 | 30 | <10 | 20 | 14 | 16 |
| Nb (ICP-AES) | 6.0 | 7.2 | -- | 3.3 | 12.9 | -- | -- |
| Ta | 0.663 | 0.801 | 2.050 | 0.232 | 0.820 | 0.910 | 1.120 |
| Th | 7.09 | 14.40 | 18.90 | 6.01 | 28.90 | 1.80 | 5.90 |
| U | 2.67 | 4.42 | 5.20 | 2.01 | 4.52 | 0.50 | 1.70 |
| Co (ICP) | 4 | 7 | -- | 31 | 20 | -- | -- |
| Co | 2.76 | 3.96 | 0.3 | 27.20 | 16.50 | 28.4 | 25.6 |
| Cr (ICP) | 4 | 11 | -- | 64 | 31 | -- | -- |
| Cr | 2.29 | 8.39 | 4.6 | 71.50 | 27.90 | 34.4 | 43.5 |
| Ni (ICP) | <2 | 4 | -- | 34 | 35 | -- | -- |
| Ni | 11.3 | 8.0 | -- | 30.3 | 42.0 | -- | -- |
| Sc (ICP) | 3 | 5 | -- | 28 | 17 | -- | -- |
| Sc | 3.50 | 4.25 | 2.65 | 2.28 | 11.40 | 24.5 | 23.9 |
| V (ICP) | 20 | 26 | -- | 201 | 121 | -- | -- |
| Zn | 56.2 | 44.4 | 27.0 | nd | 103.0 | 95.0 | 99.0 |
| Sb | 0.134 | 0.300 | 0.600 | 0.249 | 0.120 | <0.5 | 0.400 |

**Table 5.** Major oxide and trace-element composition of Late Cretaceous and Tertiary and volcanic and plutonic rocks (TKr, TKa, TKs) from the Unalakleet quadrangle, west-central Alaska—*Continued*

| Sample No. | 86ML043 | 86Pa012b | 86Pa098a | 86Pa098b | 86Pa098c | 86Pa099 | 86Pa100 |
|---|---|---|---|---|---|---|---|
| Map Unit | TKr | TKr | TKr | TKr | TKr | TKr | TKs |
| Rock Type | Rhyolite | Rhyolite dike | Dacite | Dacite | Dacite | Dacite | Rhyolite |
| Map No. | 60 | 61 | 62 | 63 | 64 | 65 | 66 |
| Township | T28S | T28S | T28S | T28S | T28S | T28S | T28S |
| Range | R11W | R10W | R3W | R3W | R3W | R2W | R2W |
| $SiO_2$ | 73.5 | 70.1 | 63.8 | 64.3 | 62.7 | 63.7 | 76.4 |
| $Al_2O_3$ | 13.5 | 14.8 | 15.4 | 16.0 | 16.2 | 15.8 | 12.6 |
| $Fe_2O_3$ | 0.32 | 2.15 | 4.52 | 4.61 | 4.47 | 4.84 | 0.57 |
| FeO | 0.09 | 0.57 | 0.21 | 0.21 | 0.64 | 0.28 | 0.08 |
| MgO | <0.2 | 0.85 | 0.40 | 0.58 | 1.19 | 1.17 | 0.17 |
| CaO | 0.60 | 2.80 | 3.28 | 3.41 | 4.31 | 4.34 | 0.39 |
| $Na_2O$ | 3.80 | 4.30 | 3.60 | 3.20 | 3.39 | 3.44 | 2.65 |
| $K_2O$ | 4.08 | 1.92 | 2.58 | 2.65 | 2.50 | 2.72 | 5.51 |
| $TiO_2$ | 0.06 | 0.38 | 0.60 | 0.62 | 0.69 | 0.64 | 0.17 |
| $P_2O_5$ | 0.04 | 0.20 | 0.22 | 0.22 | 0.24 | 0.23 | 0.03 |
| MnO | 0.07 | 0.05 | 0.02 | 0.01 | 0.02 | 0.03 | <0.01 |
| $CO_2$ | <0.05 | 0.15 | 0.11 | 0.07 | 0.06 | <0.05 | 0.08 |
| $H_2O+$ | 2.33 | 0.98 | 1.14 | 0.96 | 0.75 | 0.72 | 0.48 |
| $H_2O-$ | 0.80 | 0.45 | 2.99 | 2.64 | 2.33 | 1.66 | 0.94 |
| Total | 99.2 | 99.7 | 98.9 | 99.5 | 99.5 | 99.6 | 100.1 |
| | | | | | | | |
| Rb | 176.0 | 48.6 | 72.3 | 75.8 | 74.1 | 84.4 | 106.0 |
| Rb (XRF) | 160 | 44 | 68 | 70 | 70 | 78 | 110 |
| Cs | 13.50 | 1.75 | 2.49 | 2.16 | 2.58 | 2.27 | 2.15 |
| Sr (XRF) | 35 | 260 | 470 | 480 | 560 | 540 | 33 |
| Ba (XRF) | 690 | 670 | 1650 | 1700 | 1650 | 1650 | 540 |
| La | 8.8 | 20.9 | 54.7 | 53.0 | 67.3 | 39.5 | 42.8 |
| Ce | 18.2 | 44.5 | 96.9 | 84.8 | 76.1 | 69.8 | 74.3 |
| Nd | 7.1 | 17.8 | 35.8 | 34.4 | 42.8 | 26.0 | 24.4 |
| Sm | 1.75 | 3.79 | 6.31 | 6.39 | 7.00 | 4.57 | 3.66 |
| Eu | 0.247 | 1.030 | 1.340 | 1.370 | 1.610 | 1.210 | 0.463 |
| Gd | 1.84 | 3.56 | 5.02 | 5.18 | 6.01 | 3.84 | 2.69 |
| Tb | 0.263 | 0.494 | 0.710 | 0.687 | 0.783 | 0.492 | 0.314 |
| Tm | 0.141 | 0.261 | 0.324 | 0.304 | 0.289 | nd | nd |
| Yb | 0.835 | 1.610 | 1.820 | 1.740 | 1.77 | 1.330 | 0.789 |
| Lu | 0.103 | 0.235 | 0.256 | 0.252 | 0.255 | 0.189 | 0.106 |
| Y (XRF) | 10 | 18 | 20 | 20 | 22 | 14 | <10 |
| Y (ICP) | 10 | 12 | 19 | 19 | 21 | 14 | 8 |
| Zr (XRF) | 42 | 235 | 176 | 180 | 170 | 170 | 120 |
| Hf | 1.95 | 4.86 | 4.20 | 4.22 | 4.15 | 4.03 | 3.02 |
| Nb (XRF) | 18 | <10 | 14 | 15 | 17 | 14 | 22 |
| Nb (ICP-AES) | 14.9 | 6.4 | 12.3 | 12.0 | 12.0 | 11.5 | 15.5 |
| Ta | 1.590 | 0.607 | 1.040 | 1.030 | 0.930 | 0.975 | 1.360 |
| Th | 11.40 | 5.34 | 12.40 | 12.50 | 11.40 | 11.90 | 19.40 |
| U | 8.03 | 2.22 | 3.91 | 3.97 | 3.91 | 4.23 | 3.35 |
| Co (ICP) | 2 | 6 | 11 | 10 | 11 | 13 | 3 |
| Co | 0.421 | 4.81 | 7.86 | 8.38 | 9.50 | 10.30 | 1.85 |
| Cr (ICP) | 1 | 9 | 48 | 66 | 81 | 46 | 3 |
| Cr | <0.7 | 8.18 | 38.6 | 40.2 | 53.60 | 30.80 | 1.60 |
| Ni (ICP) | <2.0 | 12.0 | 37 | 45 | 53 | 51 | 5 |
| Ni | <3.1 | 16.4 | 34.8 | 42.2 | 44.0 | 39.7 | 7.76 |
| Sc (ICP) | 2 | 5 | 13 | 10 | 12 | 10 | <2 |
| Sc | 2.22 | 23.9 | 10.5 | 10.8 | 12.6 | 10.80 | 1.54 |
| V (ICP) | 3 | 32 | 68 | 72 | 80 | 75 | 5 |
| Zn | 32.8 | 48.7 | 56.7 | 74.7 | 80.3 | 62.3 | 20.7 |
| Sb | 1.6 | 0.0366 | 0.409 | 0.330 | 0.301 | 0.346 | 0.428 |

**Table 6.** Major oxide and trace-element composition of Early Cretaceous shoshonitic flows and tuffs (Kft) from the Unalakleet quadrangle, west-central Alaska

[Major elements in weight percent; trace elements in parts per million. All major oxides except FeO, $CO_2$, $H_2O+$, and $H_2O-$ by X-ray fluorescence following methods of Taggart and others (1990). FeO by titration following method of Papp and others (1990). $CO_2$ and $H_2O$ by methods of Norton and Papp (1990). Trace elements by instrumental neutron activation analysis (INAA) unless otherwise noted in first column by following acronyms: XRF, energy-dispersive X-ray fluorescence; ICP, inductively coupled plasma-emission spectrometry. Nb analyses labeled (ICP-AES) were determined using inductively coupled plasma-atomic emission spectrometry using unpublished method developed by T.L. Fries of USGS, Menlo Park, Calif. Other methods described by Baedecker (1987). nd, not accurately determined; - -, not analyzed. USGS analysts: D. Kobilis, R.G. Johnson, L.J. Schwarz, B. Scott, H.J. Rose, B.A. McCall, G. Sellers, and J.R. Lindsay, Reston, Va.; S.T. Neil and D.V. Vivit, Menlo Park, Calif.; A.J. Bartel, K. Stewart, J.E. Taggart, Jr., B. Anderson, L.A. Bradley, J.R. Budahn, R.J. Knight, D.M. McKown, J.S. Wahlberg, J.W. Baker, H.G. Neiman, F.D. Newman, and G.R. Mason, Lakewood, Colo.]

| Sample No. | 86ML022 | 86ML041d | 80ML045a | 86Pa018a | 86Pa018b | 86Pa020 | 80Pa079a |
|---|---|---|---|---|---|---|---|
| Map Unit | Kft | Kft | Kft | Kft | Kft | Kft | Kft |
| Rock Type | Shoshonitic andesite | Syenite | Shoshonite | Shoshonite | Shoshonitic andesite | Tuff | Shoshonitic andesite |
| Map No. | 67 | 68 | 69 | 70 | 71 | 72 | 73 |
| Township | T27S | T27S | T25S | T28S | T28S | T27S | T25S |
| Range | R9W | R9W | R8W | R9W | R9W | R9W | R8W |
| $SiO_2$ | 49.7 | 54.3 | 51.0 | 49.7 | 58.5 | 61.0 | 59.6 |
| $Al_2O_3$ | 16.9 | 17.3 | 19.6 | 20.3 | 15.7 | 16.8 | 18.6 |
| $Fe_2O_3$ | 3.21 | 3.09 | 3.56 | 2.20 | 1.81 | 2.77 | 2.35 |
| FeO | 4.44 | 3.14 | 3.31 | 3.54 | 4.25 | 2.10 | 2.38 |
| MgO | 5.37 | 3.80 | 3.30 | 1.50 | 1.70 | 1.00 | 0.78 |
| CaO | 5.06 | 2.88 | 7.18 | 6.72 | 5.34 | 1.02 | 2.05 |
| $Na_2O$ | 2.93 | 3.40 | 3.20 | 4.70 | 3.40 | 3.50 | 4.51 |
| $K_2O$ | 4.37 | 6.02 | 4.13 | 2.64 | 2.28 | 7.78 | 7.36 |
| $TiO_2$ | 0.92 | 0.66 | 1.04 | 0.86 | 0.30 | 0.38 | 0.54 |
| $P_2O_5$ | 0.49 | 0.36 | 0.40 | 0.28 | 0.20 | 0.10 | 0.18 |
| MnO | 0.16 | 0.16 | 0.14 | 0.11 | 0.11 | 0.10 | 0.15 |
| $CO_2$ | 0.07 | 0.09 | 0.28 | 3.64 | 2.83 | 0.34 | 0.08 |
| $H_2O+$ | 3.26 | 2.12 | 1.79 | 2.48 | 2.25 | 1.47 | 1.07 |
| $H_2O-$ | 1.20 | 0.86 | 0.69 | 0.58 | 0.42 | 0.47 | 0.27 |
| Total | 98.1 | 98.2 | 99.6 | 99.3 | 99.1 | 98.8 | 99.9 |
| | | | | | | | |
| Rb | 132.0 | 150.0 | 163.0 | 116.0 | 84.2 | 279.0 | -- |
| Rb (XRF) | 120 | 142 | 164 | 116 | 76 | 260 | 256 |
| Cs | 20.70 | 11.70 | 20.10 | 11.50 | 4.90 | 1.04 | -- |
| Sr (XRF) | 820 | 660 | 899 | 720 | 465 | 110 | 387 |
| Ba (XRF) | 6200* | 5750* | 1751 | 1450 | 1000 | 400 | 1485 |
| La | 47.1 | 43.4 | 52.0 | 39.0 | 53.4 | 107.0 | -- |
| Ce | 95.0 | 81.9 | 92.0 | 75.9 | 86.7 | 217.0 | -- |
| Nd | 36.9 | 31.2 | 41.0 | 26.5 | 30.8 | 74.4 | -- |
| Sm | 7.21 | 5.45 | 5.70 | 5.37 | 4.56 | 12.30 | -- |
| Eu | 3.080 | 2.890 | 1.680 | 1.560 | 1.260 | 0.802 | -- |
| Gd | 6.54 | 5.05 | 7.40 | 4.78 | 3.80 | 11.40 | -- |
| Tb | 0.941 | 0.737 | 0.610 | 0.664 | 0.566 | 1.600 | -- |
| Tm | 0.431 | 0.369 | 0.450 | 0.387 | 0.388 | 0.958 | -- |
| Yb | 2.570 | 2.230 | 2.700 | 2.380 | 2.120 | 6.100 | -- |
| Lu | 0.365 | 0.310 | 0.420 | 0.348 | 0.318 | 0.901 | -- |
| Y (XRF) | 30 | 30 | 28 | 24 | 20 | 64 | 46 |
| Y (ICP) | 27 | 23 | -- | 21 | 17 | 51 | -- |
| Zr (XRF) | 180 | 194 | 216 | 220 | 305 | 490 | 482 |
| Hf | 4.07 | 3.77 | 4.70 | 4.68 | 6.98 | 12.40 | -- |
| Nb (XRF) | 12 | 14 | 12 | 14 | 12 | 30 | 33 |
| Nb (ICP-AES) | 8.0 | 8.8 | -- | 9.6 | 10.0 | 26.4 | -- |
| Ta | 0.568 | 0.570 | 0.840 | 0.781 | 1.240 | 2.410 | -- |
| Th | 15.20 | 15.90 | 22.10 | 16.80 | 41.80 | 51.30 | -- |
| U | 4.87 | 4.89 | 6.40 | 5.46 | 8.84 | 18.20 | -- |
| Co (ICP) | 25 | 20 | -- | 18 | 21 | 4 | -- |
| Co | 21.60 | 13.50 | 19.90 | 16.00 | 18.20 | 3.48 | -- |
| Cr (ICP) | 113 | 80 | -- | 35 | 35 | 14 | -- |
| Cr | 88.10 | 79.70 | 69.80 | 33.6 | 28.5 | 19.4 | -- |
| Ni (ICP) | 44 | 35 | -- | 28 | 54 | 8 | -- |
| Ni | 46.6 | 44.6 | -- | 28.6 | 40.5 | 9.8 | -- |
| Sc (ICP) | 16 | 13 | -- | 14 | 20 | 4 | -- |
| Sc | 17.70 | 10.70 | 13.3 | 12.40 | 19.2 | 4.29 | -- |
| V (ICP) | 146 | 73 | -- | 132 | 59 | 15 | -- |
| Zn | 75.7 | 71.0 | 70.0 | 71.2 | 72.4 | 136 | -- |
| Sb | 0.346 | 0.295 | 1.300 | 0.371 | 0.475 | 1.53 | -- |

**Table 6.** Major oxide and trace-element composition of Early Cretaceous shoshonitic flows and tuffs (Kft) from the Unalakleet quadrangle, west-central Alaska—*Continued*

| Sample No. | 80Pa080a | 80Pa080b | 86Pa092a | 86Pa092b | 81Pa208 | 81Pa229 |
|---|---|---|---|---|---|---|
| Map Unit | Kft | Kft | Kft | Kft | Kft | Kft |
| Rock Type | Shoshonitic andesite | Shoshonitic andesite | Shoshonite | Shoshonite | Shoshonitic andesite | Syenite |
| Map No. | 74 | 75 | 76 | 77 | 78 | 79 |
| Township | T25S | T25S | T27S | T27S | T25S | T26S |
| Range | R8W | R8W | R10W | R10W | R8W | R8W |
| $SiO_2$ | 54.0 | 57.1 | 44.6 | 43.9 | 54.8 | 60.6 |
| $Al_2O_3$ | 18.0 | 17.6 | 15.3 | 14.7 | 17.4 | 17.8 |
| $Fe_2O_3$ | 1.97 | 1.54 | 3.79 | 3.74 | 2.63 | 2.60 |
| FeO | 2.74 | 3.90 | 5.53 | 5.44 | 2.70 | 1.40 |
| MgO | 1.85 | 2.42 | 4.10 | 4.00 | 1.44 | 0.66 |
| CaO | 8.85 | 4.23 | 11.20 | 11.60 | 4.86 | 0.80 |
| $Na_2O$ | 3.16 | 3.60 | 2.00 | 2.00 | 3.96 | 5.75 |
| $K_2O$ | 3.97 | 5.28 | 2.32 | 2.28 | 5.15 | 6.12 |
| $TiO_2$ | 0.96 | 0.53 | 1.52 | 1.52 | 0.53 | 0.41 |
| $P_2O_5$ | 0.40 | 0.30 | 0.68 | 0.68 | 0.16 | 0.09 |
| MnO | 0.09 | 0.10 | 0.16 | 0.17 | 0.07 | 0.13 |
| $CO_2$ | 3.26 | 2.12 | 5.46 | 5.86 | 2.30 | 0.02 |
| $H_2O+$ | 1.23 | 1.92 | 2.63 | 2.68 | 1.50 | 0.95 |
| $H_2O-$ | 0.18 | 0.42 | 0.61 | 0.54 | 0.44 | 0.32 |
| Total | 100.7 | 100.6 | 99.9 | 99.1 | 97.9 | 97.7 |
| Rb | -- | -- | 83.0 | 85.9 | 156.0 | 193.0 |
| Rb (XRF) | 144 | 128 | 82 | 76 | 158 | 185 |
| Cs | -- | -- | 2.43 | 2.43 | 3.80 | 0.90 |
| Sr (XRF) | 599 | 376 | 720 | 710 | 401 | 60 |
| Ba (XRF) | 1359 | 1737 | 1850 | 1900 | 1770 | 50 |
| La | -- | -- | 42.3 | 44.0 | 73.0 | 86.0 |
| Ce | -- | -- | 85.6 | 89.0 | 125.0 | 142.0 |
| Nd | -- | -- | 38.0 | 40.7 | 50.0 | 57.0 |
| Sm | -- | -- | 7.65 | 7.84 | 8.20 | 9.00 |
| Eu | -- | -- | 2.230 | 2.280 | 1.800 | 0.680 |
| Gd | -- | -- | 7.01 | 6.98 | 6.80 | 7.60 |
| Tb | -- | -- | 0.903 | 0.965 | 0.890 | 0.970 |
| Tm | -- | -- | 0.403 | 0.410 | 0.540 | 0.440 |
| Yb | -- | -- | 2.340 | 2.440 | 4.100 | 4.200 |
| Lu | -- | -- | 0.333 | 0.336 | 0.530 | 0.480 |
| Y (XRF) | 36 | 42 | 34 | 28 | 39 | 39 |
| Y (ICP) | -- | -- | 27 | 27 | -- | -- |
| Zr (XRF) | 162 | 326 | 160 | 160 | 350 | 379 |
| Hf | -- | -- | 3.67 | 3.69 | 7.80 | 8.30 |
| Nb (XRF) | 14 | 24 | 12 | 10 | 19 | 18 |
| Nb (ICP-AES) | -- | -- | 8.2 | 8.2 | -- | -- |
| Ta | -- | -- | 0.586 | 0.575 | 1.450 | 1.740 |
| Th | -- | -- | 12.80 | 13.00 | 36.50 | 35.70 |
| U | -- | -- | 3.72 | 4.18 | 11.10 | 11.10 |
| Co (ICP) | -- | -- | 28 | 28 | -- | -- |
| Co | -- | -- | 24.30 | 24.90 | 9.90 | 1.70 |
| Cr (ICP) | -- | -- | 107 | 91 | -- | -- |
| Cr | -- | -- | 111.0 | 104.00 | 140.00 | 2.80 |
| Ni (ICP) | -- | -- | 42 | 44 | -- | -- |
| Ni | -- | -- | 46.1 | 48.8 | -- | -- |
| Sc | -- | -- | 24 | 23 | 6.99 | 2.87 |
| Sc (ICP) | -- | -- | 22.00 | 21.70 | -- | -- |
| V (ICP) | -- | -- | 211 | 213 | -- | -- |
| Zn | -- | -- | 84.2 | 84.0 | 93.0 | 116.0 |
| Sb | -- | -- | 0.235 | 0.195 | 0.500 | 0.600 |

**Table 7.** Major oxide and trace-element composition of Middle and Late Jurassic plutonic rocks (Jt) from the Unalakleet quadrangle, west-central Alaska

[Major elements in weight percent; trace elements in parts per million. All major oxides except FeO, $CO_2$, $H_2O+$, and $H_2O-$ by X-ray fluorescence following methods of Taggart and others (1990). FeO by titration following method of Papp and others (1990). $CO_2$ and $H_2O$ by methods of Norton and Papp (1990). Trace elements by instrumental neutron activation analysis (INAA) unless otherwise noted in first column by following acronyms: XRF, energy-dispersive X-ray fluorescence; ICP, inductively coupled plasma-emission spectrometry. Nb analyses labeled (ICP-AES) were determined using inductively coupled plasma-atomic emission spectrometry using unpublished method developed by T.L. Fries of USGS, Menlo Park. Other methods described by Baedecker (1987). nd, not accurately determined; - -, not analyzed. USGS analysts: R.G. Johnson, L.J. Schwarz, B. Scott, H.J. Rose, B.A. McCall, G. Sellers, and J.R. Lindsay, Reston, Va.; S.T. Neil and D.V. Vivit, Menlo Park, Calif.; J.E. Taggart, Jr., B. Anderson, L.A. Bradley, J.R. Budahn, R.J. Knight, D.M. McKown, J.S. Wahlberg, J.W. Baker, H.G. Neiman, F.D. Newman, and G.R. Mason, Lakewood, Colo.]

| Sample No. | 86ML036 | 86Pa005 | 86Pa084a | 86Pa084b | 80Pa002a | 80Pa012a |
|---|---|---|---|---|---|---|
| Map Unit | Jt | Jt | Jt | Jt | Jt | Jt |
| Rock Type | Altered tonalite | Altered tonalite | Gabbro | Gabbro | Trondhjemite | Hbd Tonalite |
| Map No. | 80 | 81 | 82 | 83 | 84 | 85 |
| Township | T27S | T27S | T27S | T27S | T21S | T19S |
| Range | R12W | R11W | R12W | R12W | R9W | R8W |
| $SiO_2$ | 57.3 | 58.6 | 50.6 | 51.5 | 69.4 | 50.3 |
| $Al_2O_3$ | 15.6 | 16.6 | 15.2 | 16.5 | 14.0 | 17.2 |
| $Fe_2O_3$ | 2.57 | 2.05 | 4.19 | 5.37 | 1.87 | 2.49 |
| FeO | 3.82 | 4.36 | 4.86 | 5.34 | 2.29 | 5.96 |
| MgO | 3.70 | 3.30 | 8.40 | 4.70 | 1.50 | 5.86 |
| CaO | 5.18 | 6.48 | 8.08 | 8.06 | 3.32 | 7.71 |
| $Na_2O$ | 3.70 | 3.40 | 3.40 | 3.40 | 3.76 | 4.05 |
| $K_2O$ | 1.80 | 1.58 | 0.64 | 0.80 | 1.59 | 1.09 |
| $TiO_2$ | 0.86 | 0.90 | 0.66 | 1.38 | 0.38 | 0.99 |
| $P_2O_5$ | 0.24 | 0.22 | 0.06 | 0.10 | 0.11 | 0.19 |
| MnO | 0.11 | 0.12 | 0.21 | 0.19 | 0.07 | 0.20 |
| $CO_2$ | 1.59 | 0.20 | <0.05 | <0.05 | <0.01 | 0.01 |
| $H_2O+$ | 2.23 | 1.56 | 2.31 | 1.38 | 1.01 | 2.41 |
| $H_2O-$ | 0.35 | 0.16 | 0.24 | 0.18 | 0.28 | 0.33 |
| Total | 99.1 | 99.5 | 98.9 | 98.9 | 99.6 | 98.8 |
| Rb | 37.2 | 30.0 | 7.1 | 11.3 | - - | - - |
| Rb (XRF) | 26 | 24 | <10 | 12 | 31 | 23 |
| Cs | 2.09 | 0.415 | 0.685 | 0.96 | - - | - - |
| Sr (XRF) | 345 | 435 | 475 | 425 | 202 | 573 |
| Ba (XRF) | 540 | 560 | 305 | 305 | 662 | 532 |
| La | 10.7 | 10.5 | 2.31 | 3.38 | - - | - - |
| Ce | 27.0 | 24.2 | 5.96 | 8.71 | - - | - - |
| Nd | 14.8 | 15.3 | 4.41 | 6.56 | - - | - - |
| Sm | 3.45 | 3.83 | 1.45 | 2.06 | - - | - - |
| Eu | 0.989 | 1.030 | 0.603 | 1.050 | - - | - - |
| Gd | 3.69 | 3.80 | 1.90 | 2.36 | - - | - - |
| Tb | 0.620 | 0.585 | 0.343 | 0.403 | - - | - - |
| Tm | 0.389 | 0.346 | 0.190 | 0.263 | - - | - - |
| Yb | 2.430 | 2.200 | 1.080 | 1.640 | - - | - - |
| Lu | 0.349 | 0.334 | 0.155 | 0.240 | - - | - - |
| Y (XRF) | 22 | 16 | <10 | 14 | 26 | 11 |
| Y (ICP) | 21 | 21 | 14 | 14 | - - | - - |
| Zr (XRF) | 110 | 120 | 40 | 62 | 107 | 58 |
| Hf | 3.36 | 3.31 | 0.892 | 1.12 | - - | - - |
| Nb (XRF) | <10 | <10 | <10 | <10 | <5 | <5 |
| Nb (ICP-AES) | 3.5 | 3.1 | 2.4 | 2.0 | - - | - - |
| Ta | 0.203 | 0.185 | 0.044 | 0.067 | - - | - - |
| Th | 2.01 | 2.83 | 0.291 | 0.265 | 3.8 | - - |
| U | 1.07 | 1.28 | 0.104 | nd | -0.963 | - - |
| Co (ICP) | 20 | 22 | 29 | 29 | - - | - - |
| Co | 18.70 | 20.70 | 33.00 | 28.60 | - - | - - |
| Cr (ICP) | 44 | 45 | 23 | 21 | - - | - - |
| Cr | 42.70 | 39.80 | 174.00 | 20.50 | - - | - - |
| Ni (ICP) | 24 | 25 | 19 | 18 | - - | - - |
| Ni | 19.0 | 28.1 | 64.5 | 23.0 | - - | - - |
| Sc | 21 | 22 | 35 | 35 | - - | - - |
| Sc (ICP) | 20.30 | 22.00 | 34.00 | 34.50 | - - | - - |
| V (ICP) | 155 | 171 | 341 | 343 | - - | - - |
| Zn | 73.2 | 86.8 | 103.0 | 92.8 | - - | - - |
| Sb | 0.799 | 0.412 | nd | 0.130 | - - | - - |

**Table 7.** Major oxide and trace-element composition of Middle and Late Jurassic plutonic rocks (Jt)) from the Unalakleet quadrangle, west-central Alaska—*Continued*

| Sample No. | 80Pa015a | 80Pa051 | 80ML025 | 80ML034 | 80Pa060a |
|---|---|---|---|---|---|
| Map Unit | Jt | Jt | Jt | Jt | Jt |
| Rock Type | Trondhjemite | Gabbro | Tonalite | Trondhjemite | Trondhjemite |
| Map No. | 86 | 87 | 88 | 89 | 90 |
| Township | T20S | T24S | T22S | T23S | T21S |
| Range | R8W | R10W | R9W | R10W | R8W |
| $SiO_2$ | 72.4 | 49.5 | 60.1 | 73.1 | 66.5 |
| $Al_2O_3$ | 14.2 | 20.3 | 15.9 | 13.6 | 15.0 |
| $Fe_2O_3$ | 1.40 | 2.01 | 2.04 | 1.11 | 0.84 |
| FeO | 1.22 | 5.02 | 5.04 | 0.93 | 2.63 |
| MgO | 0.82 | 5.99 | 3.30 | 0.64 | 1.82 |
| CaO | 3.02 | 11.90 | 6.52 | 1.19 | 2.15 |
| $Na_2O$ | 4.03 | 2.79 | 3.10 | 3.10 | 4.96 |
| $K_2O$ | 1.51 | 0.45 | 0.91 | 4.52 | 2.31 |
| $TiO_2$ | 0.32 | 0.50 | 0.88 | 0.26 | 0.42 |
| $P_2O_5$ | 0.15 | 0.05 | 0.10 | <0.1 | 0.14 |
| MnO | 0.06 | 0.13 | 0.12 | 0.05 | 0.09 |
| $CO_2$ | <0.01 | 0.03 | 0.01 | <0.01 | 0.90 |
| $H_2O+$ | 0.62 | 1.83 | 1.40 | 0.59 | 1.66 |
| $H_2O-$ | 0.02 | 0.34 | 0.12 | 0.18 | 0.18 |
| Total | 99.8 | 100.8 | 99.5 | 99.3 | 99.6 |
| Rb | -- | -- | 21.5 | 117.0 | -- |
| Rb (XRF) | 24 | 18 | 24 | 118 | 39 |
| Cs | -- | -- | 0.60 | 1.00 | -- |
| Sr (XRF) | 242 | 552 | 330 | 182 | 515 |
| Ba (XRF) | 533 | 167 | 275 | 1158 | 471 |
| La | -- | -- | 9.0 | 13.0 | -- |
| Ce | -- | -- | 20.0 | 39.5 | -- |
| Nd | -- | -- | 13.0 | 13.0 | -- |
| Sm | -- | -- | 4.70 | 3.20 | -- |
| Eu | -- | -- | 0.950 | 0.565 | -- |
| Gd | -- | -- | 4.35 | 3.60 | -- |
| Tb | -- | -- | 0.380 | 0.310 | -- |
| Tm | -- | -- | 0.455 | 0.335 | -- |
| Yb | -- | -- | 2.550 | 2.100 | -- |
| Lu | -- | -- | 0.425 | 0.325 | -- |
| Y (XRF) | 27 | 11 | 30 | 23 | 17 |
| Y (ICP) | -- | -- | -- | -- | -- |
| Zr (XRF) | 87 | 5 | 99 | 197 | 84 |
| Hf | -- | -- | 2.35 | 5.65 | -- |
| Nb (XRF) | < 5 | < 5 | < 5 | 5 | < 5 |
| Nb (ICP-AES) | -- | -- | -- | -- | -- |
| Ta | -- | -- | 0.270 | 0.510 | -- |
| Th | 2.5 | -- | 2.20 | 8.36 | -- |
| U | 0.948 | -- | 1.20 | 2.79 | -- |
| Co (ICP) | -- | -- | -- | -- | -- |
| Co | -- | -- | 19.40 | 2.95 | -- |
| Cr (ICP) | -- | -- | -- | -- | -- |
| Cr | -- | -- | 11.80 | 2.60 | -- |
| Ni (ICP) | -- | -- | -- | -- | -- |
| Ni | -- | -- | -- | -- | -- |
| Sc (ICP) | -- | -- | -- | -- | -- |
| Sc | -- | -- | 21.95 | 5.10 | -- |
| V (ICP) | -- | -- | -- | -- | -- |
| Zn | -- | -- | 80.0 | 24.5 | -- |
| Sb | -- | -- | 1.30 | 1.35 | -- |

**Table 8.** Major oxide and trace-element composition of Paleozoic(?) and Mesozoic(?) altered basalt and diabase (MzPzb) from the Unalakleet quadrangle, west-central Alaska

[Major elements in weight percent; trace elements in parts per million. All major oxides except FeO, $CO_2$, $H_2O+$, and $H_2O-$ by X-ray fluorescence following methods of Taggart and others (1990). FeO by titration following method of Papp and others (1990). $CO_2$ and $H_2O$ by methods of Norton and Papp (1990). Trace elements by instrumental neutron activation analysis (INAA) unless otherwise noted in first column by following acronyms: XRF, energy-dispersive X-ray fluorescence; ICP, inductively coupled plasma-emission spectrometry. Nb analyses labeled (ICP-AES) were determined using inductively coupled plasma-atomic emission spectrometry using unpublished method developed by T.L. Fries of USGS, Menlo Park, Calif. Other methods described by Baedecker (1987). nd, not accurately determined; - -, not analyzed. USGS analysts: S.T. Neil and D.V. Vivit, Menlo Park, Calif.; B. Anderson, L.A. Bradley, J.R. Budahn, R.J. Knight, and D.M. McKown, Lakewood, Colo.]

| Sample No. | 86ML007 | 86ML026 | 86ML028 | 86Pa073 | 86Pa105 | 86Pa106 |
|---|---|---|---|---|---|---|
| Map Unit | MzPzb | MzPzb | MzPzb | MzPzb | MzPzb | MzPzb |
| Rock Type | Metadiabase | Metadiabase | Metadiabase | Metadiabase | Metadiabase | Metadiabase |
| Map No. | 91 | 92 | 93 | 94 | 95 | 96 |
| Township | T28S | T28S | T28S | T27S | T22S | T23S |
| Range | R10W | R10W | R12W | R12W | R9W | R9W |
| $SiO_2$ | 47.9 | 50.2 | 50.4 | 49.2 | 47.9 | 47.9 |
| $Al_2O_3$ | 19.1 | 14.1 | 15.1 | 15.0 | 14.4 | 13.9 |
| $Fe_2O_3$ | 1.85 | 8.19 | 4.86 | 2.06 | 3.42 | 3.39 |
| FeO | 5.30 | 5.23 | 6.34 | 5.21 | 6.56 | 6.86 |
| MgO | 6.80 | 4.60 | 4.00 | 9.70 | 8.11 | 8.87 |
| CaO | 12.40 | 5.96 | 8.21 | 9.56 | 11.30 | 10.80 |
| $Na_2O$ | 2.60 | 4.90 | 4.00 | 3.10 | 2.57 | 2.64 |
| $K_2O$ | 0.08 | 0.14 | 0.06 | 0.40 | 0.11 | 0.14 |
| $TiO_2$ | 0.98 | 2.00 | 1.56 | 0.54 | 1.31 | 1.43 |
| $P_2O_5$ | 0.10 | 0.34 | 0.22 | 0.02 | 0.12 | 0.13 |
| MnO | 0.12 | 0.26 | 0.18 | 0.14 | 0.13 | 0.16 |
| $CO_2$ | <0.05 | <0.05 | 1.23 | 1.42 | <0.05 | 0.07 |
| $H_2O+$ | 2.19 | 1.30 | 3.34 | 2.99 | 3.32 | 3.25 |
| $H_2O-$ | 0.12 | 1.39 | 0.25 | 0.32 | 0.44 | 0.27 |
| Total | 99.5 | 98.6 | 99.8 | 99.7 | 99.7 | 99.8 |
| Rb | 4.6 | nd | nd | 13.1 | nd | 4.04 |
| Rb (XRF) | <10 | <10 | <10 | <10 | <10 | <10 |
| Cs | nd | 0.225 | 0.179 | 0.639 | nd | 0.115 |
| Sr (XRF) | 230 | 148 | 180 | 300 | 140 | 180 |
| Ba (XRF) | <30 | 100 | 56 | 80 | <30 | <30 |
| La | 2.55 | 6.56 | 5.17 | 1.62 | 3.64 | 3.2 |
| Ce | 8.15 | 18.4 | 14.9 | 5.44 | 10.4 | 9.7 |
| Nd | 7.04 | 14.9 | 11.5 | 4.98 | 9.38 | 9.0 |
| Sm | 2.30 | 4.80 | 4.10 | 1.85 | 3.36 | 3.27 |
| Eu | 0.887 | 1.820 | 1.500 | 0.664 | 1.340 | 1.270 |
| Gd | 3.16 | 6.14 | 5.31 | 2.69 | 4.71 | 4.62 |
| Tb | 0.530 | 1.040 | 0.893 | 0.558 | 0.792 | 0.787 |
| Tm | 0.376 | 0.614 | 0.575 | 0.330 | 0.472 | 0.492 |
| Yb | 2.100 | 3.850 | 3.540 | 1.990 | 2.980 | 3.070 |
| Lu | 0.305 | 0.571 | 0.522 | 0.297 | 0.437 | 0.453 |
| Y (XRF) | 16 | 34 | 26 | 14 | 23 | 23 |
| Y (ICP) | 19 | 30 | 28 | 18 | 27 | 26 |
| Zr (XRF) | 74 | 120 | 112 | 32 | 88 | 92 |
| Hf | 1.63 | 2.80 | 2.72 | 0.989 | 2.26 | 2.29 |
| Nb (XRF) | <10 | <10 | <10 | <10 | <10 | <10 |
| Nb (ICP-AES) | 2.7 | 3.4 | 3.1 | 1.9 | 2.0 | 2.0 |
| Ta | 0.113 | 0.223 | 0.172 | 0.110 | 0.139 | 0.206 |
| Th | 0.116 | 0.341 | 0.227 | 0.337 | 0.195 | 0.18 |
| U | nd | 0.17 | 0.15 | nd | 0.24 | nd |
| Co (ICP) | 33 | 34 | 34 | 39 | 48 | 43 |
| Co | 31.90 | 33.70 | 29.20 | 39.80 | 42.30 | 40.1 |
| Cr (ICP) | 233 | 9 | 5 | 282 | 390 | 328 |
| Cr | 207.00 | 7.65 | 5.34 | 282.00 | 278.00 | 259.00 |
| Ni (ICP) | 105 | 7 | 7 | 86 | 91 | 84 |
| Ni | 94.4 | 17.9 | 15.0 | 78.4 | 84.4 | 65.8 |
| Sc (ICP) | 29 | 43 | 36 | 50 | 42 | 40 |
| Sc | 28.10 | 43.00 | 31.70 | 51.70 | 40.40 | 41.40 |
| V (ICP) | 174 | 431 | 346 | 180 | 237 | 230 |
| Zn | nd | 108.0 | 84.7 | 35.6 | 12.0 | 39.0 |
| Sb | nd | nd | 2.250 | 0.520 | 0.601 | nd |

**Table 9.** Table summarizing compositional distinction between map units in the lithotectonic terranes in the Unalakleet quadrangle, west-central Alaska

| Map Unit | Rock types | Distinctive features | Rare-earth elements (REE) | Alkalis ($K_2O$, Rb) | High-field-strength elements (Zr, Ta, Nb) | Strontium (Sr) | $TiO_2$, MgO |
|---|---|---|---|---|---|---|---|
| Kft | Flows, pyroclastic flows, some plutonic rocks | Very high alkali contents. Pluton commonly very pink. Biotite occurs in some flows | Strong to very strong light-rare-earth element (LREE) enrichment (fig. 12*A*) | Very high. $K_2O$ greater than 2.2 weight percent. Rb greater than 50 parts per million (ppm) | Zr, Nb, and Ta contents are higher than the other units, but Nb and Ta still show negative anomalies on spidergrams (figs. 12*B*, 16) | High. Decreases sharply with increasing $SiO_2$ (fig. 14) | Lower $TiO_2$ and MgO than the other units, but some overlap prevents this from being diagnostic (figs. 13, 15) |
| Kv | Mostly clastic rocks, some flows | Composition similar to unit Jt, but not plutonic and more varied | Enriched LREE to flat patterns (fig. 17) | Moderate. Like unit Jt, unless removed by alteration | Low, like unit Jt (fig. 17) | Like unit Jt (fig. 14) | Appears to have slightly higher $TiO_2$ than unit Jt (figs. 13, 15) |
| Jt | Mostly plutonic rocks. Locally highly sheared and metasomatized | Only plutonic rocks; moderate calc-alkalic composition | Moderate LREE enrichment (fig. 18) | Moderate. $K_2O$ usually less than 2.5 weight percent, unless metasomatized. Rb less than 50 ppm | Low. Zr and Nb increase with increasing $SiO_2$, but are generally low (figs. 14, 16) | Moderate. Generally decreases with increasing $SiO_2$ (fig. 14) | MgO decreases sharply with increasing $SiO_2$. $TiO_2$ shows two trends (figs. 13, 15) |
| MzPzb | Fine-grained diabase. Abundant prehnite veins. Often metamorphosed to lower greenschist facies | REE patterns are distinct | LREE depleted to flat patterns (fig. 19) | Low. $K_2O$ less than 0.5 weight percent. Rb less than 20 ppm | Moderate Zr and Nb contents. No Nb and Ta anomaly on spidergrams (fig. 14, 16, 19) | Low. Less than 250 ppm (fig. 14) | Large variation. Not very distinctive (figs. 13, 15) |